

Dear Sir,

This paper describes the synthesis of new diols from a renewable resource and their polymerization, representing a more sustainable route to polyacetals. The synthetic protocols for the transformation of the castor oil derivatives into linear and branched diols were developed taking into account the sustainability criteria (reactions at room temperature, avoiding the use of solvents or using solvents from renewable origin).

The novelty of the work relies not only on the valorization of heptaldehyde in polymer chemistry, a castor oil by-product, but also on expanding the use of 10-undecenoic acid in acetal polymers. Moreover, degradability play a key role in polymer sustainability and developing new polyacetals can promote new advances in this area. According to these considerations, we think this paper is suitable for publication in European Polymer Journal.

Sincerely,

## Answer to the comments from the editors and reviewers:

### -Reviewer 1

- This manuscript from Dr. Marina Galia and co-authors is an interesting and novel contribution in the field of bio-based polymers (here polyacetals). The manuscript is well written and the data carefully discussed. I recommend publication after the authors take into account the following remarks:

1. The introduction section and pages 13/14 are a bit long; I think these parts could be shortened.

The introduction and the discussion regarding the polyacetal synthesis on pages 13/14 have been shortened.

2. Table 1: why the yields are not 100%? What are the by-products formed?

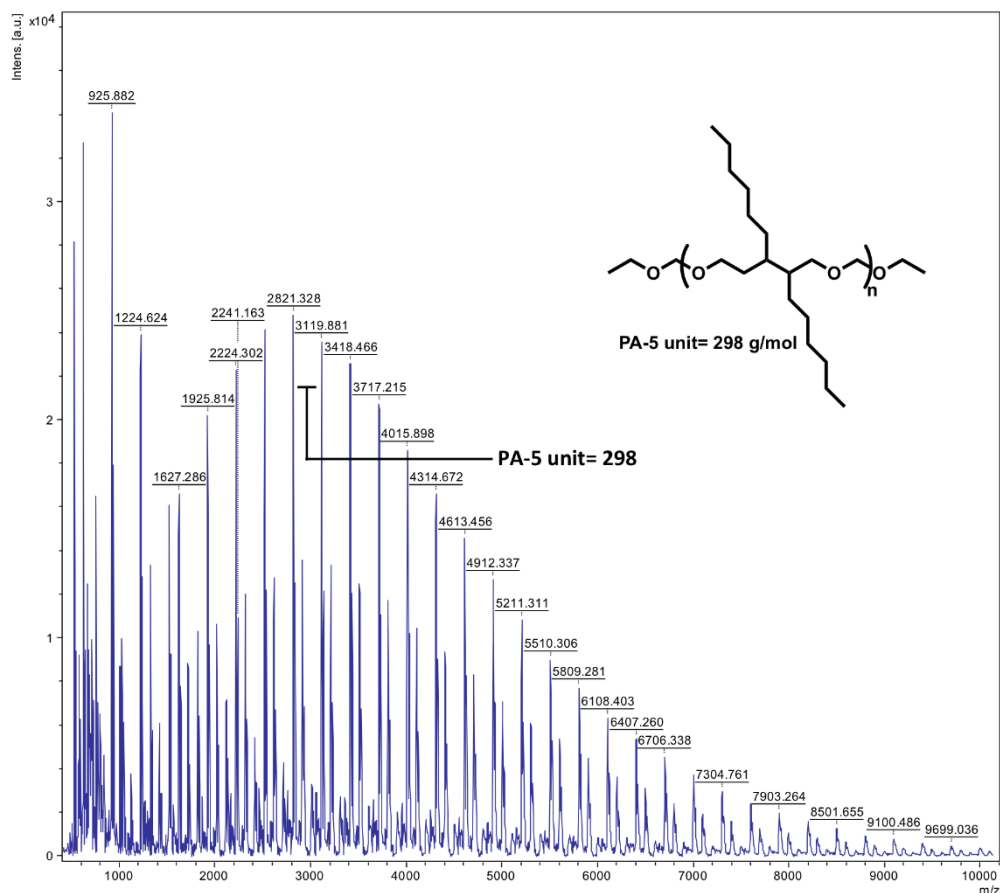
We think that soluble dimers, trimers and low molecular weight oligomers are lost during the workup procedure (dissolution in dichloromethane, quenching of the catalyst with aqueous NaOH and precipitation into methanol). Moreover, as it is mentioned in the paper (page 15, line 10), the formation of cyclic acetals cannot be discarded, especially for shorter monomer 5 which leads to an unusually low yield for PA5.

3. MALDI analysis of the polyacetals should be performed to check the formation or not of cyclics. The SEC traces exhibit a shoulder that could be assigned to cyclics?

MALDI analysis has been attempted for all the homopolymers as well as for copolymer PA1-5 (3:1). After testing different matrices and cationizing agents at various concentrations, we only obtained signal for PA5 (using 2-[(2E)-3-(4-tert-butylphenyl)-2-methylprop-2-enylidene]malononitrile (DCTB) as matrix and NaCl as cationizing agent). The MALDI is the one shown in the next figure. As can be seen, a major peak series which spacing between peaks is the expected repeating unit value is observed. However, a very complicated pattern with different peaks can also be observed that cannot be easily explained and that is strongly dependent of the laser power. It is difficult to be sure if the MALDI is representative of the polymer structure or if the polymer structure is affected by the irradiation and vacuum conditions, thus giving complicate processes and unexpected reactions. So, we think that this information cannot be considered conclusive.

SEC data in Figure S38 show a very broad molecular weight distribution according to a  $\bar{D}=1.8$ . No bimodal distributions that could be attributed to the presence of cyclic oligomers are observed for any of the polymers or copolymers. Thus, we cannot confirm the presence of cyclic oligomers, nor to exclude it. As a

step growth polymerization their formation could occur, so low amounts can be present.



4. A last suggestion would be to implement rheology tests on these novel polyacetals.

A rheological characterization would be very interesting, but to our understanding should be directed to a specific application. As will be mentioned below, the monomers and polymers of this work can be applied in different fields and the goal of this paper was to carry out the synthesis and characterization rather than the design for a specific application.

-Reviewer 2

-

*The current paper of Cadiz and colleagues is a nice piece of work on creating a platform on linear and branched acetal polymers from castor oil via acetal metathesis by expanding the toolbox of castor oil based polymers. Hence, I suggest accepting this paper after taking into account the following minor revisions and comments:*

*According the authors, the NMR studies indicated that the polyacetals degrade down to parent diols, thus I am wondering if it is possible to isolate the respective diols and reuse them in subsequent polymerization?*

Yes, this would be possible as they are polyacetals. So, this can be foreseen as very advantageous for certain applications from the point of view of sustainability.

*I would like to recommend subjecting the polyacetals, particularly the copolymers, to MS (explicitly MALDI-ToF)-analysis in order to determine the ration of each polymer repeat unit; and hence to see if the proton NMR spectroscopy observations are corroborated by the MALDI-ToF-MS characterization of the polymers.*

As above mentioned, no conclusive results have been obtained from MALDI. Moreover, the quantification of the ratio of each copolymer repeat unit by MALDI would be very difficult.

*Last but not least, could the authors specify what kind of applications are foreseen for the co(polymers)?*

Due to their hydrolytic degradability, linear polyacetals have been considered as a substitutes of commodity plastics like polyethylene or PLA. They show high crystallinity and hydrophobicity, so the copolymerization of long chain diols with branched ones offers the opportunity to modulate these properties. Moreover, biomedical applications of polyacetals are widely explored for sensing, diagnostics, tissue engineering and targeted drug delivery. The monomers described in our work can also be used to tune the degradation properties in this field.

## HIGHLIGHTS

Synthetic protocols are developed to prepare new diols from heptanal

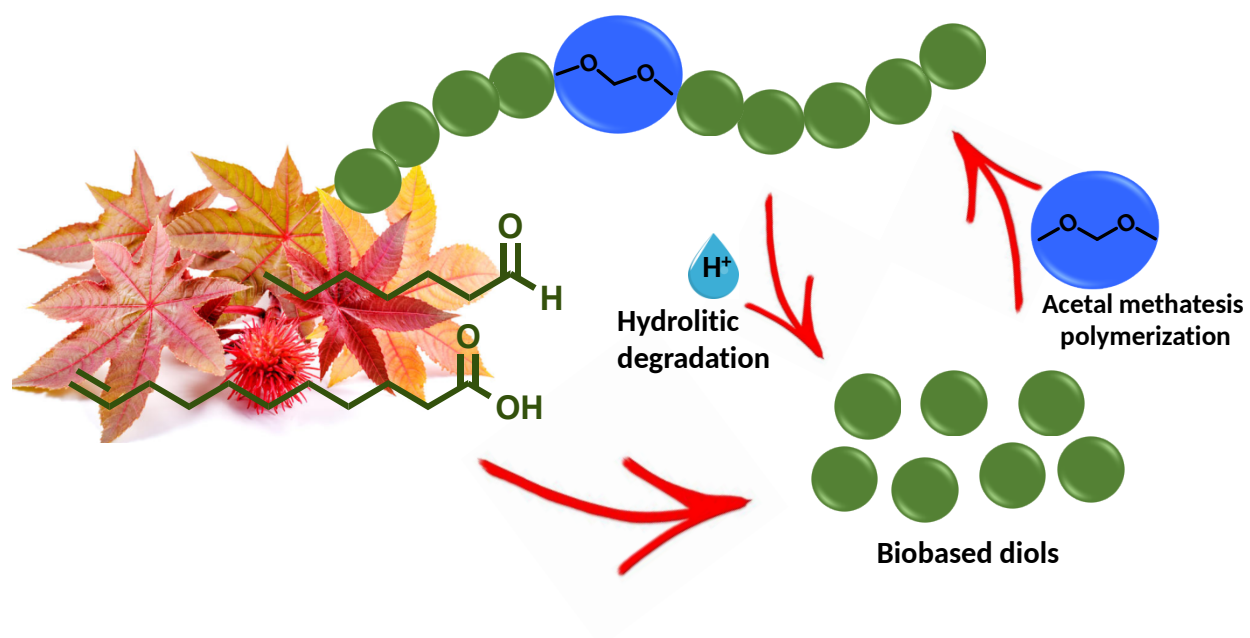
Linear and branched polyacetals are obtained by acetal metathesis polymerization

Similar acidic degradation patterns are obtained regardless of polyacetal structure

Graphical Abstract

Linear and branched acetal polymers from castor oil via acetal metathesis polymerization

Adrian Moreno, Gerard Lligadas, Juan Carlos Ronda, Marina Galià and Virginia Cádiz



# Linear and branched acetal polymers from castor oil via acetal metathesis polymerization

Adrian Moreno, Gerard Lligadas, Juan Carlos Ronda, Marina Galià and Virginia Cádiz

Universitat Rovira i Virgili, Departament de Química Analítica I Química Orgànica, Laboratory  
of Sustainable Polymers, Marcel·lí Domingo 1, 43007 Tarragona, Spain

**KEYWORDS:** Polyacetals, castor oil, heptanal, 10-undecenoic acid, renewable resources, plant oils

## ABSTRACT

Synthetic protocols to prepare new diols were developed to revalorize heptanal and 10-undecenoic acid castor oil derivatives. The Acetal Metathesis Polymerization of these diols yielded linear and branched renewable polyacetals and copolyacetals with number average molecular weights in the range 14000 to 27000 g mol<sup>-1</sup>. Thermally robust semicrystalline or amorphous materials were obtained. Polyacetals were hydrolytically degradable down to parent diols under slightly acidic media and no significant differences on the degradation pattern were observed among them.

## Introduction

Polymers are an indispensable component of our modern society and the major output of the chemical industry. Nearly all polymers are derived from non-renewable fossil resources and their disposal at their end of use brings about several environmental problems. The development of polymers that are sustainable from combined environmental, societal, human health and economic perspectives is a major challenge in polymer science. [1] The key to shifting to sustainable alternatives will be to obtain both existing and new low-cost polymers with competitive performance properties from renewable resources. Moreover, polymers that can be easily recycled, autonomously degraded to innocuous byproducts over reasonable time scales or safely incinerated to recover their embedded energy must be developed to address the end-of-life concerns.

The next generation of environmentally friendly commodity plastics will derive from sustainable feedstocks based on biomass. A particularly relevant option is to replace oil based resources by plant oils and their derived fatty acids, and castor oil is one of the most valuable choices. Their high versatility and exclusion of alimentary sector convert this material into a good candidate to explore new routes to obtain biopolymers. Castor oil derivatives have been employed in the synthesis of different kind of polymers such as polyesters, polyamides and polyurethanes among others.[2] However, the bioderived plastics suffer from the same end of life issues as fossil derived plastics and they persist in the environment long after their use. The design of durable products susceptible to rapid degradation at the end of their life plays a key role in sustainability.

Acetals are excellent candidates for facilitating degradation due to their acid-sensitive nature. The structural variations of the acetal moiety affect its sensitivity, thus allowing the fine-tuning of degradation.[3] Their incorporation in the main chain or as pendant group of a non-degradable

backbone and their use in a variety of areas have been reported.[4-9] Hydrolytically sensitive polyacetals can be designed to degrade in aqueous environments.[10] Moreover, landfill leachate is slightly acidic and polyacetals should be degradable regardless of landfill depth and level of microbial activity, thus they are useful to improve the environmental degradability of commodity plastics. A more sustainable solution is the production of polyacetals from renewable resources and the use of plant oils,[11, 12] carbohydrates[13, 14] and lignin[15, 16] has been described.

The aim of this work was the synthesis of novel polyacetals sourced from castor oil as biorenewable feedstock that do not compete with food production. Its main constituent, ricinoleic acid, can be subjected to thermal cracking to obtain 10-undecenoic acid and heptanal. 10-Undecenoic acid has been widely used in polymer chemistry.[17, 18] However, the use of heptanal as an intermediate in polymer chemistry is practically non-existent.[19] In this work, both starting materials have been used to synthesize biobased diols that were polymerized and copolymerized to obtain renewable polyacetals by acetal metathesis polymerization (AMP).[12] Initial results on the hydrolytic degradability of the polyacetals are presented.

## **Experimental section**

### *Materials*

The following chemicals were obtained from Aldrich and used as received: trimethyl phosphonoacetate (98%), 1,8-diazabicyclo-[5.4.0]undec-7-ene (DBU, 99%), 2-mercaptoethanol

(98%), *p*-toluenesulfonic acid (*p*-TSA, 97%), 1,10-decanediol (**1**, 99%), 10-undecenoic acid (98%), 1-octene (99%), lithium aluminum hydride (powder, 97%), potassium *tert*-butoxide (98%), palladium on carbon (10% wt), methyl 3-mercaptopropionate (98%), 3-chloroperbenzoic acid (mCPBA, 70%), hydrogen peroxide (50% wt). Heptanal (96%) was obtained from Arkema. 10-undecen-1-ol was synthesized from 10-undecenoic acid using LiAlH<sub>4</sub> following a reported procedure.[20] Methyl 2-nonenoate was obtained from heptanal as previously described.[19] Diethoxymethane (DEM) from Aldrich was dried and distilled over CaH<sub>2</sub> and stored under inert conditions. THF was distilled from sodium and stored under inert conditions. Other solvents were used in technical grade as received.

### *Instrumentation*

NMR spectra were recorded on a Varian VNMRS400. The samples were dissolved in CDCl<sub>3</sub>, and <sup>1</sup>H and <sup>13</sup>C NMR spectra were recorded at room temperature with tetramethylsilane as an internal standard. ESI MS were run on a chromatographic system Agilent 1200 liquid chromatography coupled to 6210 Time of Flight (TOF) mass spectrometer from Agilent Technologies with an ESI interface.

Size exclusion chromatography (SEC) analysis was performed with an Agilent 1200 series system equipped with an Agilent 1100 series refractive-index detector. The analysis was performed at 35°C on the three column system: 3µm PLgel MIXED-E, 5µm PLgel MIXED-D, 20µm PLgel MIXED-A at a nominal flow rate of 1.0 mL/min and a sample concentration of 0.1% w/w in THF as solvent. The calibration curves for SEC analysis were obtained with polystyrene standards from Polymer Laboratories with molecular weights ranging from 500 to 400,000 Da.

Differential scanning calorimetry (DSC) measurements were carried out with a Mettler DSC822e thermal analyzer with N<sub>2</sub> as the purge gas and using heating and cooling rates of 10°C min<sup>-1</sup>. All data reported were collected from the second heating cycle. Thermal stability studies were carried out with a Mettler TGA/SDTA851e/LF/1100 with N<sub>2</sub> as the purge gas at a scanning rate of 10 °C/min.

#### *Monomer synthesis and characterization*

Diols **2**, **3**, **4** and **5** were obtained and characterized as described in the supplementary information (SI 1.1-1.7 and Figures S1-S12)

#### *Polymer synthesis*

Polyacetals **PA1**, **PA2**, **PA3**, **PA4** and **PA5** and copolyacetals **PA1-4** (1:1), **PA1-5** (1:1 and 3:1) and **PA2-5** (1:1) (Scheme 3) were synthesized according to the following general procedure. **PA1** was also obtained from 3,5,16,18-tetraoxaicosane (decanediol bis-acetal) (SI 1.8, Figure S13).

General procedure: In a flame dried 50 mL Schlenk tube, 1.0 g of diol, 1.5% mol of *p*-TSA and DEM (6:1 mol DEM:mol diol) were charged under argon atmosphere. The reaction mixture was heated to 80 °C for 30 minutes and during the next 3 hours, a 15 seconds argon flow was applied each 30 minutes. The temperature was then increased to 90°C and dynamic vacuum was applied for 1 minute at intervals of 30 minutes during 1.5 hours to allow the removal of the volatile side product. Finally, additional 1.5% mol of *p*-TSA was added, the reaction was heated to 115 °C and was conducted under vacuum for 5 hours. Once cool, the product was dissolved in the minimum amount of dichloromethane and 1 mL of aqueous 1M NaOH solution was added to quench the

acid catalyst. The polymer was precipitated into 300 mL of cold methanol, filtered and washed several times with cold methanol, acetone and ether and dried under vacuum until constant weight.

### PA1

**1** (1.0 g, 5.73 mmol), *p*-TSA (15 mg, 0.08 mmol) and DEM (4.10 mL, 32.78 mmol) were used. The polymer was obtained as a white solid in a 82% yield.

Alternatively, a 100 mL round bottom flask was charged with 1.32 g (4.8 mmol) of 3,5,16,18-tetraoxaicosane and 26 mg (1.5 mol%) of (*p*-TSA). The mixture was stirred under inert atmosphere and the temperature was increased to 115 °C for 3 hours. A 10 seconds argon flow was applied each 15 minutes during this period. Next, vacuum was applied, first 30 minutes at 115°C and then 8 hours a 150°C. Once cool, the above mentioned work-up procedure was applied to give the polymer as a white powder in 80% yield. The overall yield over the two steps was 77%.

<sup>1</sup>H NMR [CDCl<sub>3</sub>, TMS, δ (ppm)] (Figure SI.22): 4.64 (s, O-CH<sub>2</sub>-O, 2H), 3.49 (t, O-CH<sub>2</sub>, 4H), 1.53 (m, O-CH<sub>2</sub>-CH<sub>2</sub>, 4H), 1.37-1.27 (m, aliphatic chain, 12H).

<sup>13</sup>C NMR [CDCl<sub>3</sub>, TMS, δ (ppm)] (Figure SI.23): 95.1, 67.8, 29.5, 29.4, 26.2.

### PA2

**2** (1.0 g, 4.0 mmol), *p*-TSA (11 mg, 0.06 mmol) and DEM (2.8 mL, 23 mmol) were used. **PA2** was isolated as a slightly yellow solid (75% yield).

<sup>1</sup>H NMR [CDCl<sub>3</sub>, TMS, δ (ppm)] (Figure S24): 4.72, 4.69, 4.67 (s, -O-CH<sub>2</sub>-O-, 2H), 3.71 (q, O-CH<sub>2</sub>-CH<sub>2</sub>-S, 2H), 3.52 (q, O-CH<sub>2</sub>-CH<sub>2</sub>, 2H), 2.71 (t, O-CH<sub>2</sub>-CH<sub>2</sub>-S-CH<sub>2</sub>, 2H), 2.53

(t, O-CH<sub>2</sub>-CH<sub>2</sub>-S-CH<sub>2</sub>, 2H), 1.56 (m, O-CH<sub>2</sub>-CH<sub>2</sub>-S-CH<sub>2</sub>-CH<sub>2</sub>; O-CH<sub>2</sub>-CH<sub>2</sub>, 4H), 1.36-1.27 (m, aliphatic chain, 14H).

<sup>13</sup>C NMR [CDCl<sub>3</sub>, TMS, δ (ppm)] (Figure S25): 95.3, 95.2, 95.1, 68.0, 67.8, 67.2, 67.1, 32.5, 32.4, 31.8, 29.7-28.8 (8C), 26.2

### PA3

**3** (1.0 g, 3.56 mmol), *p*-TSA (10 mg, 0.05 mmol) and DEM (2.54 mL, 20 mmol) were used. **PA3** was isolated as a solid. (84% yield).

Alternatively, 0.3g (1.36 mmol) of **PA2** were dissolved in 9 mL of THF, followed by the addition of 20 mL of a mCPBA solution in THF (0.6 g, 2.72 mmol). The reaction mixture was stirred at room temperature for 2 hours. After that, the reaction mixture was washed with Na<sub>2</sub>S<sub>2</sub>O<sub>3</sub> and NaHCO<sub>3</sub>. The resulting organic phases were dried over MgSO<sub>4</sub> and concentrated. The resulting polymer, were purified by precipitation in cold methanol. **PA3** was isolated as a grey solid (88% yield).

<sup>1</sup>H NMR [CDCl<sub>3</sub>, TMS, δ (ppm)] (Figure S26): 4.72, 4.69, 4.67 (s, -O-CH<sub>2</sub>-O, 2H), 3.96 (q, O-CH<sub>2</sub>-CH<sub>2</sub>-SO<sub>2</sub>, 2H), 3.52 (t, O-CH<sub>2</sub>-CH<sub>2</sub>, 2H), 3.22, (t, O-CH<sub>2</sub>-CH<sub>2</sub>-SO<sub>2</sub>-CH<sub>2</sub>, 2H), 3.06, (t, O-CH<sub>2</sub>-CH<sub>2</sub>-SO<sub>2</sub>-CH<sub>2</sub>, 2H), 1.78, (m, HO-CH<sub>2</sub>-CH<sub>2</sub>-SO<sub>2</sub>-CH<sub>2</sub>-CH<sub>2</sub>, 2H) 1.58 (OH-CH<sub>2</sub>-CH<sub>2</sub>, 2H), 1.43-1.28, (m, aliphatic chain, 14H).

<sup>13</sup>C NMR [CDCl<sub>3</sub>, TMS, δ (ppm)] (Figure S27): 95.4, 95.2, 68.4, 67.8, 61.6, 61.13, 55.0, 54.8, 54.5, 29.3-28.4 (9C), 25.9, 22.6

### PA4

**4** (1.0 g, 4.2 mmol), *p*-TSA (11 mg, 0.06 mmol) and DEM (3.05 mL, 24.4 mmol) were used. **PA4** was isolated as a yellow viscous liquid (80% yield).

<sup>1</sup>H NMR [CDCl<sub>3</sub>, TMS, δ (ppm)] (Figure S28): 4.65 (s, O-CH<sub>2</sub>-O, 2H), 3.67 (m, O-CH<sub>2</sub>-CH<sub>2</sub>-CH, 2H), 3.60 (t, O-CH<sub>2</sub>-CH<sub>2</sub>-CH<sub>2</sub>, 2H), 2.71 (m, S-CH, 1H), 2.56 (t, S-CH<sub>2</sub>, 2H), 1.81 (m, HO-CH<sub>2</sub>-CH<sub>2</sub>, HO-CH<sub>2</sub>-CH<sub>2</sub>-CH, 3H), 1.65 (m, HO-CH<sub>2</sub>-CH<sub>2</sub>-CH, 1H), 1.55 (m, S-CH-CH<sub>2</sub>-(CH<sub>2</sub>)<sub>4</sub>, 2H), 1.45-1.28 (m, aliphatic chain, 8H), 0.88 (t, CH<sub>3</sub>, 3H).

<sup>13</sup>C NMR [CDCl<sub>3</sub>, TMS, δ (ppm)] (Figure S29): 95.3, 66.3, 65.3, 42.6, 35.1, 34.8, 31.7, 29.9, 29.2, 26.8, 26.6, 22.6, 14.7

#### **PA5**

**5** (1.0 g, 3.5 mmol), *p*-TSA (9.9 mg, 0.05 mmol) and DEM (2.5 mL, 20 mmol) were used. **PA5** was isolated as a yellow viscous liquid (80% yield).

<sup>1</sup>H NMR [CDCl<sub>3</sub>, TMS, δ (ppm)] (Figure S30): 4.62 (m, O-CH<sub>2</sub>-O, 2H), 3.51-3.42 (m, O-CH<sub>2</sub>-CH<sub>2</sub>, O-CH<sub>2</sub>-CH, 4H), 1.62 (m, O-CH<sub>2</sub>-CH<sub>2</sub>-CH, O-CH<sub>2</sub>-CH, 4H), 1.34-1.27 (m, aliphatic chain, 22H), 0.88 (t, CH<sub>3</sub>, 6H).

<sup>13</sup>C NMR [CDCl<sub>3</sub>, TMS, δ (ppm)] (Figure S31): 95.3, 68.6, 66.8, 40.7, 35.6, 31.9, 30.8, 30.0, 29.7, 29.3, 29.4, 29.1, 28.0, 27.8, 22.6, 14.0

#### **PA1-4**

**1** (0.3 g, 1.74 mmol), **4** (0.4 g, 1.74 mmol), *p*-TSA (10 mg, 0.05 mmol) and DEM (2.5 mL, 20 mmol) were used. **PA1-4** (1:1) was isolated as a slightly yellow viscous liquid (83% yield).

$^1\text{H}$  NMR [ $\text{CDCl}_3$ , TMS,  $\delta$  (ppm)] (Figure S32): 4.66 (s, O-CH $_2$ -O, 4H), 3.67 (m, O-CH $_2$ -CH $_2$ -CH, 2H), 3.60 (t, O-CH $_2$ -CH $_2$ -CH $_2$ , 2H), 3.51 (t, O-CH $_2$ -CH $_2$ -(CH $_2$ ) $_5$ , 4H), 2.71 (m, S-CH, 1H), 2.57 (t, S-CH $_2$ , 2H), 1.85 (m, HO-CH $_2$ -CH $_2$ , HO-CH $_2$ -CH $_2$ -CH, 3H), 1.75 (m, HO-CH $_2$ -CH $_2$ -CH, 1H), 1.56 (m, S-CH-CH $_2$ -(CH $_2$ ) $_4$ -CH $_3$ , O-CH $_2$ -CH $_2$ -(CH $_2$ ) $_4$ , 6H), 1.43-1.28 (m, aliphatic chain, 18H), 0.88 (t, CH $_3$ , 3H).

$^{13}\text{C}$  NMR [ $\text{CDCl}_3$ , TMS,  $\delta$  (ppm)] (Figure S33): 95.2, 95.1, 67.9, 67.7, 66.2, 65.2, 42.6, 35.1, 34.8, 31.7, 29.9-29.2 (12C), 22.5, 14.5

#### **PA1-5 (1:1)**

**1** (0.5 g, 2.86 mmol), **5** (0.5 g, 1.75 mmol), *p*-TSA (10 mg, 0.05 mmol) and DEM (2.5 mL, 20 mmol) were used. **PA1-5** (1:1) was isolated as a slightly yellow viscous liquid (80% yield).

$^1\text{H}$  NMR [ $\text{CDCl}_3$ , TMS,  $\delta$  (ppm)] (Figure S34): 4.66 (s, O-CH $_2$ -O, 2H), 4.65 (s, O-CH $_2$ -O, 2H), 3.51 (t, O-CH $_2$ -(CH $_2$ ) $_9$ , 4H), 3.43-3.40 (m, O-CH $_2$ -CH $_2$ , O-CH $_2$ -CH, 4H), 1.57 (m, O-CH $_2$ -CH $_2$ -CH, O-CH $_2$ -CH, O-CH $_2$ -CH $_2$ -(CH $_2$ ) $_8$ , 8H), 1.44-1.26 (m, aliphatic chain, 22H), 0.88 (t, CH $_3$ , 6H).

$^{13}\text{C}$  NMR [ $\text{CDCl}_3$ , TMS,  $\delta$  (ppm)] (Figure S35): 95.3, 95.1, 68.0, 67.7, 66.6, 40.2, 35.5, 31.8, 31.1-28.1 (18C), 22.6, 14.0.

#### **PA1-5 (3:1)**

**1** (0.3 g, 1.74 mmol), **5** (0.13 g, 0.43 mmol), *p*-TSA (6 mg, 0.03 mmol) and DEM (1.6 mL, 12.4 mmol) were used. **PA1-5** (3:1) was isolated as a slightly yellow powder (80%, yield).

## PA2-5

**1** (0.3 g, 1.74 mmol), **2** (0.43 g, 1.74 mmol), *p*-TSA (10 mg, 0.05 mmol) and DEM (2.5 mL, 20 mmol) were used. **PA2-5** (1:1) was isolated as a slightly yellow viscous liquid (86%, yield).

$^1\text{H}$  NMR [ $\text{CDCl}_3$ , TMS,  $\delta$  (ppm)] (Figure S36): 4.72-4.66 (m,  $-\text{O}-\underline{\text{CH}_2}-\text{O}-$ , 4H), 3.70 (q,  $\text{O}-\underline{\text{CH}_2}-\text{CH}_2-\text{S}$ , 2H), 3.51 (m,  $\text{O}-\underline{\text{CH}_2}-(\text{CH}_2)_7$ ,  $\text{O}-\underline{\text{CH}_2}-\text{CH}$ ,  $\text{O}-\underline{\text{CH}_2}-\text{CH}_2-\text{CH}$  6H), 2.72, (t,  $\text{O}-\text{CH}_2-\underline{\text{CH}_2}-\text{S}$ , 2H), 2.54 (t,  $\text{O}-\text{CH}_2-\text{CH}_2-\text{S}-\underline{\text{CH}_2}$ , 2H), 1.71-1.51 (m,  $\text{S}-\text{CH}_2-\underline{\text{CH}_2}$ ,  $\text{O}-\text{CH}_2-\underline{\text{CH}_2}-(\text{CH}_2)_7$ ,  $\text{O}-\text{CH}_2-\underline{\text{CH}_2}-\underline{\text{CH}}$ ,  $\text{O}-\text{CH}_2-\underline{\text{CH}}$  8H), 1.36-1.27 (m, aliphatic chain, 36H), 0.88 (t,  $\underline{\text{CH}_3}$ , 6H).

$^{13}\text{C}$  NMR [ $\text{CDCl}_3$ , TMS,  $\delta$  (ppm)] (Figure S37): 95.3, 95.2, 67.9, 67.8, 67.3, 67.1, 40.27, 36.6, 36.1, 32.4, 31.8, 30.8-26.6 (19C), 22.6, 14.0

### *Hydrolytic degradation of PAs*

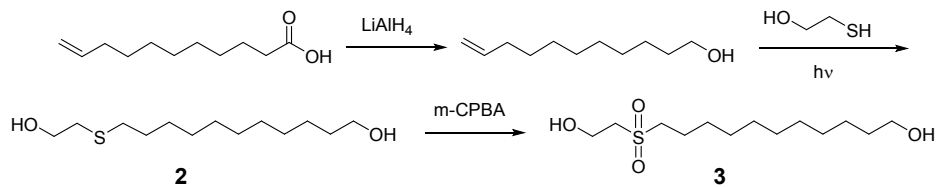
Solution degradation studies were performed following the next procedure: Solutions of 20 mg of the corresponding polyacetal in 4 mL chloroform were prepared at 25°C. Different volumes of 1M HCl solution in dioxane were added to obtain 0.02M, 0.04M and 0.06M polymer solutions. Aliquots were taken at different times and worked up by passing the liquid through a basic short alumina column. Solvent was removed by evaporation and the resulting residues were analyzed by SEC. Degradation was carried out under the same conditions using NMR tubes and monitored by  $^1\text{H}$  NMR.

## Results and discussion

### Diol monomer synthesis

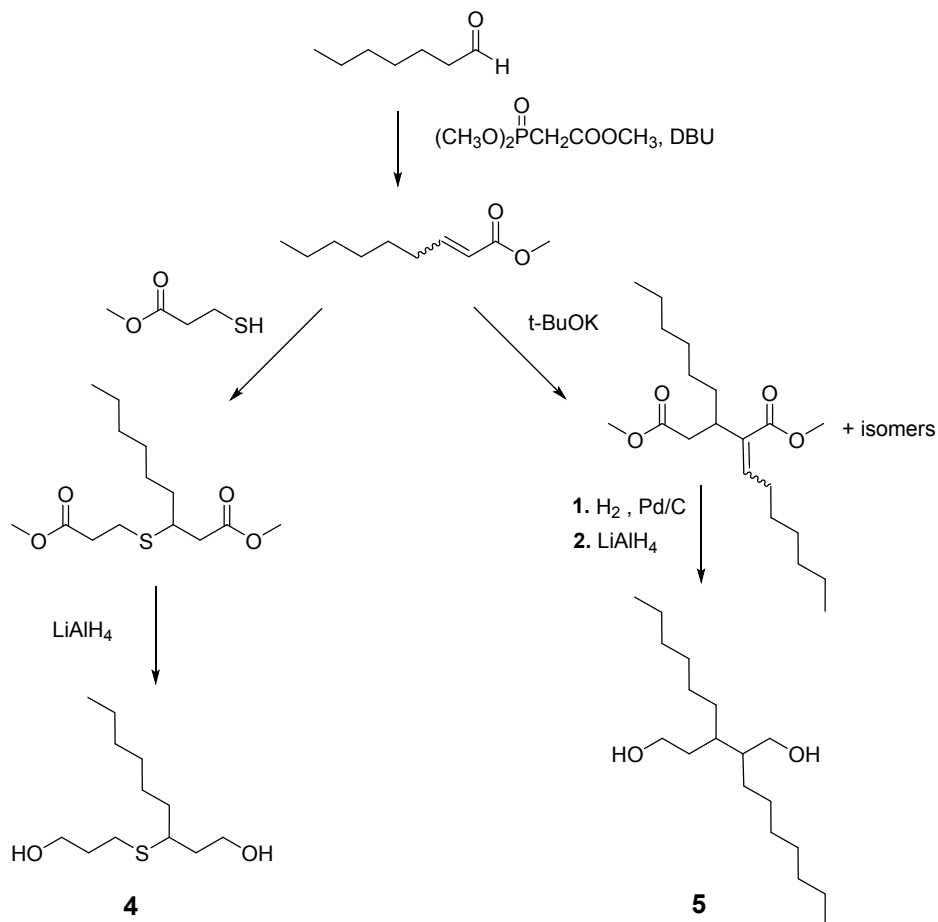
Two linear and two branched diols have been designed for the synthesis of polyacetals. Long linear primary diols have been described to polymerize successfully.[12] 1,10-decanediol (**1**) was used in this work for comparison. Our approach to linear diols consisted on the use of a sulfur-containing diol derived from 10-undecenoic acid (**2**, Scheme 1). Diol **3** was obtained after the oxidation of the sulfide moieties to sulfone. This modification is expected to increase polarity, thus changes in the thermal behavior and crystallinity of its derived polymers could be expected.

The thiol-ene addition is an efficient route to the development of a set of renewable monomers from castor oil derivatives.[21, 22, 23] Thiol-ene coupling of 2-mercaptoethanol and 10-undecenol was used to obtain the diol monomer **2**. This reaction was carried out at room temperature in absence of photoinitiator and using an excess of thiol, and the sulfur containing diol **2** was obtained in high yield. Diol monomer **3** has been obtained by oxidation of the sulfide moiety to sulfone using *m*-chloroperbenzoic acid. Attempts to carry out the reaction using H<sub>2</sub>O<sub>2</sub> as oxidizing agent led to a mixture of sulfoxide and sulfone even at long reaction times.



**Scheme 1.** Synthesis of diols **2** and **3** from renewable 10-undecenoic acid

Two branched diols, **4** and **5** (Scheme 2), have been obtained from heptanal. Their polymerization would lead to polymers containing aliphatic side chains that are expected to show lower crystallinity degrees thus broadening the properties profile of the polyacetals obtained in this work. Moreover, **4** offers the possibility to be oxidized as previously described.



**Scheme 2.** Synthesis of diols **4** and **5** from renewable heptanal

The Horner-Wadsworth-Emmons (HWE) reaction is one of the most popular and powerful method for the generation of C-C double bonds.[24] This modification of the Wittig reaction is widely used for the preparation of  $\alpha,\beta$ -unsaturated esters. It has several

advantages over the Wittig reaction, which are a result of the strong nucleophilic nature of the phosphonate carbanion created during the reaction. This increase in nucleophilicity allows milder reaction conditions, tolerance of a variety of functional groups and use of less electrophilic aldehydes and ketones. Heptanal was functionalized by HWE reaction using trimethyl phosphonoacetate and DBU (Scheme 2).[19] The obtained  $\alpha,\beta$ -unsaturated ester can be further functionalized using the nucleophile-catalyzed Michael addition of thiols, a reaction which possess many features of a click reaction, facilitating the rapid and orthogonal addition of thiols to electron-deficient enes in a quantitative manner with low amounts of commercially available catalysts.[25] The thio-Michael addition of 3-mercaptopropionate to methyl 2-nonenolate was carried out in bulk at room temperature using DBU as a catalyst at a loading of 2 mol%. 100%  $\alpha,\beta$ -unsaturated ester conversion was reached in 1 hour and after column chromatography purification, 3-((3-methoxy-3-oxopropyl)thio)nonanoate was obtained in a 88% yield. Diol **4** was obtained as a viscous oil from the diester by using  $\text{LiAlH}_4$  as reductive agent in a 85% yield after purification.

The catalytic dimerization of alkenoates has been described as a powerful method for the synthesis of unsaturated substituted diesters. These dimers can be easily converted to other unsaturated and saturated monomers.[26] The catalytic dimerization of methyl 2-nonenolate was carried out at room temperature using potassium *tert*-butoxide in THF. The mixture of *E*- and *Z*-isomers and the double bond isomer side products was converted to saturated pentanedioate by hydrogenation over Pd/C and further reduced to diol **5** in an 77% overall yield.

### *Acetal polymer synthesis*

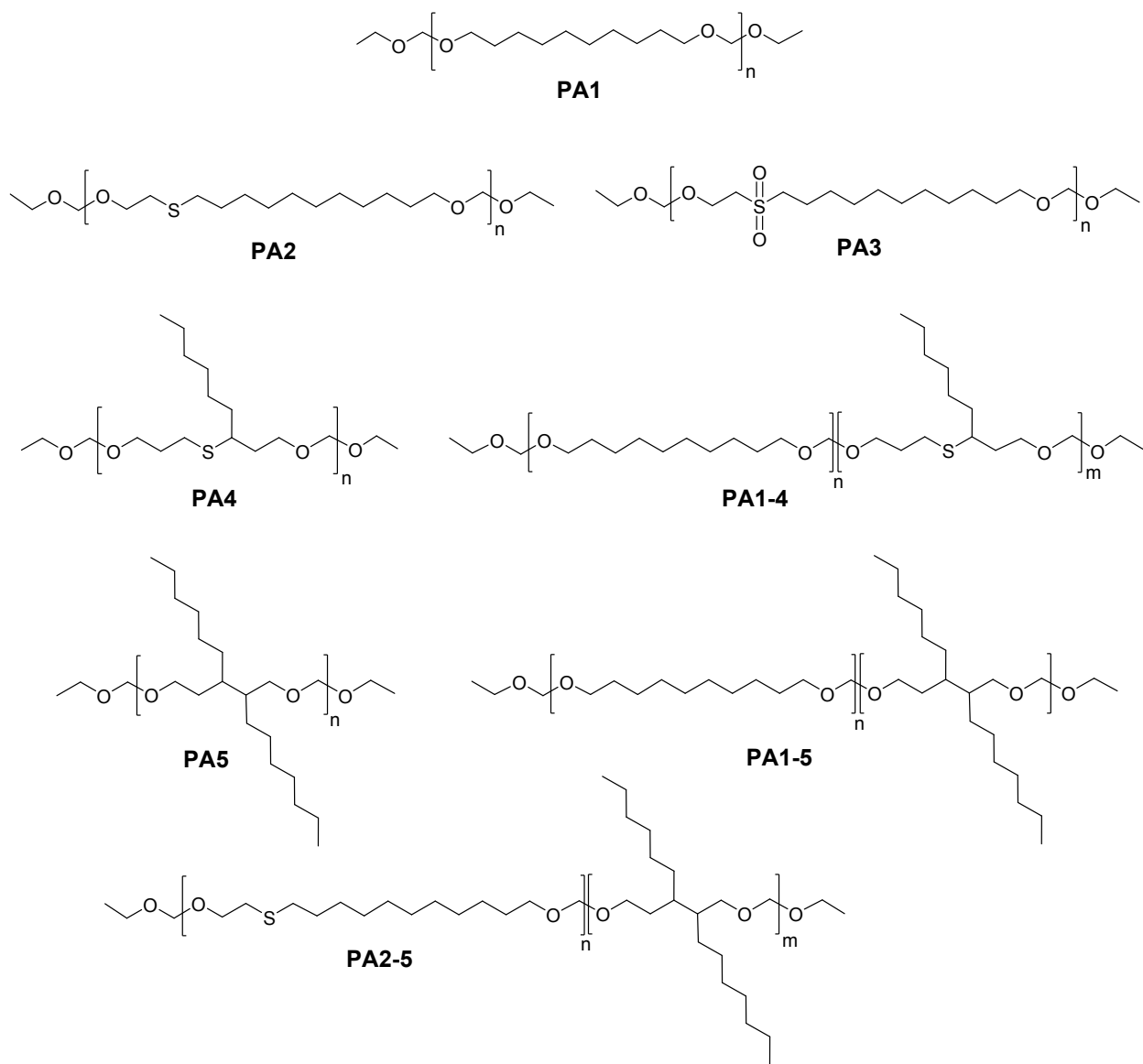
After synthesizing the diol monomers, we set out to evaluate their acid catalyzed acetal interchange polymerization or acetal metathesis polymerization (AMP). This last term was coined due to similarities between a metal catalyzed acyclic diene metathesis polymerization (ADMET) and the acid catalyzed diacetal polymerization.[12] ADMET and AMP are step growth polymerizations driven by the loss of a low boiling point molecule that achieve high polymerization degree by continuous removal of this volatile by-product.

As a first attempt, the direct conversion of the diol and diethoxymethane (DEM) to polyacetal was investigated. Commercially available 1,10-decanediol (**1**), a castor oil derivative, was treated with an excess of DEM in the presence of a catalytic amount of *p*-toluenesulfonic acid (*p*-TSA, 1.5 % mol) under inert atmosphere. The reaction mixture was heated at 80 °C and bubbling was observed, which indicated the loss of DEM and side product ethanol. The polymerization was carried out by steeply increasing the temperature to 200°C and applying dynamic vacuum. An insoluble fraction (30-15%) was isolated in all cases, which turn out to be insoluble in common organic solvents at elevated temperatures, according to its crosslinked nature. The soluble fraction was precipitated into cold methanol, leading to polymers with  $M_n$  around 15000 g/mol, high polydispersities and low yields.

As a different approach, the polymerization was carried out from decanediol bis-acetal (SI 1.8, Figures S13). The reaction was carried out overnight at room temperature and using the same amounts of **1**, *p*-TSA and DEM to afford the corresponding bis-acetal in 80% yield after column chromatography purification. The bis-acetal polymerization was carried out under dynamic vacuum (Experimental part). The reaction mixture in this case was soluble, thus indicating that

crosslinking was avoided. A higher yield (80%) was achieved, and lower  $M_n$  (11800) and  $\bar{D}$  (1.9) were obtained.

To increase the molecular weight, the more efficient one-pot strategy was investigated by avoiding harsh reaction conditions (temperature and time under vacuum, see experimental part). A soluble polymer with a  $M_n=21000$  and  $\bar{D}=1.8$  with a yield of 86% was obtained. Increasing time of the last step to 15 hours did not improve significantly  $M_n$ ,  $\bar{D}$  or yield. These last reaction conditions were used for the synthesis of polyacetals from diols **2**, **3**, **4** and **5** (Scheme 3). Yields and molecular weights are collected in Table 1.  $M_n$  for longer diols **1**, **2** **3** and **4** are higher than for shorter **5**. In this case, the lower number of methylene units could favor the formation of a cyclic acetal, thus lowering molecular weight and yield.[12]



**Scheme 3.** Polyacetals and copolyacetals synthesized via acetal methathesis polymerization from biobased diols.

**Table 1.** Synthesis and thermal properties of the polyacetals.

PA	Yield (%)	M <sub>n</sub> <sup>a</sup> (g/mol)	Đ <sup>a</sup>	T <sub>c</sub> <sup>b</sup> (°C)	ΔH <sub>c</sub> <sup>b</sup> (J/g)	T <sub>m</sub> <sup>c</sup> (°C)	ΔH <sub>f</sub> <sup>c</sup> (J/g)	T <sub>5%</sub> <sup>d</sup> (%)	T <sub>max</sub> <sup>e</sup> (°C)
<b>PA1</b>	87	21000	2.1	39	82	51,60	20, 77	390	443
<b>PA2</b>	84	17600	1.8	-14, 4, 20 <sup>g</sup>	7, 36, 65 <sup>g</sup>	17, 35	31, 58	281	347
<b>PA3</b>	88	15600	2.6	-8, 8, 39	3, 44	10, 50, 67	8, 13, 31	317	360, 439
	84 <sup>f</sup>	13500 <sup>f</sup>	2.1						
<b>PA4</b>	75	16000	2.4	-	-	-	-	294	357
<b>PA5</b>	60	8800	1.9	-	-	-	-	340	427
<b>PA1-4</b> (1:1)	75	27500	1.5	-	-	-	-	320	384
<b>PA1-5</b> (1:1)	91	16500	1.9	-	-	-	-	380	431
<b>PA1-5</b> (3:1)	88	14000	2.5	17	44	31, 44	2, 33	322	431
<b>PA2-5</b> (1:1)	71	14200	1.9	-	-	-	-	355	391

[a] Molecular weight and Đ from SEC [b] Crystallization temperature and enthalpy from DSC [c] Melting temperature and enthalpy from DSC [d] Temperature corresponding to the 5% weight loss from TGA [e] Maximum weight loss temperature from TGA [f] Obtained from **PA2** by oxidation [g] Crystallization temperature and enthalpy from a second DSC heating scan.

The polymer structures were characterized by NMR spectroscopy. The <sup>1</sup>H NMR spectrum of **PA2** (Figure 1) shows the characteristic signals of the methylenes linked to O (**a** and **a'**) and to S (**b** and **c**) as well as signals corresponding to the aliphatic main chain. Signals corresponding to the acetal methylene (**A**) appear at 4.72, 4.69 and 4.67 ppm. These signals were attributed to the existence of head-to-tail, head-to-head and tail-to-tail sequences and were unequivocally assigned by using model compounds (SI 1.9, Figures S14-S21). The expected signals for the acetal methylene and the other methylenes can be seen in the <sup>13</sup>C NMR spectrum. No signals due to end

groups or indicative of other structures are present either in  $^1\text{H}$  or in  $^{13}\text{C}$  NMR, thus indicating the formation of the expected structure for **PA2**. The spectra for the other polyacetals are also consistent with the target structures (SI Figures S22-S37).

**PA3** was also obtained from **PA2** by oxidation. Using *m*-chloroperbenzoic acid the complete conversion to sulfone was achieved at room temperature in 2 hours, while using  $\text{H}_2\text{O}_2$  complete conversion required 24 hours. No significant variations in molecular weight or molecular weight distribution were observed by SEC (SI Figure 38) and no signals attributable to polymer degradation could be observed by NMR spectroscopy in any case (SI Figures S26 and S27).

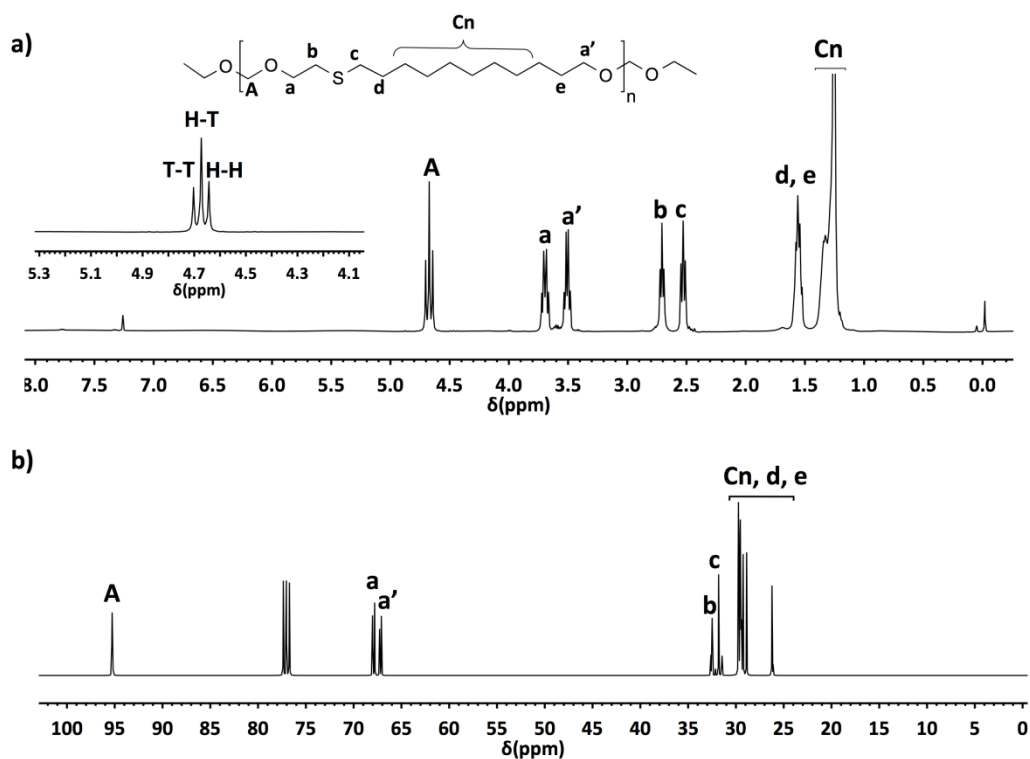


**Figure 1.**  $^1\text{H}$ (a) and  $^{13}\text{C}$ (b) NMR spectra of **PA2** ( $\text{CDCl}_3$ ,  $\delta$ (ppm))

### *Thermal and hydrolytic properties*

The thermal properties of PAs were analyzed by DSC and TGA. Heating DSC thermograms revealed a semicrystalline nature for **PA1**, **PA2** and **PA3** and all of them show crystallization exotherms in a further cooling DSC scan (Figure 2a). In a second heating melting endotherms with maximum temperatures of 60 °C (**PA1**), 17 and 35 °C (**PA2**) and 10, 50 and 67 °C (**PA3**) can be observed (Figure 2b). **PA2** show also a crystallization endotherm in this second heating at 18 °C. The dependence of the polyalkylene acetal melting temperature as a function of the number of methylene units of the diol monomer has been described.[27] The melting and crystallization points of polyacetals increase as the number of acetal units is reduced, thus resembling those of linear polyethylene. For acetal groups, a gauche conformation is preferred as a result of the anomeric effect. This conformation is not compatible with the all-trans methylene conformation and a high density of acetal units disturb the formation of a polyethylene-like orthorhombic structure, leading to heterogeneous morphologies and broad melting transitions. A similar effect can be seen for **PA2** that contains both acetal and sulfide units, thus indicating that the sulfide unit behaves like the acetal unit. Moreover, the polymer regularity can be diminished by the presence of different regiosequences, leading to heterogeneous polymer crystals. This fact could explain the appearance of two broad melting endotherms and a crystallization endotherm in the DSC plot of this polymer. **PA3** show a DSC pattern similar to **PA1** in both, cooling and second heating scans. Two effects have to be taken into account in this case, the disruption of the conformation due to the presence of sulfone moieties and the strong polarity of these groups. The dipole-dipole interactions between them can result in an interchain bonding, thus reducing the disturbing effect of the sulfone moieties and resulting in a more pronounced propensity to formation of ordered layers of functional groups.

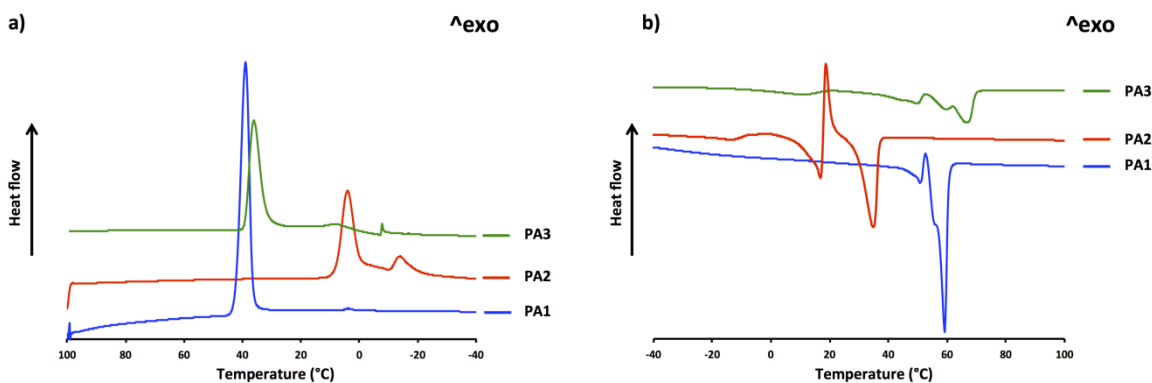


**Figure 2.** Cooling (a) and second heating (b) DSC plots of **PA1**, **PA2** and **PA3**

**PA4** and **PA5** were found to be in the liquid state at room temperature and DSC at lower temperatures did not exhibit a melting point, according to a totally amorphous nature, in spite of  $T_g$  was not observed by DSC. The amorphous character can be expected from the presence of aliphatic side chains that hinder chain packing and decrease van der Waals interactions as well as to the existence of regioirregularities.

TGA plots show that there is only one weight loss step in all cases with initial weight loss temperatures ( $T_{5\%}$ ) ranging from 280 to 390 °C (Figure 3 and Table 1). Sulfur containing **PA2**, **PA3** and **PA4** display significantly lower thermal stability than **PA1** and **PA5**. Moreover, sulfone containing **PA3** show two weight loss steps.

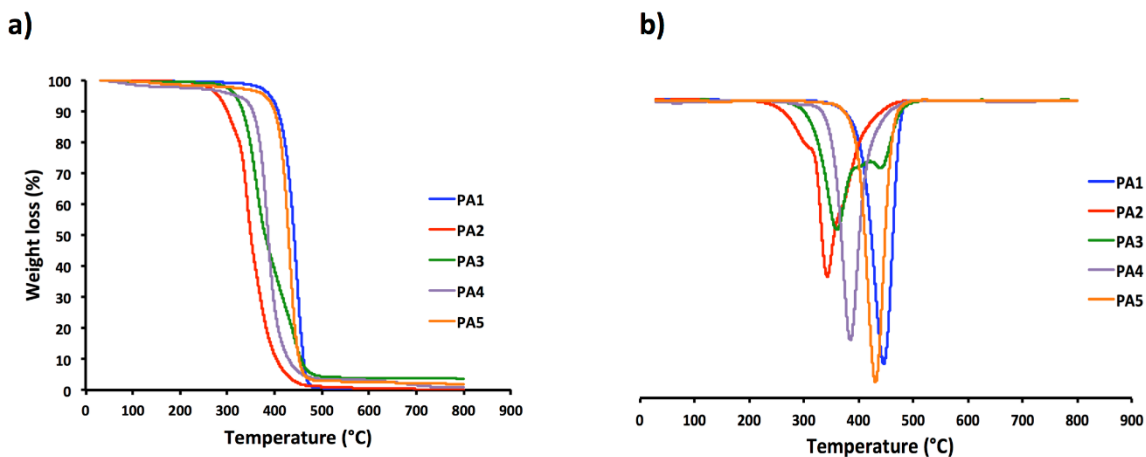


**Figure 3.** TGA (a) and DTGA (b) plots of **PA1**, **PA2**, **PA3**, **PA4** and **PA5**

To further modulate the thermal properties, we copolymerized **1** or **2** as linear diols with **4** or **5** as branched diols using the above described procedure to yield copolyacetals of different branching degrees (Scheme 3). Lower molecular weights are obtained for copolymers from **5**, according to its lower polymerization reactivity. The structures of the copolymers were characterized by NMR (SI Figures S32-S37). All copolymers compositions were found to be concordant to the initial monomer ratios in the polymerization mixtures as determined by the ratio of the  $^1\text{H}$  NMR signals intensities (signals at 4.7 and 0.88 ppm, corresponding to the acetal and methyl protons, respectively)

Copolymers containing equimolar amounts of monomers were liquids at room temperature. Only **PA1-5(3:1)** was a semicrystalline material. Figure 4 shows the DSC cooling (a) and second heating (b) plots of **PA1**, **PA1-5 (1:1)** and **PA1-5(3:1)**. As can be seen, using equimolar amounts of monomers leads to the loss of crystallinity when comparing to **PA1**. However, a lower amount of branched **5** favors the formation of branch-free regions of linear polymer chains, resulting in increased van der Waals interactions and higher crystallinities.

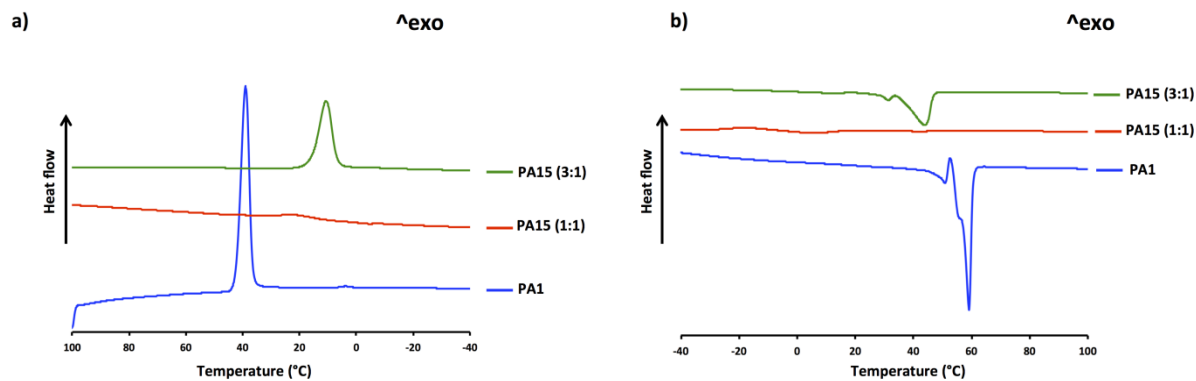


**Figure 4.** Cooling (a) and second heating (b) DSC plots of **PA1**, **PA15(1:1)** and **PA15(3:1)**

As for polyacetals, TGA analysis of copolyacetals showed one weight loss step in all cases. The thermal stability of the copolymers seems not to be affected by the linear or branched nature of the starting diols, but sulfur containing polyacetals show lower thermal stability as previously observed (Figure 5 and Table1)

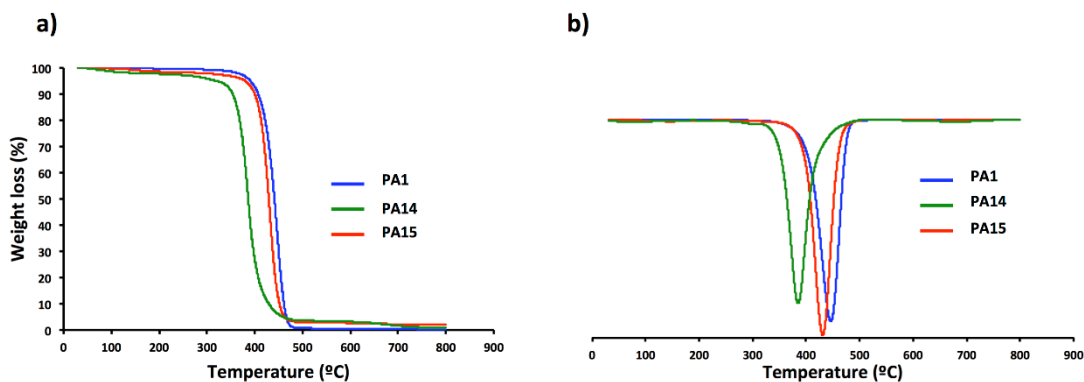


**Figure 5.** TGA (a) and DTGA (b) plots of **PA1**, **PA14** and **PA15**

Polyacetals are known to be sensitive to acid-catalyzed hydrolytic cleavage. The degradation rate of linear long-chain polyacetals decreases with increasing length of the methylene sequences.[11] For polydecylene acetal, the rate of degradation measured by the diminution in the number average molecular weight has been described to be between that of the isotactic poly L-lactide and commercially available NatureWorks® PLA600.[12]

Preliminary degradation studies were performed on **PA1**. A polymer solution with a concentration of 20 mg mL<sup>-1</sup> was prepared in chloroform and HCl was added to obtain 0.02, 0.04 and 0.06 M concentrations. The degradation was monitored at 25°C by SEC at 30 minutes, 1 hour, 2 hours and 4 hours and a clear dependence on acid concentration could be observed. For the lower acid concentration, 60% molecular weight decrease is observed in 4 hours, while the decrease reaches 90% for the higher concentration (Figure 6a).

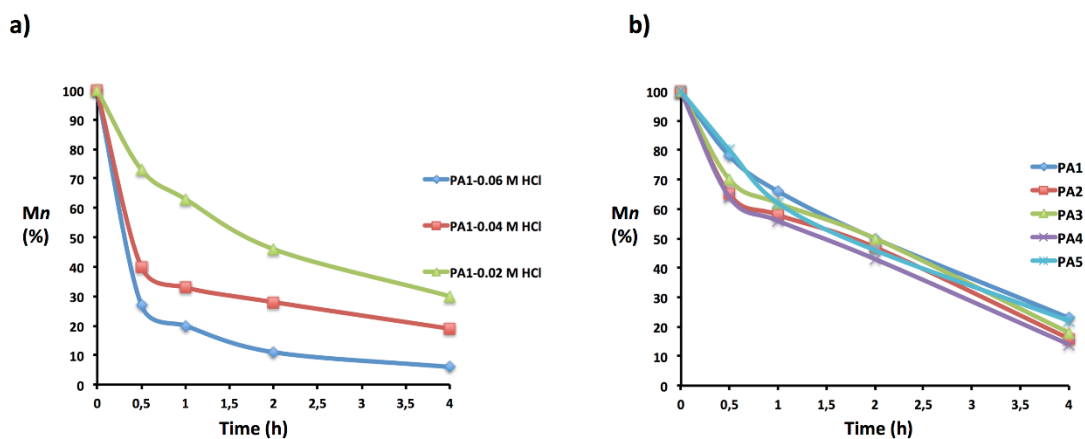


**Figure 6.** Hydrolysis studies measured by  $(M_n/M_n \text{ initial}) \times 100$  a) of **PA1** for different acid media concentrations b) for the different polyacetals (**PA1-PA5**) in 0.04 M HCl

The hydrolysis process was also monitored by <sup>1</sup>H NMR spectroscopy. Spectra were recorded at the different times and the intensity decrease of the acetal singlet at 4.67 ppm was observed, according to the cleavage of this unit (Figure 7). New signals can be observed at 4.66, 3.59, 3.51

and 1.23 ppm, which can be assigned to the end group methylene and methyl protons, according to a molecular weight decrease, and at 3.64 ppm corresponding to the diol methylene protons. This indicates that the polyacetal degrades to the initial diols.

Finally, the degradation of the polyacetals **PA1** to **PA5** was investigated in acidic 0.04 M HCl medium at 25°C. (Figure 6, b) (SI Figure S39). Small differences can be observed only in the first 30 minutes, when sulfur containing PAs seems to degrade faster, but a similar degradation pattern is observed for higher reaction times, reaching values around 80% in all cases. Thus, in spite of the different crystallinity properties and polarities, that could influence the hydrophilicity of the polymers, no differences on the degradation rate can be found.

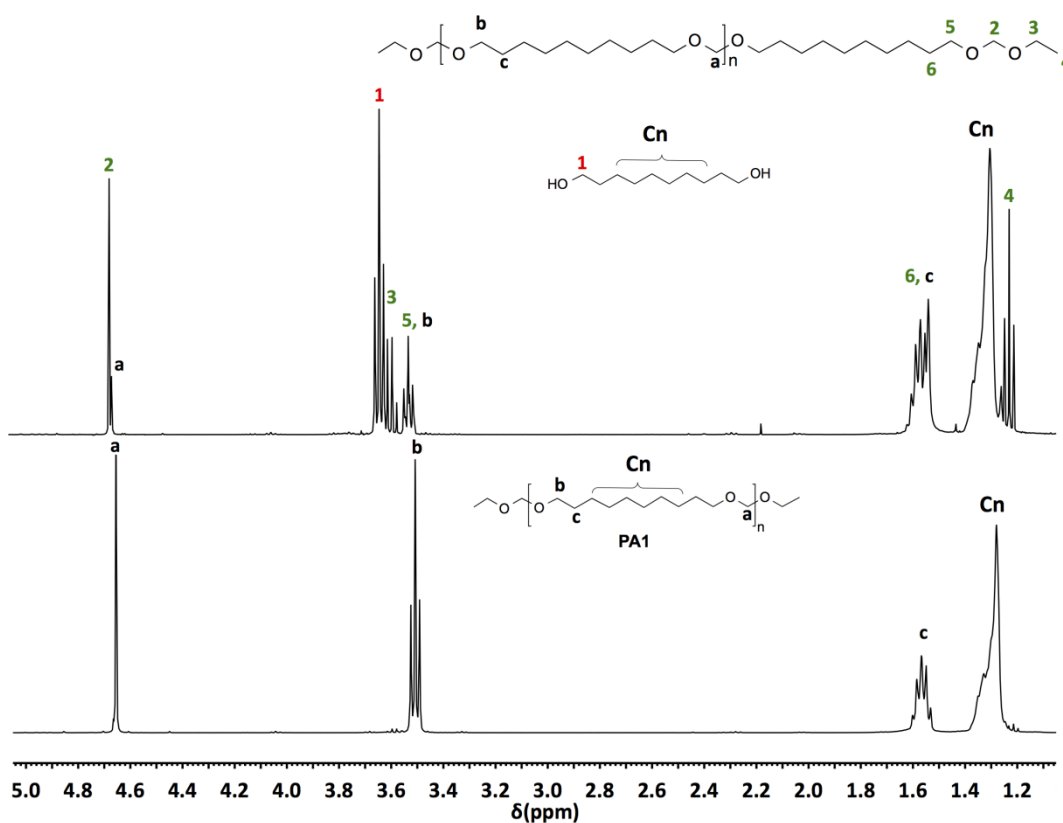


**Figure 7.** <sup>1</sup>H NMR spectrum of the hydrolysis products of **PA1** at 4 hours in 0.04 M HCl

## *Conclusion*

Heptanal was used for the first time to prepare biorenewable polyacetals. Heptanal is of special interest since it is a by-product of ricinoleic acid thermal cracking scarcely used in polymer chemistry. Synthetic protocols were developed to prepare new branched diols from this castor oil derivative. AMP was applied to linear and branched diols to prepare polyacetals and copolyacetals with number average molecular weight in the range 14000 to 27000 g mol<sup>-1</sup>. The optimization of the process using common acid catalyst under vacuum allowed the direct conversion of the diols to the polymers. Linear polyacetals and copolyacetal **PA1-5(3:1)** turn out to be semicrystalline materials of low melting points while branched polyacetals and copolyacetals were found to be liquid at room temperature. The polymers are thermally robust and the thermal stability seems to be lower for the sulfur containing ones. Polyacetals were hydrolytically degradable under slightly acidic media as showed by SEC measurements and no significant differences on the degradation pattern were observed among them. NMR studies showed that the polyacetals degrade down to parent diols. Thus, renewable and degradable polyacetals developed in this work meet the two criteria of sustainable materials.

## SUPPLEMENTARY INFORMATION

Synthesis and characterization data of diol monomers and model compounds. <sup>1</sup>H and <sup>13</sup>C NMR spectra of monomers, model compounds, polyacetals and copolyacetals. SEC data for the synthesis of PA3 from PA2. SEC data of hydrolytic degradation of PA1 and PA2.

## ACKNOWLEDGMENT

Financial support from the MINECO (Ministerio de Economía y Competitividad) (MAT2014-53652-R, MAT2017-8266) is gratefully acknowledged. G.L. acknowledges the Serra Húnter Programme (Generalitat de Catalunya). A. M. was supported by an FPI grant (BES-2015-072662) from MINECO.

## References

- [1] D.K. Schneiderman, M.A. Hillmyer, 50th Anniversary Perspective: There is a Great Future in Sustainable Polymers, *Macromolecules* 50 (2017) 3733-3749.
- [2] H. Mutlu, M.A.R. Meier, Castor oil as a renewable resource for the chemical industry, *Eur. J. Lipid Sci. Technol.* 112 (2010) 10–30.
- [3] B. Liu, S. Thayumanavan, Substituent effects on the pH sensitivity of acetals and ketals and their correlation with encapsulation stability in polymeric nanogels, *J. Am. Chem. Soc.* 139 (2017) 2306-2317.
- [4] S.E. Paramonov, E.M. Bachelder, T.T. Beaudette, S.M. Standley, C.C. Lee, J. Dashe, J.M.J. Fréchet, Fully acid-degradable biocompatible polyacetal microparticles for drug delivery, *Bioconjugate Chem.* 19 (2008) 911-919.
- [5] R. Tomlinson, M. Klee, S. Garrett, J. Heller, R. Duncan, S. Brocchini, Pendent chain functionalized polyacetals that display pH-dependent degradation: A platform for the development of novel polymer therapeutics, *Macromolecules* 35 (2002) 473-480.
- [6] S. Chatterjee, S. Ramakrishnan, Hyperbranched polyacetals with tunable degradation rates, *Macromolecules* 44 (2011) 4658-4664.
- [7] R.A. Shenoi, J.K. Jayaprakash, J.L. Hamilton, B.F.L. Lai, S. Horte, R.K. Kainthan, J.P. Varghese, K.G. Rajeev, M. Manoharan, J.N. Kizhakkedathu, Branched multifunctional polyether polyketals: Variation of ketal group structure enables unprecedented control over polymer degradation in solution and within cells, *J. Am. Chem. Soc.* 134 (2012) 14945-14957.

[8] S. Samanta, D.R. Bogdanowicz, H.H. Lu, J.T. Koberstein, Polyacetals: water soluble, pH-degradable polymers with extraordinary temperature response, *Macromolecules* 49 (2016) 1858-1854.

[9] H. Matsukizono, T. Endo, Reworkable polyhydroxyurethane films with reversible acetal networks obtained from multifunctional six-membered cyclic carbonates, *J. Am. Chem. Soc.* 140 (2018) 884-887.

[10] Martin, R.T.; Camargo, L.P.; Miller, S.; Marine degradable polymers. *Green. Chem.* 2014, 16, 1768-1773.

[11] S. Chilkali, F. Stempfle, S. Mecking, Long-Chain polyacetals from plant oils. *Macromol. Rapid Commun.* 33 (2012) 1126-1129.

[12] A.G. Pemba, J.A. Flores, S.A. Miller, Acetal metathesis polymerization (AMP): A method for synthesizing biorenewable polyacetals, *Green Chem.* 15 (2013) 325-329.

[13] B. S. Rajput, S. R. Gaikwad, S. K. Menon, S. H. Chikkali, Sustainable polyacetals from isohexides, *Green Chem.* 16 (2014) 3810-3818.

[14] B.S. Rajput, U. Chander, K. Arole, F. Stempfle, S. Menon, S. Mecking, S.H. Chikkali, Synthesis of renewable copolyacetals with tunable degradation, *Macromol. Chem. Phys.* 217 (2016) 1396-1410.

[15] A.G. Pemba, M. Rostagno, T.A. Lee, S.A. Miller, Cyclic and spirocyclic polyacetal ethers from lignin-based aromatics, *Polym. Chem.* 5 (2014) 3214-3221.

[16] M. Rostagno, E.J. Price, A.G. Pemba, I. Ghiriviga, K.A. Abboud, S.A. Miller, Sustainable polyacetals from erythritol and bioaromatics, *J. Appl. Polym. Sci.* 133 (2016) 44089-44100.

[17] G. Lligadas, J.C. Ronda, M. Galià, V. Cádiz, Oleic and undecylenic acids as renewable feedstocks in the synthesis of polyols and polyurethanes, *Polymers* (2010) 440–453.

[18] S. Bigot, M. Daghrir, A. Mhanna, G. Boni, S. Pourchet, L. Lecamp, L. Plasseraud, Undecylenic acid: A tunable bio-based synthon for materials applications, *Eur. Polym. J.* 74 (2016) 26-37.

[19] L. Ruiz, A. Aghmiz, A.M. Masdeu-Bultó, G. Lligadas, J.C.Ronda, M. Galià, V. Cádiz, Upgrading castor oil: from heptanal to non-isocyanate poly(amide-hydroxyurethane)s, *Polymer* 124 (2017) 226-234.

[20] R. González-Paz, C. Lluch, G. Lligadas, J.C. Ronda, M. Galià, V. Cádiz, A Green approach towards oleic- and undecylenic acid-derived polyurethanes, *J. Polym. Sci. Part A Polym. Chem.* 49 (2011) 2407-2416.

[21] O. Türünç, M.R.M. Meier, Fatty acid derived monomers and related polymers via thiol-ene (click)additions, *Macromol. Rapid Commun.* 31 (2010) 1822-1826.

[22] T. Lebarbé, L. Maisonneuve, T.H.N. Nguyen, B. Gadenne, C. Alfos, H. Cramail, Methyl 10-undecenoate as a raw material for the synthesis of renewable semi-crystalline polyesters and poly(ester amide)s, *Polym. Chem.* 3 (2012) 2842-2851.

[23] G. Lligadas, J.C.Ronda, M. Galià, V. Cádiz. Monomers and polymers from plant oils via click chemistry reactions, *J. Polym. Sci. Part A Polym. Chem.* 51 (2013) 2111-2124.

[24] J.A. Bisceglia, L.R. Orelli, Recent progress in the Horner- Wadsworth-Emmons reaction, *Curr. Org. Chem.* 19 (2015) 744-775.

[25] J.W. Chan, C.E. Hoyle, A.B. Lowe, M. Bowman, Nucleophile-Initiated Thiol-Michael Reactions: Effect of Organocatalyst, Thiol, and Ene, *Macromolecules* 43 (2010) 6381-6388.

[26] J.C.A. Flanagan, E.J. Kang, N.I. Strong, R.M. Waymouth, Catalytic dimerization of crotonates, *ACS Catal.* 5 (2015) 5328-5332.

[27] P. Ortmann, I. Heckler, S. Mecking, Physical properties and hydrolytic degradability of polyethylene-like polyacetals and polycarbonates, *Green Chem.* 16 (2014) 1816-1827.



Supplementary information for

# Linear and branched acetal polymers from castor oil via acetal metathesis polymerization

Adrian Moreno, Gerard Lligadas, Juan Carlos Ronda, Marina Galià and Virginia Cádiz  
Universitat Rovira i Virgili, Departament de Química Analítica I Química Orgànica,  
Laboratory of Sustainable Polymers, Marcel·lí Domingo 1, 43007 Tarragona, Spain

## Table of contents

1. Monomer synthesis and characterization data
  - 1.1 Synthesis of 11-((2-hydroxyethyl)thio)undecan-1-ol (**2**)
  - 1.2 Synthesis of 11-((2-hydroxyethyl)sulfonyl)undecan-1-ol (**3**)
  - 1.3 Synthesis of methyl 3-((3-methoxy-3-oxopropyl)thio)nonanoate
  - 1.4 Synthesis of 3-((3-hydroxypropyl)thio)nonan-1-ol (**4**)
  - 1.5 Synthesis of dimethyl 2-heptylidene-3-hexylpentandioate
  - 1.6 Synthesis of dimethyl 2-heptyl-3-hexylpentanedioate
  - 1.7 Synthesis of 2-heptyl-3-hexylpentane-1,5-diol (**5**)
  - 1.8 Synthesis of 3,5,16,18-tetraoxaicosane (decanediol bis-acetal)
  - 1.9 Synthesis of model compounds
    - 1.9.1. Synthesis of 2-(octylthio)ethan-1-ol
    - 1.9.2. General procedure for the transacetalization reaction.
    - 1.9.3. Synthesis of 9,11-dioxaoctadecane
    - 1.9.4. Synthesis of 12,14-dioxa-9,17-dithiapentacosane
    - 1.9.5. Synthesis of 12,14-dioxa-9-thiadocosane

## 2. Figures

Figure S1. <sup>1</sup>H NMR spectrum of **2**

Figure S2. <sup>13</sup>C NMR spectrum of **2**

Figure S3. <sup>1</sup>H NMR spectrum of **3**

Figure S4. <sup>13</sup>C NMR spectrum of **3**

Figure S5. <sup>1</sup>H NMR spectrum of methyl 3-((3-methoxy-3-oxopropyl)thio)nonanoate

Figure S6.  $^{13}\text{C}$  NMR spectrum of methyl 3-((3-methoxy-3-oxopropyl)thio)nonanoate

Figure S7.  $^1\text{H}$  NMR spectrum of **4**

Figure S8.  $^{13}\text{C}$  NMR spectrum of **4**

Figure S9.  $^1\text{H}$  NMR spectrum of dimethyl 2-heptylidene-3-hexylpentandioate isomer mixture and non conjugated product

Figure S10.  $^1\text{H}$  NMR spectrum of dimethyl 2-heptyl-3-hexylpentanedioate

Figure S11.  $^1\text{H}$  NMR spectrum of **5**

Figure S12.  $^{13}\text{C}$  NMR spectrum of **5**

Figure S13.  $^1\text{H}$  NMR spectrum of 3,5,16,18-tetraoxaicosane (decanediol bis-acetal)

Figure S14.  $^1\text{H}$  NMR spectrum of 2-(octylthio)ethan-1-ol

Figure S15.  $^{13}\text{C}$  NMR spectrum of 2-(octylthio)ethan-1-ol

Figure S16.  $^1\text{H}$  NMR spectrum of 9,11-dioxaoctadecane

Figure S17.  $^{13}\text{C}$  NMR spectrum of 9,11-dioxaoctadecane

Figure S18.  $^1\text{H}$  NMR spectrum of 12,14-dioxa-9,17-dithiapentacosane

Figure S19.  $^{13}\text{C}$  NMR spectrum of 12,14-dioxa-9,17-dithiapentacosane

Figure S20.  $^1\text{H}$  NMR spectrum of 12,14-dioxa-9-thiadocosane

Figure S21.  $^{13}\text{C}$  NMR spectrum of 12,14-dioxa-9-thiadocosane

Figure S22.  $^1\text{H}$  NMR spectrum of **PA1**

Figure S23.  $^{13}\text{C}$  NMR spectrum of **PA1**

Figure S24.  $^1\text{H}$  NMR spectrum of **PA2**

Figure S25.  $^{13}\text{C}$  NMR spectrum of **PA2**

Figure S26.  $^1\text{H}$  NMR spectrum of **PA3**

Figure S27.  $^{13}\text{C}$  NMR spectrum of **PA3**

Figure S28.  $^1\text{H}$  NMR spectrum of **PA4**

Figure S29.  $^{13}\text{C}$  NMR spectrum of **PA4**

Figure S30.  $^1\text{H}$  NMR spectrum of **PA5**

Figure S31.  $^{13}\text{C}$  NMR spectrum of **PA5**

Figure S32.  $^1\text{H}$  NMR spectrum of **PA1-4**

Figure S33.  $^{13}\text{C}$  NMR spectrum of **PA1-4**

Figure S34.  $^1\text{H}$  NMR spectrum of **PA1-5 1:1**

Figure S35.  $^{13}\text{C}$  NMR spectrum of **PA1-5 1:1**

Figure S36.  $^1\text{H}$  NMR spectrum of **PA2-5**

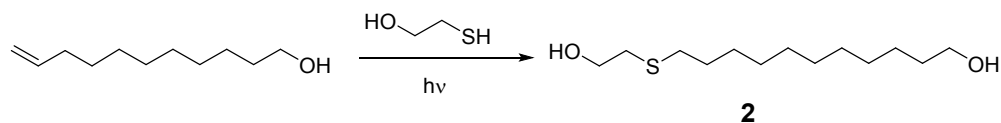
Figure S37.  $^{13}\text{C}$  NMR spectrum of **PA2-5**

Figure S38. GPC traces of **PA2** and **PA3**

Figure S39. GPC degradation traces of **PA1** and **PA2**

## 1. Monomer synthesis and characterization data

### 1.1 Synthesis of 11-((2-hydroxyethyl)thio)undecan-1-ol (2)

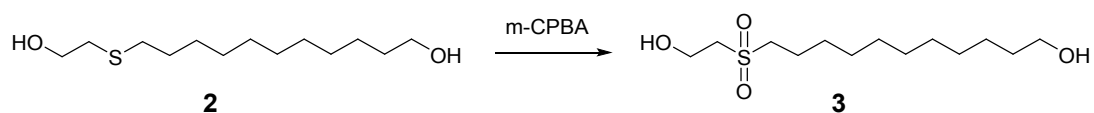


A 25 ml round-bottom flask was charged with 6.0 g (35.2 mmol) of 10-undecen-1-ol and 6.2 ml of 2-mercaptoethanol (88 mmol). The reaction was carried out at room temperature by irradiation with two 9W UV-lamps ( $\lambda=365$  nm). After 45 minutes a white solid was formed. The completion of reaction was confirmed by <sup>1</sup>H-NMR spectroscopy through the complete disappearance of the C-C double bond signals. The crude mixture was crystallized from diethyl ether, filtered and washed with cold diethyl ether and dried under vacuum to afford a powder white solid (93% yield).

<sup>1</sup>H NMR [CDCl<sub>3</sub>, TMS,  $\delta$  (ppm)] (Figure S1): 3.71 (t, HO-CH<sub>2</sub>-CH<sub>2</sub>-S-, 2H), 3.63 (t, HO-CH<sub>2</sub>-, 2H), 2.72 (t, HO-CH<sub>2</sub>-CH<sub>2</sub>-S-, 2H), 2.51 (t, CH<sub>2</sub>-S-, 2H), 1.57 (m, HO-CH<sub>2</sub>-CH<sub>2</sub>-, -CH<sub>2</sub>-CH<sub>2</sub>-S-, 4H), 1.37 -1.27 (m, aliphatic chain, 14 H).

<sup>13</sup>C NMR [CDCl<sub>3</sub>, TMS,  $\delta$  (ppm)] (Figure S2): 63.0, 60.1, 35.3, 32.3, 31.6, 29.7, 29.5, 29.4, 29.3, 29.2, 29.1, 28.1, 25.7

### 1.2 Synthesis of 11-((2-hydroxyethyl)sulfonyl)undecan-1-ol (3)



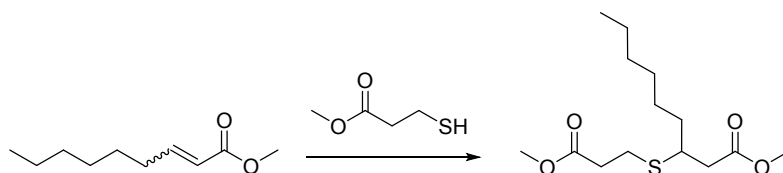
14 g (57 mmol) of mCPBA was dissolved in 50 mL of THF in a 100 round-bottom flask, followed by the addition 7 g (28.17 mmol) of 2. The reaction mixture was carried out at room temperature for 2 hours. The crude reaction was extracted several times with a solution of 5% Na<sub>2</sub>S<sub>2</sub>O<sub>5</sub> followed by 5% NaHCO<sub>3</sub> solution and finally brine. The collected organic phases were dried over MgSO<sub>4</sub> and concentrated. The crude product was

crystallized from hexane:diethyl ether (9/1), filtered, washed with cold diethyl ether and dried under vacuum to afford a powder white solid (97% yield).

$^1\text{H}$  NMR [ $\text{CDCl}_3$ , TMS,  $\delta$  (ppm)] (Figure S3): 4.15 (t, HO- $\text{CH}_2$ - $\text{CH}_2$ - $\text{SO}_2$ -, 2H), 3.65 (t, HO- $\text{CH}_2$ -, 2H), 3.21 (t, HO- $\text{CH}_2$ - $\text{CH}_2$ - $\text{SO}_2$ -, 2H), 3.11 (t,  $\text{CH}_2$ - $\text{SO}_2$ -, 2H), 2.58 (t, OH, 1H), 1.78 (m, - $\text{CH}_2$ - $\text{CH}_2$ - $\text{SO}_2$ -, 2H), 1.58 (m, OH- $\text{CH}_2$ - $\text{CH}_2$ -, 2H), 1.44-1.28 (m, aliphatic chain, 14 H).

$^{13}\text{C}$  NMR [ $\text{CDCl}_3$ , TMS,  $\delta$  (ppm)] (Figure S4): 63.0, 56.4, 54.7, 54.6, 32.7, 29.4, 29.3, 29.1, 28.9, 28.8, 28.4, 25.7, 21.7

### 1.3 Synthesis of methyl 3-((3-methoxy-3-oxopropyl)thio)nonanoate

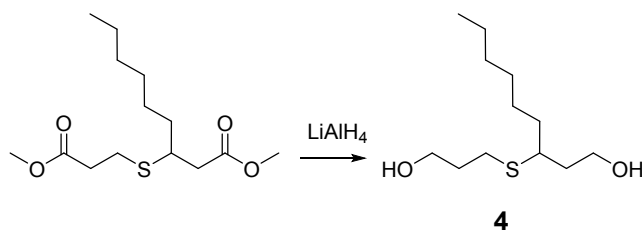


To a 250 ml round-bottom flask were added 10.0 g (58.78 mmol) of methyl 2-nonenoate and 6.50 ml of methyl 3-mercaptopropionate (58.73 mmol). The flask was placed in an ice/water bath to keep the reaction mixture between 0-5 °C and subsequently 0.18 ml (1.17 mmol) of DBU was added dropwise during 20 minutes. The reaction mixture was stirred 1 hour and 30 ml of ethyl ether was added. After that, the crude reaction was washed three times with an aqueous acid solution (10% of HCl) and finally with brine. The resulting organic phase was dried over  $\text{MgSO}_4$  and the solvent was removed under reduced pressure to afford a yellow oil. The obtained crude product was purified by column chromatography using hexane:ethyl acetate (7:3) as eluent, to afford the pure compound as yellow pale oil (88% yield).

$^1\text{H}$  NMR [ $\text{CDCl}_3$ , TMS,  $\delta$  (ppm)] (Figure S5): 3.68 (s, - $\text{OCH}_3$ , 6H), 3.03 (m, -S- $\text{CH}$ -, 1H), 2.78 (t, -S- $\text{CH}_2$ -, 2H), 2.57 (dt, - $\text{CH}_2$ -CO-, 2H), 1.57 (m, S-CH- $\text{CH}_2$ - $(\text{CH}_2)_4$ , 2H), 1.43-1.25 (m, - $(\text{CH}_2)_4$ , aliphatic chain, 8H), 0.87 (t,  $\text{CH}_3$ , 3H).

$^{13}\text{C}$  NMR [ $\text{CDCl}_3$ , TMS,  $\delta$  (ppm)] (Figure S6): 172.4, 172.2, 51.9, 51.8, 42.2, 40.9, 35.2, 34.8, 31.8, 29.2, 26.9, 25.8, 22.7, 14.2.

#### 1.4 Synthesis of 3-((3-hydroxypropyl)thio)nonan-1-ol (4)

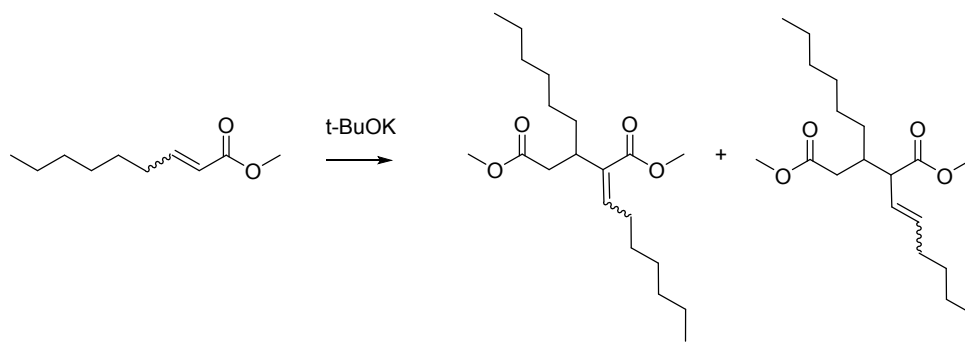


To a 500 ml round-bottom two necked flask, 3.92 g of  $\text{LiAlH}_4$  (0.10 mol) and 200 ml of anhydrous THF were mixed under argon atmosphere. Methyl 3-((3-methoxy-3-oxopropyl)thio)nonanoate (20 g, 68.8 mmol) was added using an addition funnel during 20 minutes. The reaction mixture was stirred at room temperature for 4 hours. The excess of  $\text{LiAlH}_4$  was removed by adding dropwise 100 ml ethyl acetate followed by the addition of 50 ml of 10%  $\text{H}_2\text{SO}_4$  aqueous solution and the phases were separated. The aqueous phase was washed three times with diethyl ether. The combined organic phases were washed with aqueous basic solution (10%  $\text{NaHCO}_3$ ) and brine. Finally the organic layer was dried over  $\text{MgSO}_4$ , filtered and the solvent was removed under reduced pressure to obtain a colorless oil. The obtained product was purified by column chromatography using hexane:ethyl acetate (10/1) as eluent, to afford pure compound as a colorless viscous oil (85% yield).

$^1\text{H}$  NMR [ $\text{CDCl}_3$ , TMS,  $\delta$  (ppm)] (Figure SI.7): 3.85 (m,  $\text{HO}-\underline{\text{CH}_2}-\text{CH}_2-\text{CH}$ , 2H), 3.76 (m,  $\text{HO}-\underline{\text{CH}_2}$ , 2H), 2.77 (m,  $-\text{S}-\underline{\text{CH}}-$ , 1H), 2.65 (dt,  $-\text{S}-\underline{\text{CH}_2}-$ , 2H), 2.51 (m,  $\text{OH}$ , 1H), 1.85 (m,  $\text{HO}-\text{CH}_2-\underline{\text{CH}_2}$ ,  $\text{HO}-\text{CH}_2-\underline{\text{CH}_2}-\text{CH}$ , 3H), 1.70 (m,  $\text{HO}-\text{CH}_2-\underline{\text{CH}_2}-\text{CH}$ , 1H), 1.54 (m,  $\text{S}-\text{CH}-\underline{\text{CH}_2}-(\text{CH}_2)_4$ , 2H), 1.43-1.34 (m,  $-(\underline{\text{CH}_2})_4-\text{CH}_3$ , 8H), 0.89 (t,  $\underline{\text{CH}_3}$ , 3H).

$^{13}\text{C}$  NMR [ $\text{CDCl}_3$ , TMS,  $\delta$  (ppm)] (Figure SI.8): 61.9, 60.9, 43.4, 37.2, 35.7, 32.3, 31.95, 29.4, 27.0, 26.9, 22.8, 14.2.

## 1.5 Synthesis of dimethyl 2-heptylidene-3-hexylpentandioate



To a 100 ml round-bottom Schlenk 0.76 g of potassium *tert*-butoxide (6.78 mmol) and 30 ml of anhydrous THF were added. To this stirred solution, 8 g (46.99 mmol) of methyl nonenoate was added dropwise during 30 minutes. The resulting orange solution was stirred at room temperature for 6 hours. The completion of the reaction was confirmed by  $^1\text{H-NMR}$  spectroscopy by the disappearance of the double bond signal of starting material and the appearance of signals attributed to the mixture of *E*- and *Z*-isomers and the double bond isomers side products. The reaction was quenched with 0.3 ml of hydrochloric acid (37%). The solvent was eliminated under reduced pressure and 50 ml of diethyl ether was added to the resulting crude product. The mixture was washed with water and brine, dried with  $\text{MgSO}_4$ , filtered and evaporated leading the crude a mixture of isomers as a yellow oil (87 % yield).

$^1\text{H NMR}$  [ $\text{CDCl}_3$ , TMS,  $\delta$  (ppm)] (Figure S9):

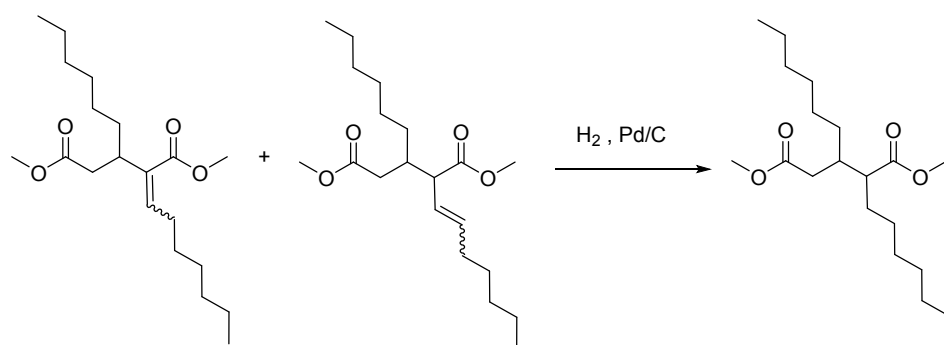
(*E*-isomer): 6.79, (t, 1H, =CH, 1H), 3.72 (s, OCH<sub>3</sub>, 3H), 3.62 (s, OCH<sub>3</sub>, 3H), 3.11 (m, -CH-(CH<sub>2</sub>)<sub>5</sub>, 1H), 2.71 (dd, CO-CH<sub>2</sub>, 1H), 2.58 (dd, 1H, CO-CH<sub>2</sub>, 2H), 2.23 (dt, =CH-CH<sub>2</sub>, 2H), 1.67 (m, CO-CH<sub>2</sub>-CH-CH<sub>2</sub>, 2H), 1.45-1.10 (m, aliphatic chain, 16H), 0.88 (t, CH<sub>3</sub>, 3H), 0.85 (t, CH<sub>3</sub>, 3H).

(*Z*-isomer): 5.83 (t, 1H, =CH, 1H), 3.74 (s, OCH<sub>3</sub>, 3H), 3.64 (s, OCH<sub>3</sub>, 3H), 2.82, (m, -CH-(CH<sub>2</sub>)<sub>5</sub>, 1H), 2.55 (dd, CO-CH<sub>2</sub>, 1H), 2.45 (dd, CO-CH<sub>2</sub>, 1H), 2.27 (dt, =CH-CH<sub>2</sub>, 2H), 1.65 (m, CO-CH<sub>2</sub>-CH-CH<sub>2</sub>, 2H), 1.44-1.15 (m, aliphatic chain, 16H), 0.87 (t, CH<sub>3</sub>, 3H), 0.86 (t, CH<sub>3</sub>, 3H).

Dimethyl 2-(hept-1-en-1-yl)-3-hexylpentanedioate

$^1\text{H-NMR}$  ( $\text{CDCl}_3$ , 400 MHz):  $\delta$  5.50-5.58 (m, =CH, 1H), 5.33-5.41 (m, =CH, 1H), 3.67 (s,  $\text{OCH}_3$ , 3H), 3.65 (s, 3H,  $\text{OCH}_3$ ), 3.00 (m,  $\text{CH-CH=CH}$ , 1H), 2.41 (dd,  $\text{CO-CH}_2$ , 2H), 2.35-2.27 (m,  $-\text{CH}(\text{CH}_2)_5\text{CH}_3$ , 1H), 2.00 (dt, = $\text{CHCH}_2-$ , 2H), 1.38-1.31 (m, aliphatic chain, 14H), 0.87 (t,  $\text{CH}_3$ , 6H).

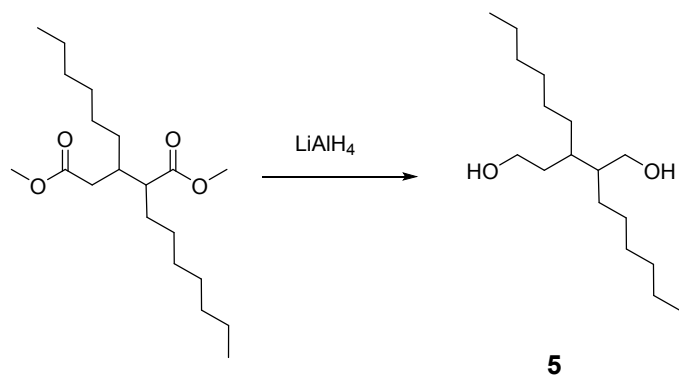
### 1.6 Synthesis of dimethyl 2-heptyl-3-hexylpentanedioate



To a 100 ml round-bottom Schlenk, 10 g of dimethyl 2-heptylidene-3-hexylpentanedioate crude mixture synthesis (29.4 mmol) and 50 ml of anhydrous methanol were added under argon atmosphere followed by the addition of 1 g of palladium on carbon (10% wt). The reaction mixture was stirred under argon atmosphere for 5 minutes, then the argon flow was substituted by hydrogen flow for 3 minutes. After that, a balloon filled with hydrogen was placed and the reaction mixture was stirred at room temperature for 5 hours. The crude reaction was filtered over celite and evaporated, affording a yellow oil (91% yield).

$^1\text{H NMR}$  [ $\text{CDCl}_3$ , TMS,  $\delta$  (ppm)] (Figure S10): 3.66 (s,  $\text{OCH}_3$ , 6H), 2.47 (m,  $\text{CH}(\text{CH}_2)_5\text{-CH}_3$ , 1H), 2.40 (dd,  $\text{CO-CH}_2$ , 1H), 2.27 (dd,  $\text{CO-CH}_2$ , 1H), 2.15 (m,  $\text{CO-CH}(\text{CH}_2)_6\text{-CH}_3$ , 1H), 1.63 (m,  $\text{CH}_2-(\text{CH}_2)_5\text{-CH}_3$ , 2H), 1.37-1.20 (m, aliphatic chain, 18H), 0.87 (t,  $\text{CH}_3$ , 6H).

### 1.7 Synthesis of 2-heptyl-3-hexylpentane-1,5-diol (5)

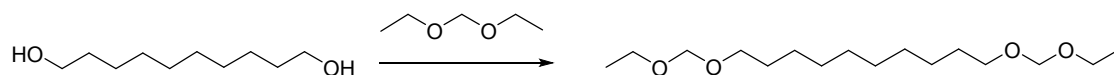


To a 250 ml round-bottom two necked flask, 2 g of LiAlH<sub>4</sub> (52.90 mmol) and 100 ml of anhydrous THF were added under argon atmosphere. Dimethyl 2-heptyl-3-hexylpentanedioate (SI.3) (12 g, 35.5 mmol) was added using an addition funnel during 10 minutes. The reaction mixture was stirred at room temperature for 6 hours. The excess of LiAlH<sub>4</sub> was removed by adding dropwise 100 ml ethyl acetate followed by the addition of 50 ml of 10% H<sub>2</sub>SO<sub>4</sub> aqueous solution and the phases were separated. The aqueous phase was washed three times with diethyl ether. The combined organic phase was washed with aqueous basic solution (10% NaHCO<sub>3</sub>) and brine. Finally the organic layer was dried over MgSO<sub>4</sub>, filtered and the solvent was removed under reduced pressure to obtain an orange oil. The obtained product was purified by column chromatography using hexane:ethyl acetate (8:2) as eluent, to afford pure 5 as colorless viscous oil (90% yield).

<sup>1</sup>H NMR [CDCl<sub>3</sub>, TMS, δ (ppm)] (Figure SI.11): 3.73 (dd, HO-CH<sub>2</sub>, 1H), 3.58 (dt, OH-CH<sub>2</sub>-CH<sub>2</sub>, 2H), 3.52 (dd, OH-CH<sub>2</sub>, 1H), 1.74-1.46 (m, HO-CH<sub>2</sub>-CH<sub>2</sub>-CH, HO-CH<sub>2</sub>-CH, 4H), 1.38-1.16 (m, aliphatic chain, 22H), 0.88 (t, CH<sub>3</sub>, 6H).

<sup>13</sup>C NMR [CDCl<sub>3</sub>, TMS, δ (ppm)] (Figure SI.12): 63.7, 63.6, 62.0, 61.5, 42.7, 42.5, 34.4, 34.3, 34.0, 32.7, 32.2-26.8 (20C), 22.7, 22.6, 12.8, 14.1

## 1.8 Synthesis of 3,5,16,18-tetraoxaicosane (decandiol bis-acetal)

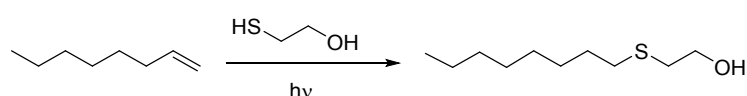


5g (24.7 mmol) of **1** and 100 mL of THF were added to a 250 mL round-bottom flask under argon atmosphere. *p*-TSA (2.47 mmol, 0.46 g) and DEM (20 mL) were added to the reaction mixture. The reaction mixture was stirred overnight at room temperature. 0.15 mL of a solution of NH<sub>4</sub>OH, were added to quench the acid catalyst, followed by several extractions with brine. The resulting organic phase was dried over MgSO<sub>4</sub> and the solvent was removed under reduced pressure. The crude was purified by flash chromatography using hexane:ethyl acetate (9/1) as eluent to afford the corresponding bis-acetal as a pale yellow oil (85 % yield).

<sup>1</sup>H NMR [CDCl<sub>3</sub>, TMS, δ (ppm)] (Figure S13): 4.66 (s, O-CH<sub>2</sub>-O, 4H), 3.59 (q, O-CH<sub>2</sub>-CH<sub>3</sub>, 4H), 3.51 (t, O-CH<sub>2</sub>, 4H), 1.57 (m, O-CH<sub>2</sub>-CH<sub>2</sub>, 4H), 1.28 (m, aliphatic chain, 12H), 1.23 (t, O-CH<sub>2</sub>-CH<sub>3</sub>, 6H).

## 1.9 Synthesis of model compounds

### 1.9.1 Synthesis of 2-(octylthio)ethan-1-ol



A 25 ml round-bottom flask was charged with 1.0 g (8.9 mmol) of 1-octene and 1.56 ml of 2-mercaptoethanol (22.25 mmol). The reaction was carried out at room temperature by irradiation with two 9W UV-lamps (λ=365 nm). After 20 minutes the completion of reaction was confirmed by <sup>1</sup>H NMR spectroscopy through the absence of the double bond signals. The crude mixture was placed in a funnel and 30 ml of ethyl acetate was added, the resulting organic layer was washed several times with water and brine. The obtained organic layer was dried over MgSO<sub>4</sub>, filtered and the solvent was eliminated at reduced

pressure to lead a colorless oil. Finally, the final product was distilled under vacuum (bp 60 °C at 0.15 mmHg) to afford pure compound as colorless oil. (80% yield)

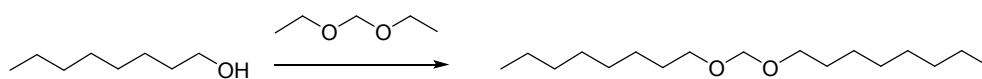
$^1\text{H}$  NMR [ $\text{CDCl}_3$ , TMS,  $\delta$  (ppm)] (Figure S14): 3.71 (t, HO- $\text{CH}_2$ , 2H), 2.72 (t, S- $\text{CH}_2$ - $\text{CH}_2$ -OH, 2H), 2.54 (t,  $\text{CH}_2$ -S- $\text{CH}_2$ - $\text{CH}_2$ -OH, 2H), 1.58 (m, S- $\text{CH}_2$ - $\text{CH}_2$ , 2H), 1.36-1.17 (m, aliphatic chain, 10H), 0.87 (t,  $\text{CH}_3$ , 3H).

$^{13}\text{C}$  NMR [ $\text{CDCl}_3$ , TMS,  $\delta$  (ppm)] (Figure S15): 60.2, 35.4, 31.8, 31.5, 30.9, 29.81, 28.8, 28.5, 22.6, 14.0.

### 1.9.2 General procedure for the transacetalization reaction.

To a 50 ml round-bottom flame dried Schlenk, the corresponding hydroxyl compound (1 mmol), *p*-TSA (0.015 mmol) and DEM (5.8 mmol) were added under argon flow. The reaction mixture was heated at 80 °C for 30 minutes. During the next 2 hours, a 1 minute argon flow was applied each 30 minutes. Then the reaction temperature was increased to 90 °C and vacuum was applied each 15 minutes during 1 h. The reaction mixture was allowed to cool and 0.5 ml of NaOH (1M) was added to quench the catalyst. Finally, the reaction mixture was placed in a funnel and extracted three times with an aqueous acid solution (10% HCl) and brine.

### 1.9.3 Synthesis of 9,10-dioxaoctadecane

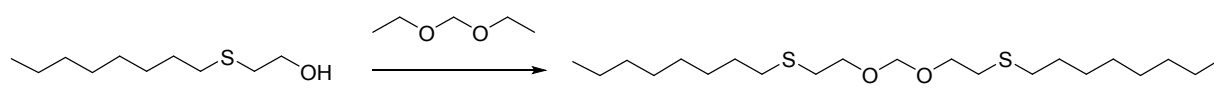


1-octanol (2.0 g, 15.32 mmol), *p*-TSA (43 mg, 2.29 mmol) and DEM (11.1 ml, 88.85 mmol) were used. The crude product was purified by a fractionated distillation (bp 77°C at 0.15 mmHg) to afford pure compound as colorless oil. (87% yield).

$^1\text{H}$  NMR [ $\text{CDCl}_3$ , TMS,  $\delta$  (ppm)] (Figure S16): 4.66 (s, O- $\text{CH}_2$ -O, 2H), 3.52 (t, O- $\text{CH}_2$ - $\text{CH}_2$ , 4H), 1.58 (m, O- $\text{CH}_2$ - $\text{CH}_2$ , 4H), 1.27 (m, aliphatic chain, 20H), 0.88 (t,  $\text{CH}_3$ , 6H).

$^{13}\text{C}$  NMR [ $\text{CDCl}_3$ , TMS,  $\delta$  (ppm)] (Figure S17): 95.2, 67.8, 31.8, 29.7, 29.4, 29.2, 26.2, 22.6, 14.0.

#### 1.9.4 Synthesis of 12,14-dioxa-9,17-dithiapentacosane

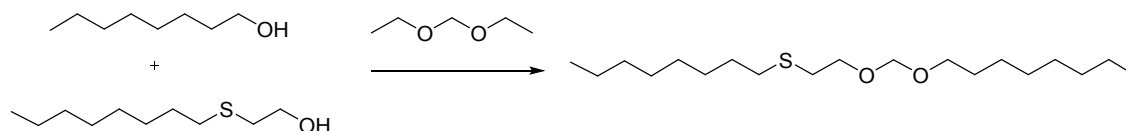


2-(octylthio)ethan-1-ol (2.0 g, 10.68 mmol), *p*-TSA (28 mg, 0.15 mmol) and DEM (7.6 ml, 61.9 mmol) were used. The crude product was purified by a fractionated distillation (bp 110 °C at 0.15 mmHg) to afford pure compound as colorless oil (87% yield).

$^1\text{H}$  NMR [ $\text{CDCl}_3$ , TMS,  $\delta$  (ppm)] (Figure S18): 4.72 (s, O- $\text{CH}_2$ -O, 2H), 3.72 (t, O- $\text{CH}_2$ - $\text{CH}_2$ -S, 4H), 2.73 (t, O- $\text{CH}_2$ - $\text{CH}_2$ -S, 4H), 2.55 (t, O- $\text{CH}_2$ - $\text{CH}_2$ -S- $\text{CH}_2$ , 4H), 1.58 (O- $\text{CH}_2$ - $\text{CH}_2$ -S- $\text{CH}_2$ - $\text{CH}_2$ , 4H), 1.36-1.27 (m, aliphatic chain, 20H), 0.88 (t,  $\text{CH}_3$ , 6H).

$^{13}\text{C}$  NMR [ $\text{CDCl}_3$ , TMS,  $\delta$  (ppm)] (Figure S19): 95.3, 67.4, 32.6, 31.8, 29.7, 29.2, 29.1, 29.0, 28.8, 22.6, 14.0.

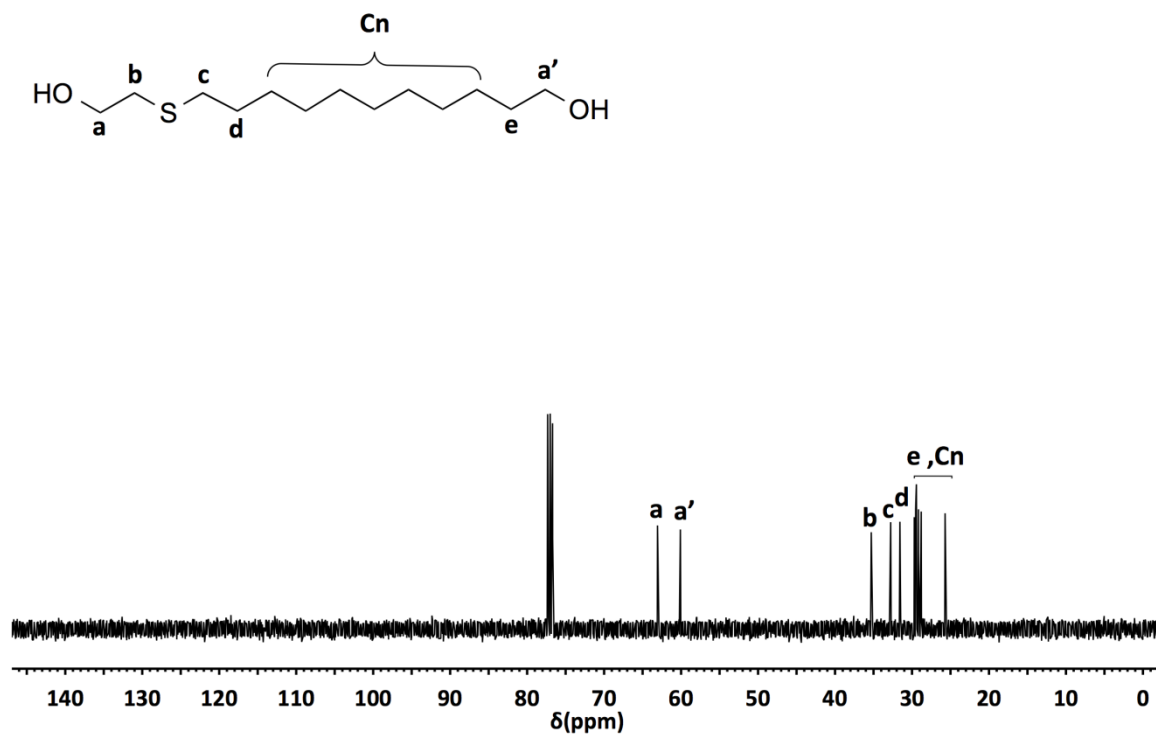
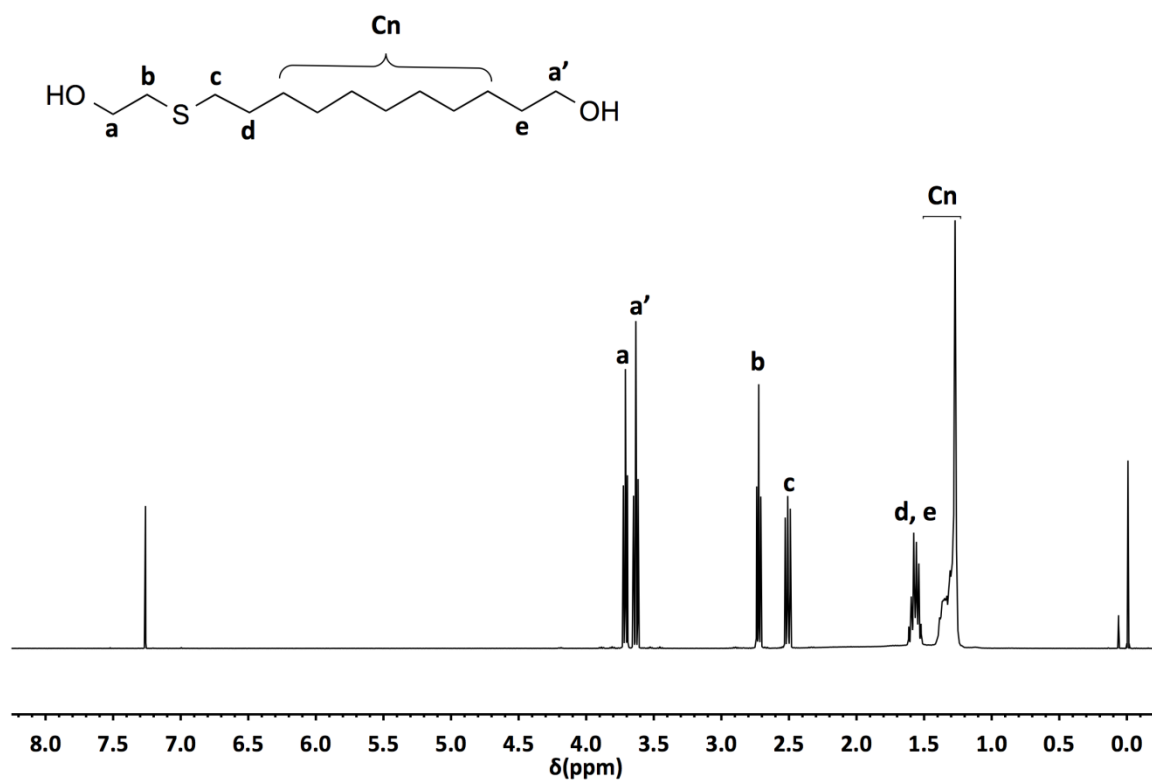
#### 1.9.5 Synthesis of 12,14-dioxa-9-thiadocosane



1-octanol (1.0 g, 7.66 mmol), 2-(octylthio)ethan-1-ol (1.0 g, 5.24 mmol), *p*-TSA (34 mg, 0.184 mmol) and DEM (9.2 ml, 73.8 mmol) were used. The crude product was purified by a fractionated distillation (bp 110 °C at 0.15 mmHg) to afford pure compound as colorless oil. (87% yield).

$^1\text{H}$  NMR [ $\text{CDCl}_3$ , TMS,  $\delta$  (ppm)] (Figure S20): 4.69 (s, O- $\text{CH}_2$ -O, 2H), 3.71 (q, O- $\text{CH}_2$ - $\text{CH}_2$ -S, 2H), 3.52 (q, O- $\text{CH}_2$ - $\text{CH}_2$ , 2H), 2.71 (t, O- $\text{CH}_2$ - $\text{CH}_2$ -S, 2H), 2.53 (t, O- $\text{CH}_2$ - $\text{CH}_2$ -S- $\text{CH}_2$ , 2H), 1.56 (m, O- $\text{CH}_2$ - $\text{CH}_2$ -S- $\text{CH}_2$ - $\text{CH}_2$ , O- $\text{CH}_2$ - $\text{CH}_2$ , 4H), 1.37-1.27 (m, aliphatic chain, 20H), 0.86 (t,  $\text{CH}_3$ , 6H).

$^{13}\text{C}$  NMR [ $\text{CDCl}_3$ , TMS,  $\delta$  (ppm)] (Figure S21): 95.3, 68.0, 67.2, 32.5, 32.4, 31.82, 31.8, 29.7, 29.7, 29.4, 29.2, 29.2, 29.2, 29.1, 28.8, 26.2, 22.6, 14.1.



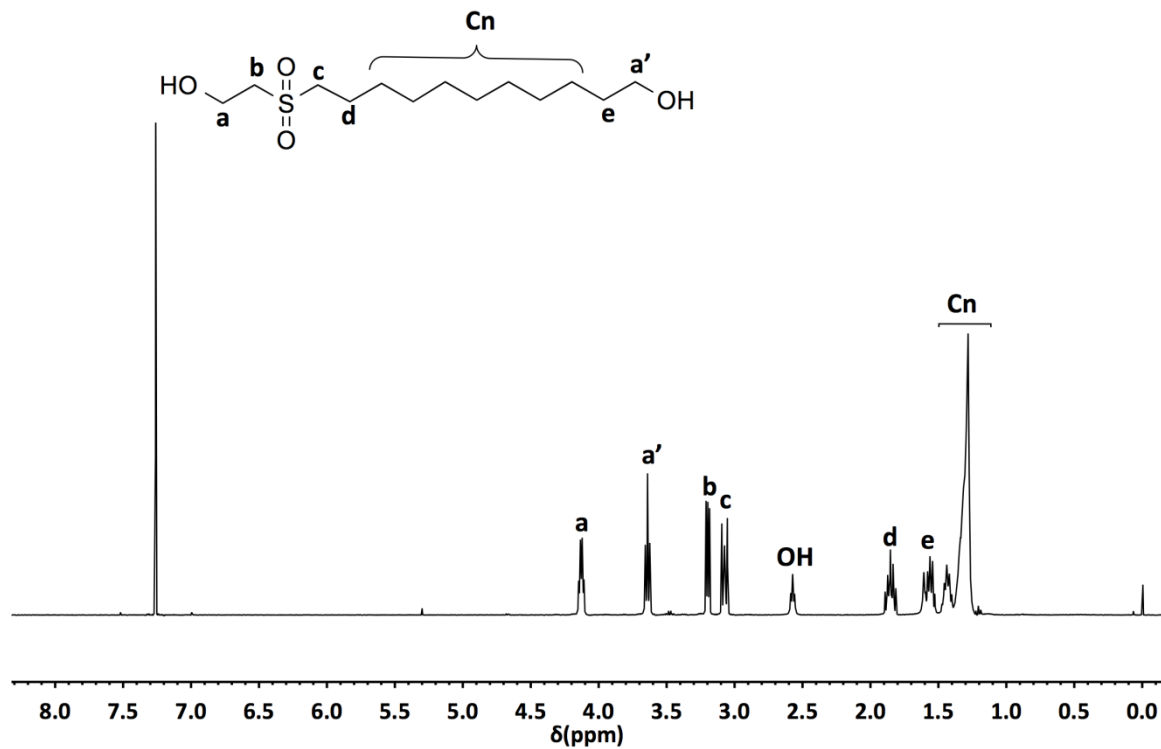


Figure S3.  $^1\text{H}$ NMR spectrum of **3** ( $\delta$  (ppm),  $\text{CDCl}_3$ )

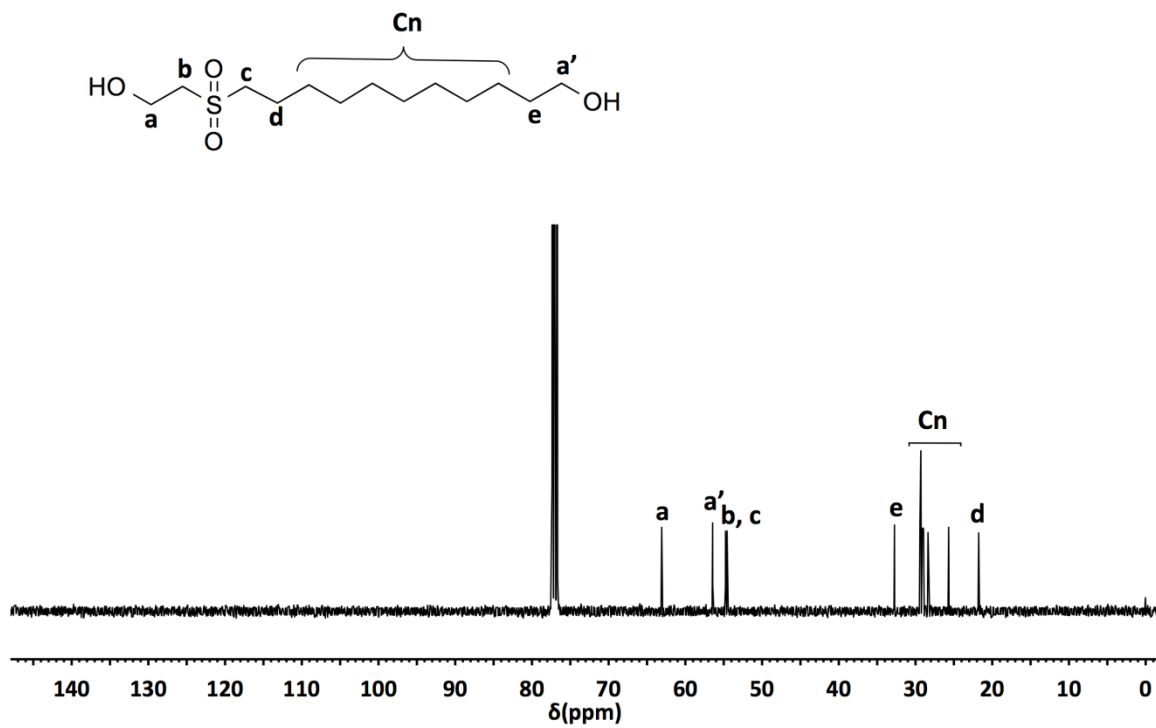


Figure S4.  $^{13}\text{C}$  NMR spectrum of **3** ( $\delta$  (ppm),  $\text{CDCl}_3$ )

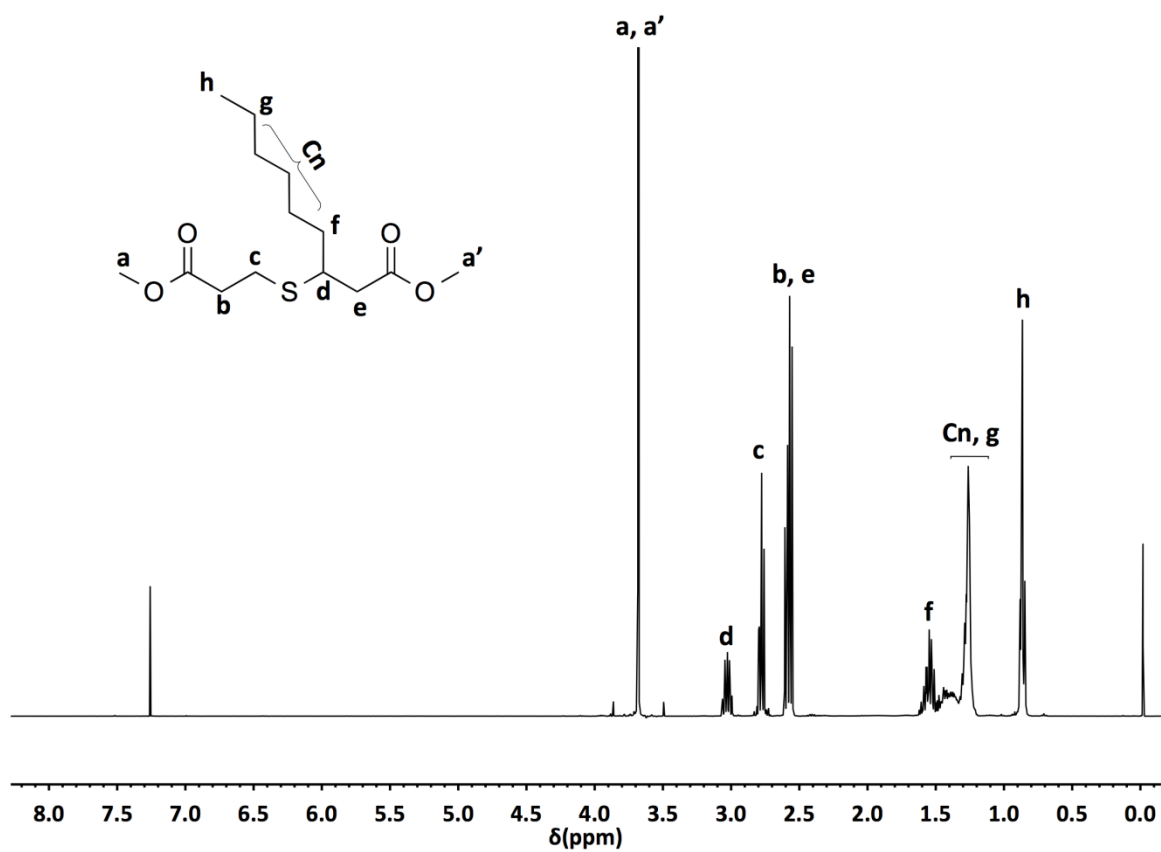


Figure S5.  $^1\text{H}$  NMR spectrum of Methyl 3-((3-methoxy-3-oxopropyl)thio)nonanoate ( $\delta$  (ppm),  $\text{CDCl}_3$ )

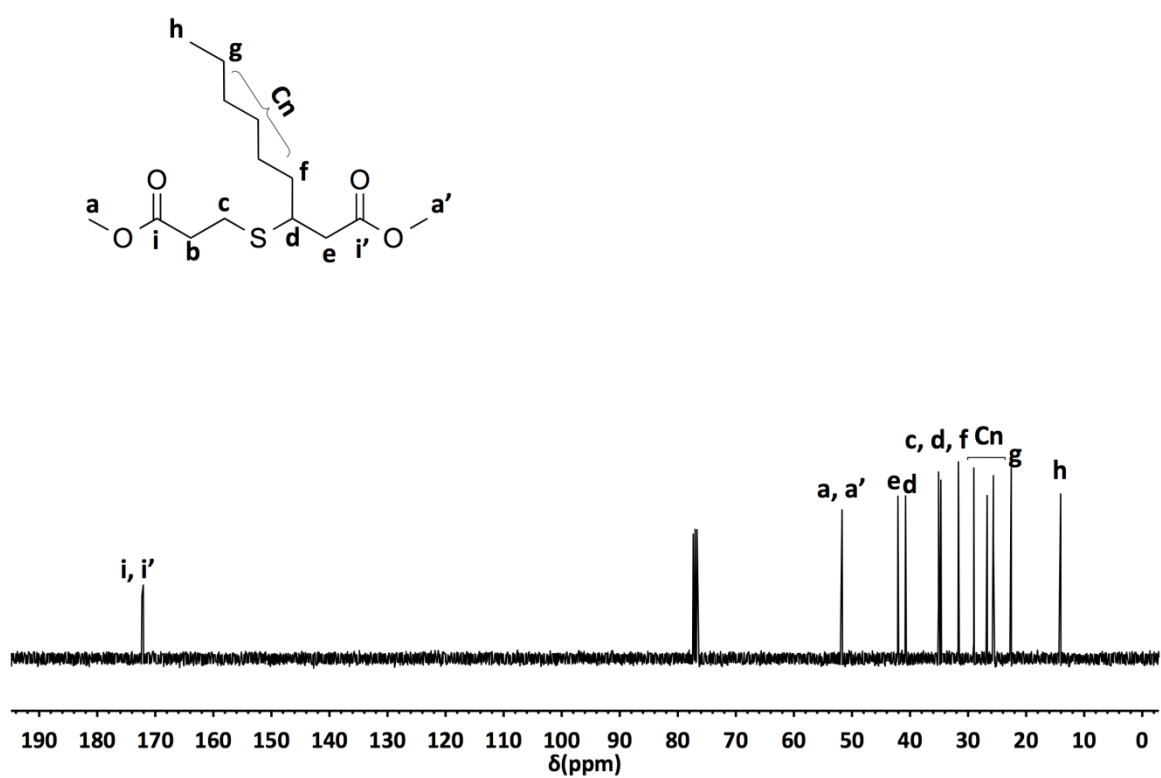


Figure S6.  $^{13}\text{C}$  NMR spectrum of Methyl 3-((3-methoxy-3-oxopropyl)thio)nonanoate ( $\delta$  (ppm),  $\text{CDCl}_3$ )

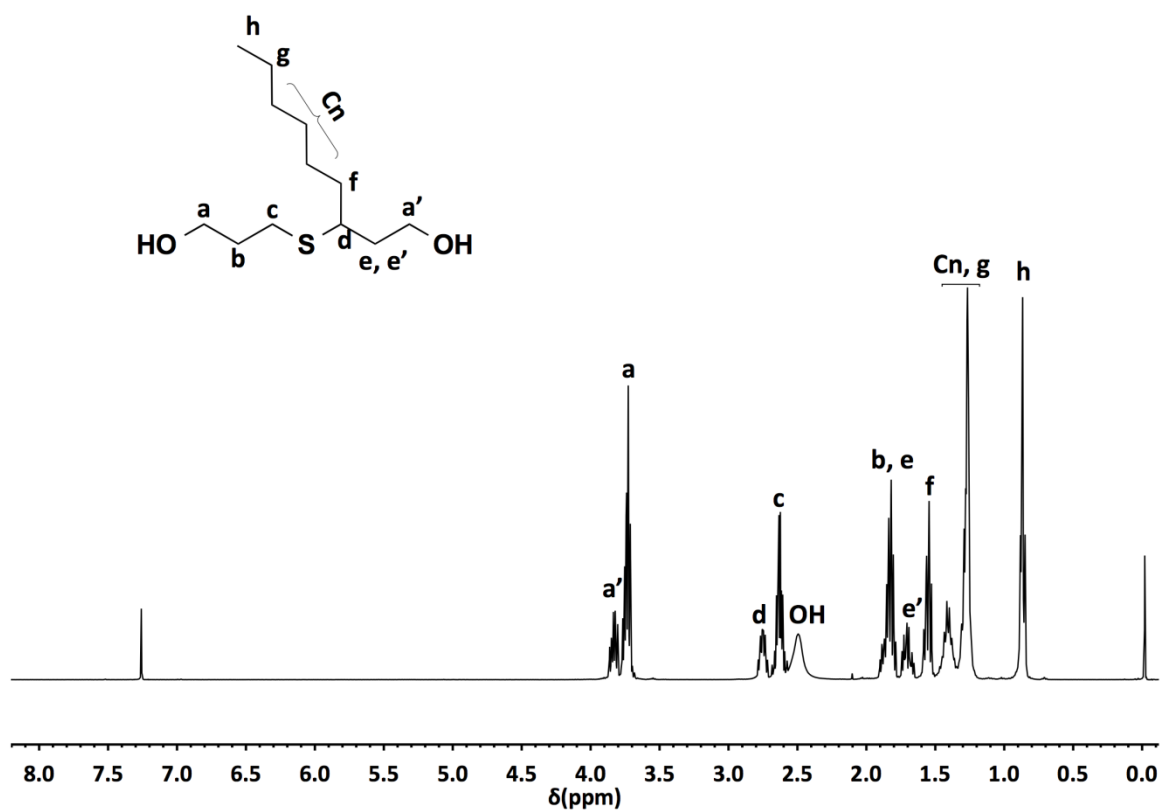


Figure S7. <sup>1</sup>H NMR spectrum of 4 (δ (ppm), CDCl<sub>3</sub>)

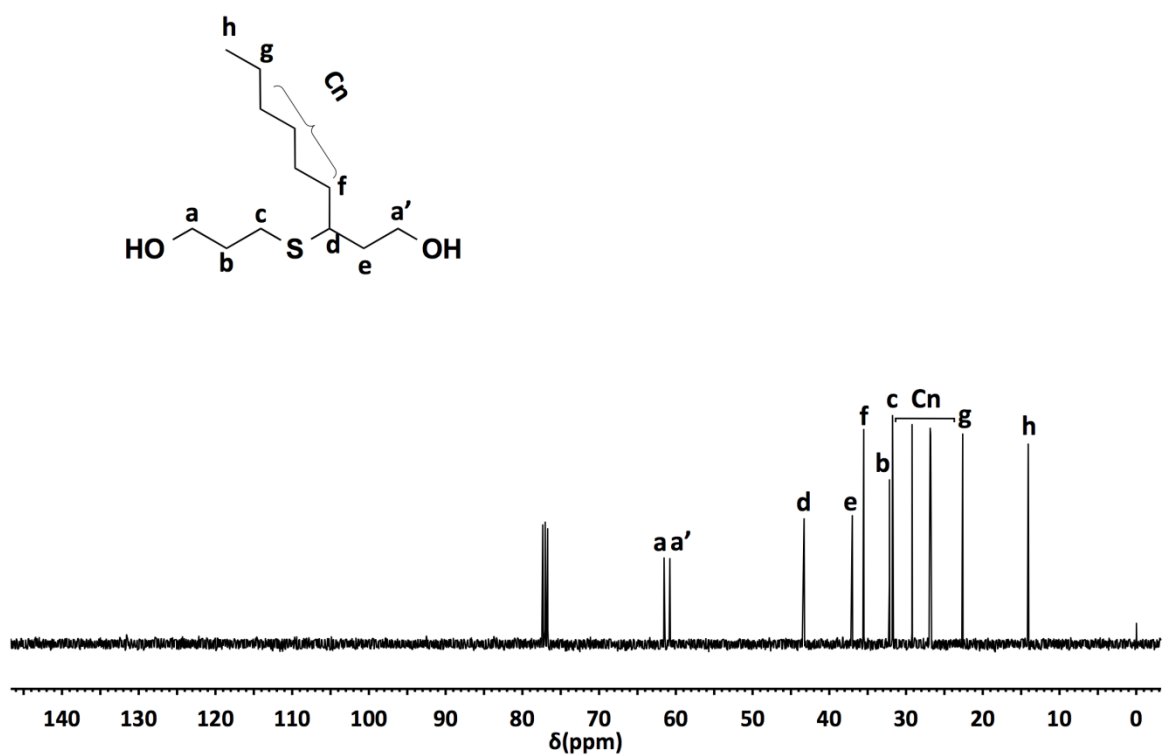


Figure S8. <sup>13</sup>C NMR spectrum of 4 (δ (ppm), CDCl<sub>3</sub>)

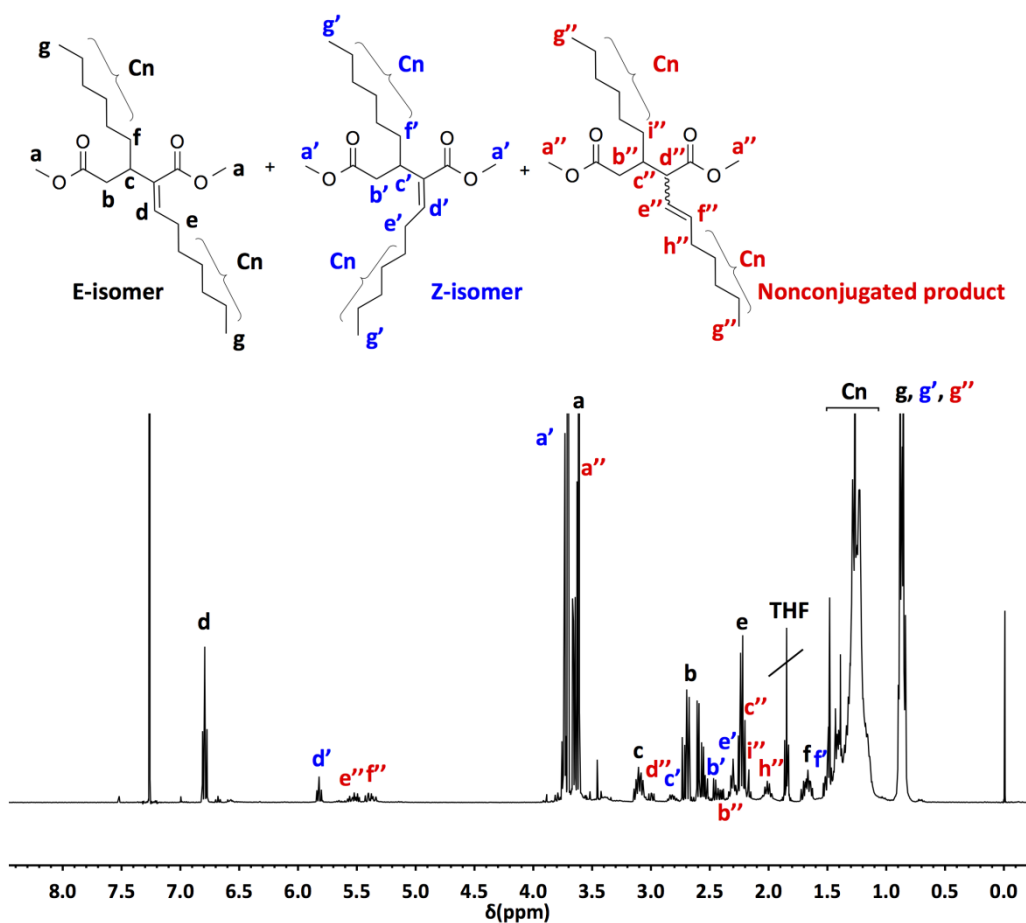


Figure S9.  $^1\text{H}$  NMR spectrum of dimethyl 2-heptylidene-3-hexylpentandioate isomer mixture and non conjugated product ( $\delta$  (ppm),  $\text{CDCl}_3$ )

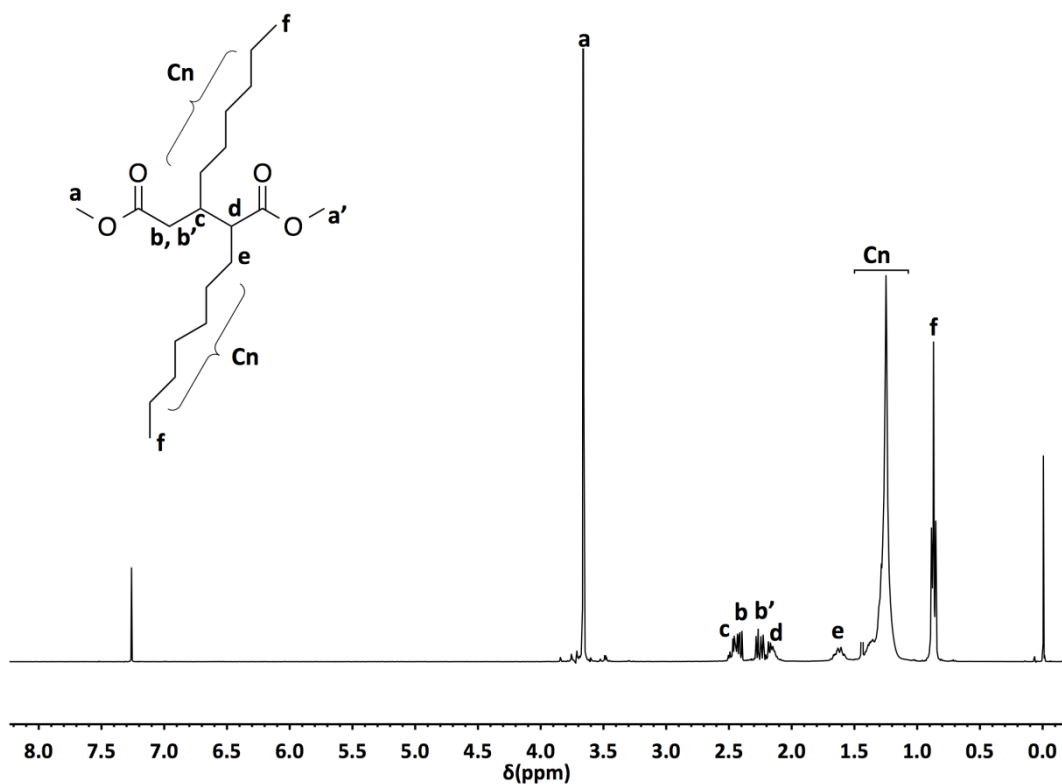


Figure S10.  $^1\text{H}$  NMR spectrum of dimethyl 2-heptyl-3-hexylpentanedioate ( $\delta$  (ppm),  $\text{CDCl}_3$ )

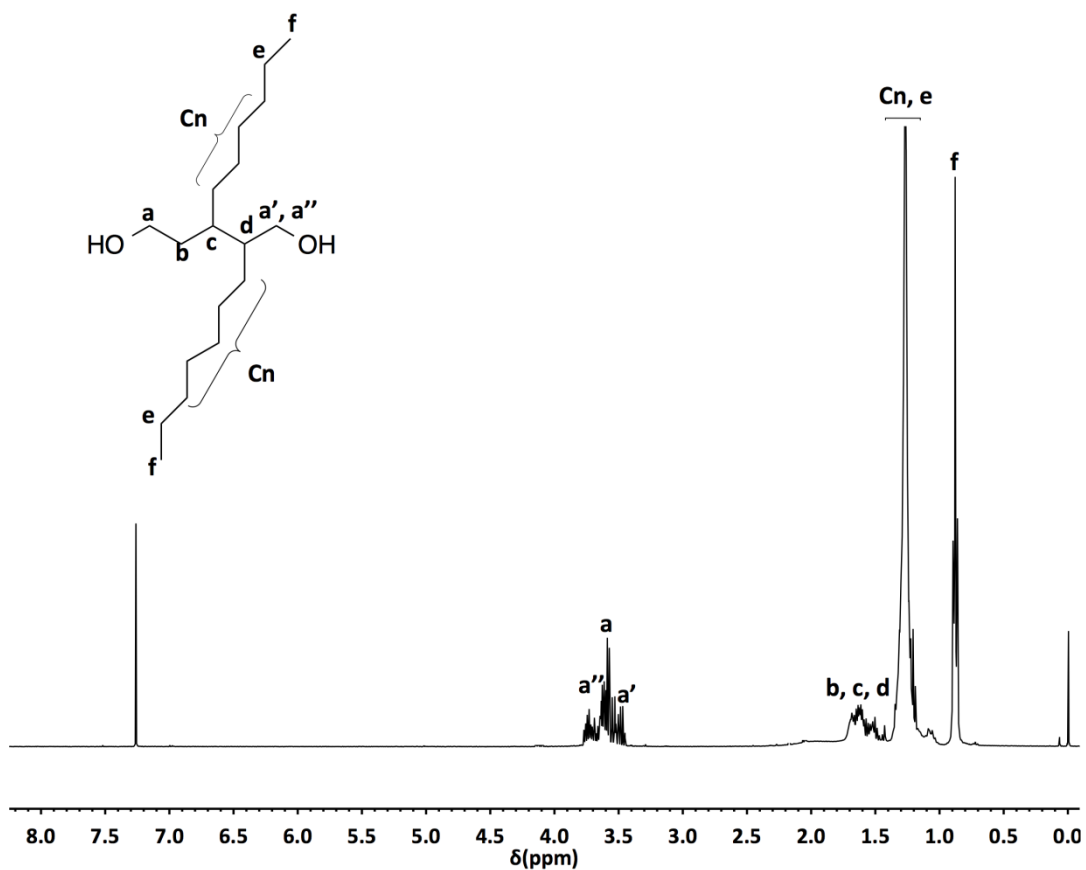


Figure S11.  $^1\text{H}$  NMR spectrum of 5 ( $\delta$  (ppm),  $\text{CDCl}_3$ )

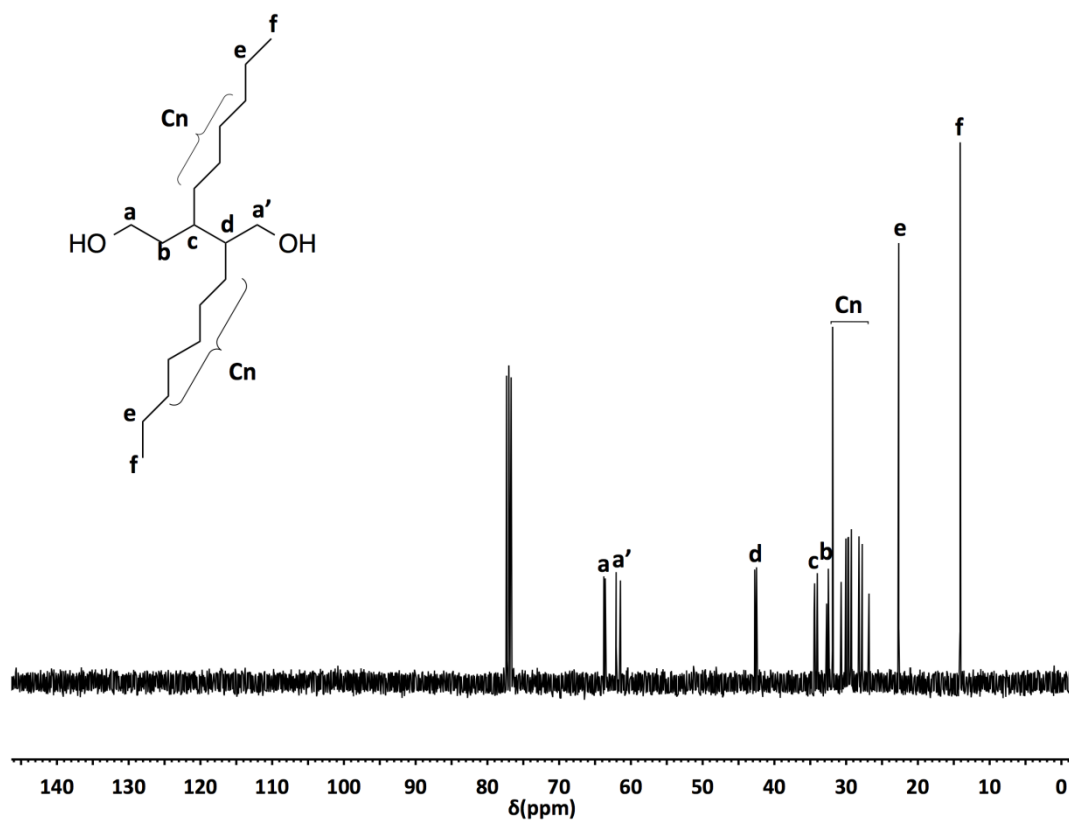


Figure S12.  $^{13}\text{C}$  NMR spectrum of 5 ( $\delta$  (ppm),  $\text{CDCl}_3$ )

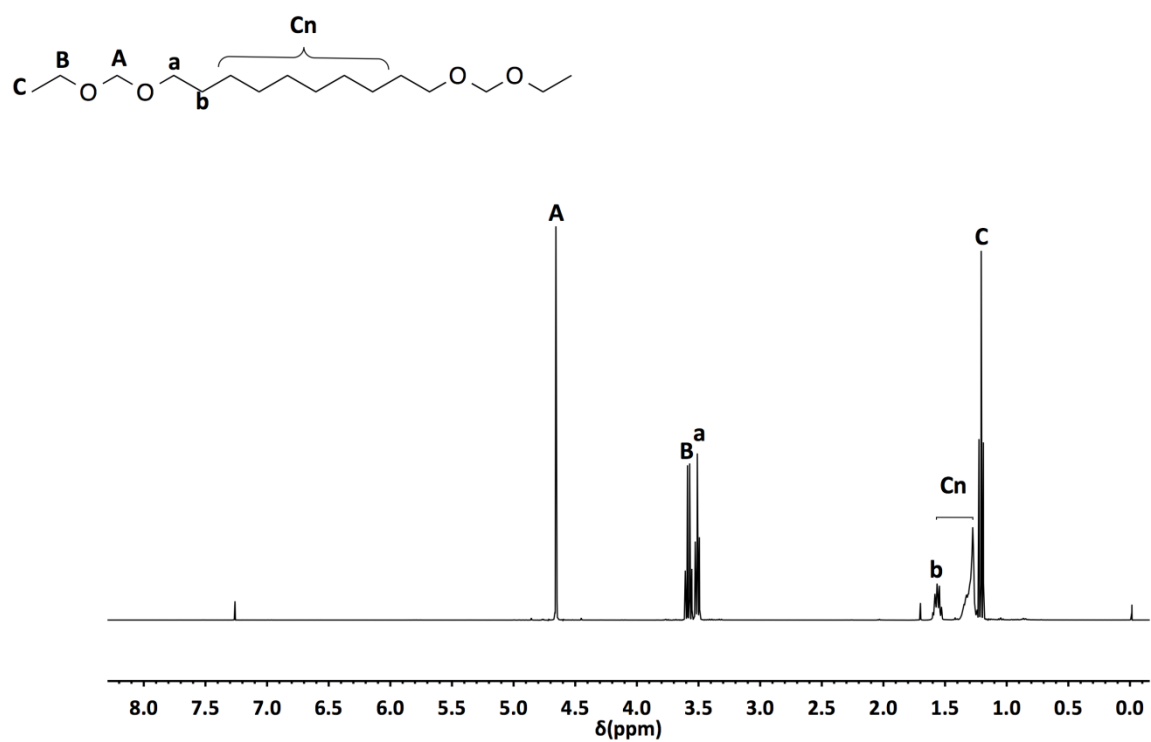


Figure S13. <sup>1</sup>H NMR spectrum of 3,5,16,18-tetraoxaicosane (δ (ppm), CDCl<sub>3</sub>)

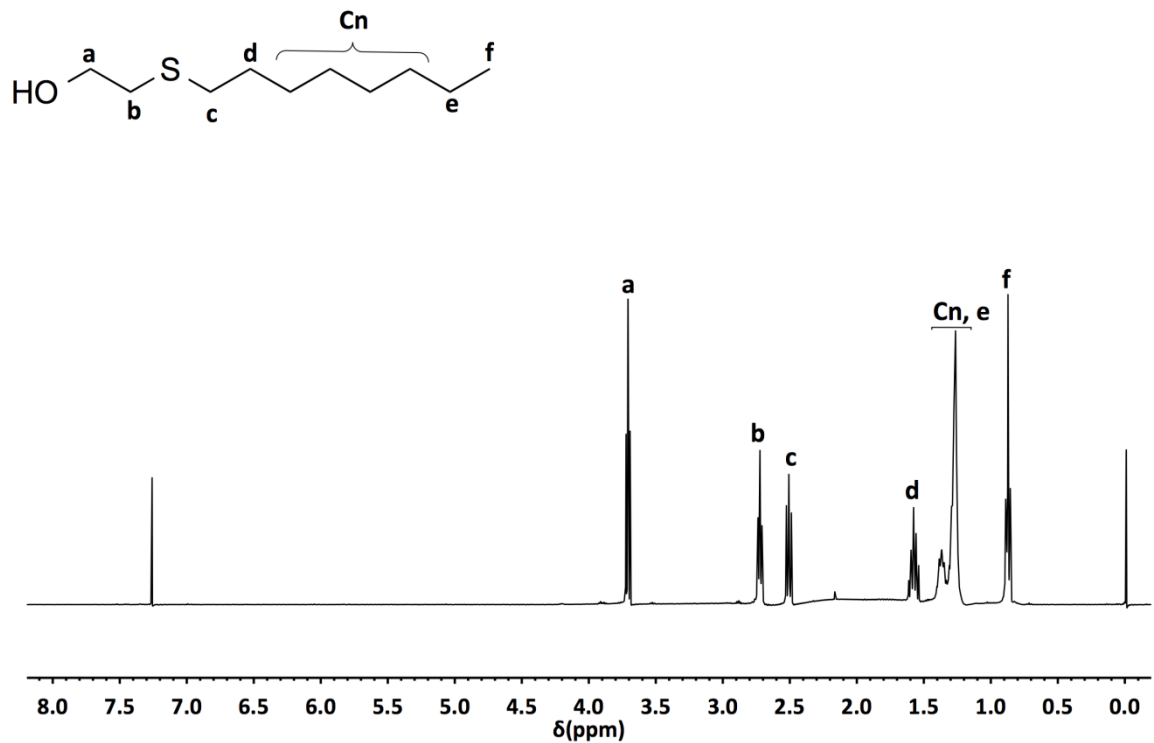


Figure S14. <sup>1</sup>H NMR spectrum of 2-(octylthio)ethan-1-ol (δ (ppm), CDCl<sub>3</sub>)

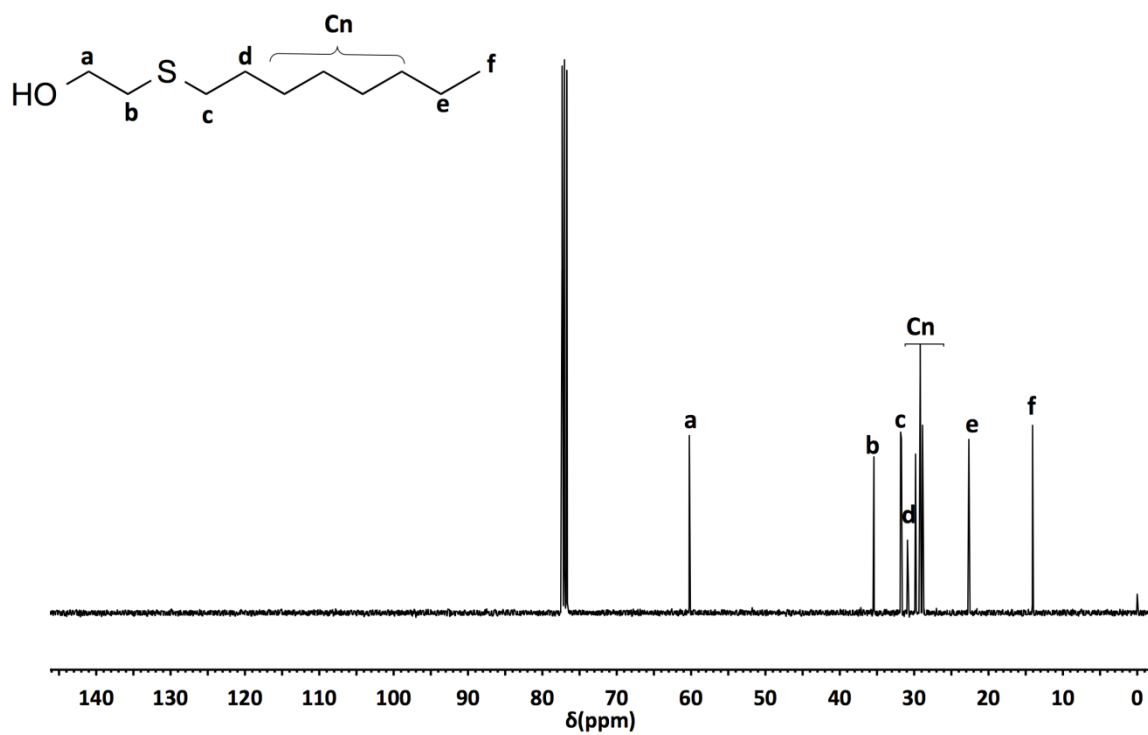


Figure S15.  $^{13}\text{C}$  NMR spectrum of 2-(octylthio)ethan-1-ol ( $\delta$  (ppm),  $\text{CDCl}_3$ )

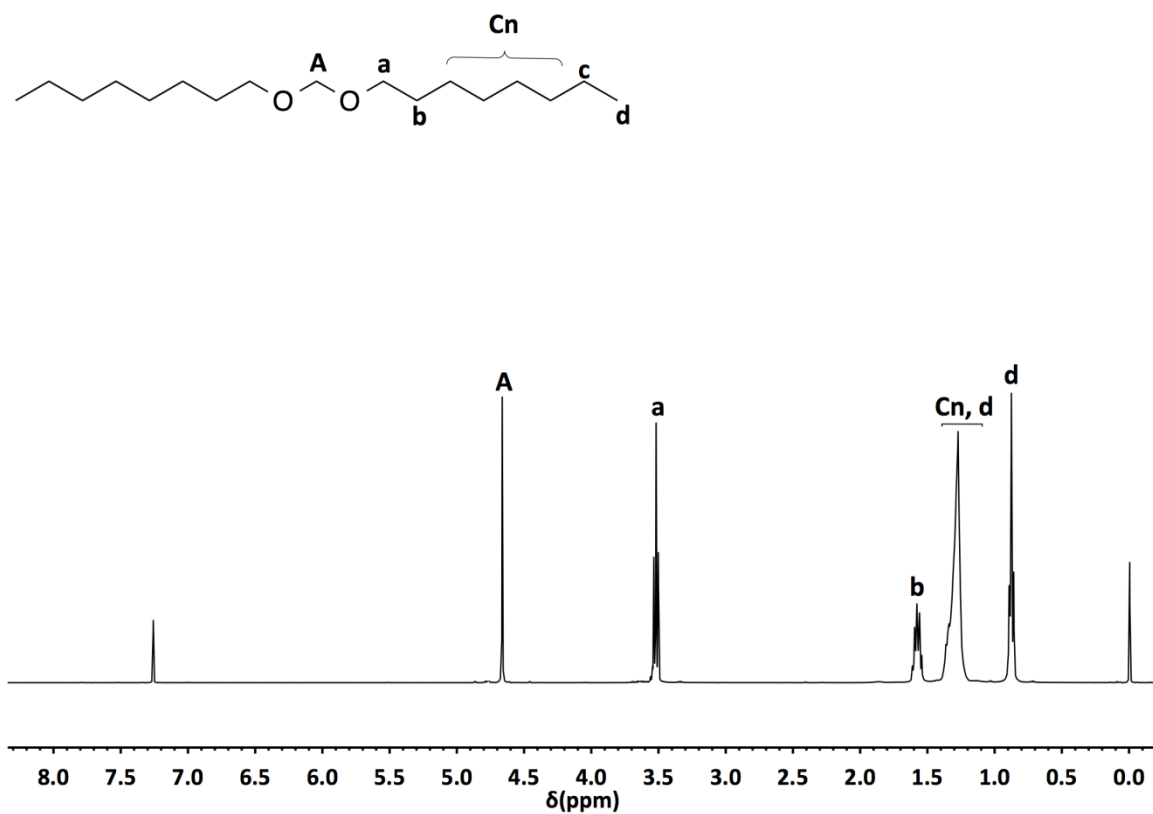


Figure S16.  $^1\text{H}$  NMR spectrum of 9,11-dioxaoctadecane ( $\delta$  (ppm),  $\text{CDCl}_3$ )

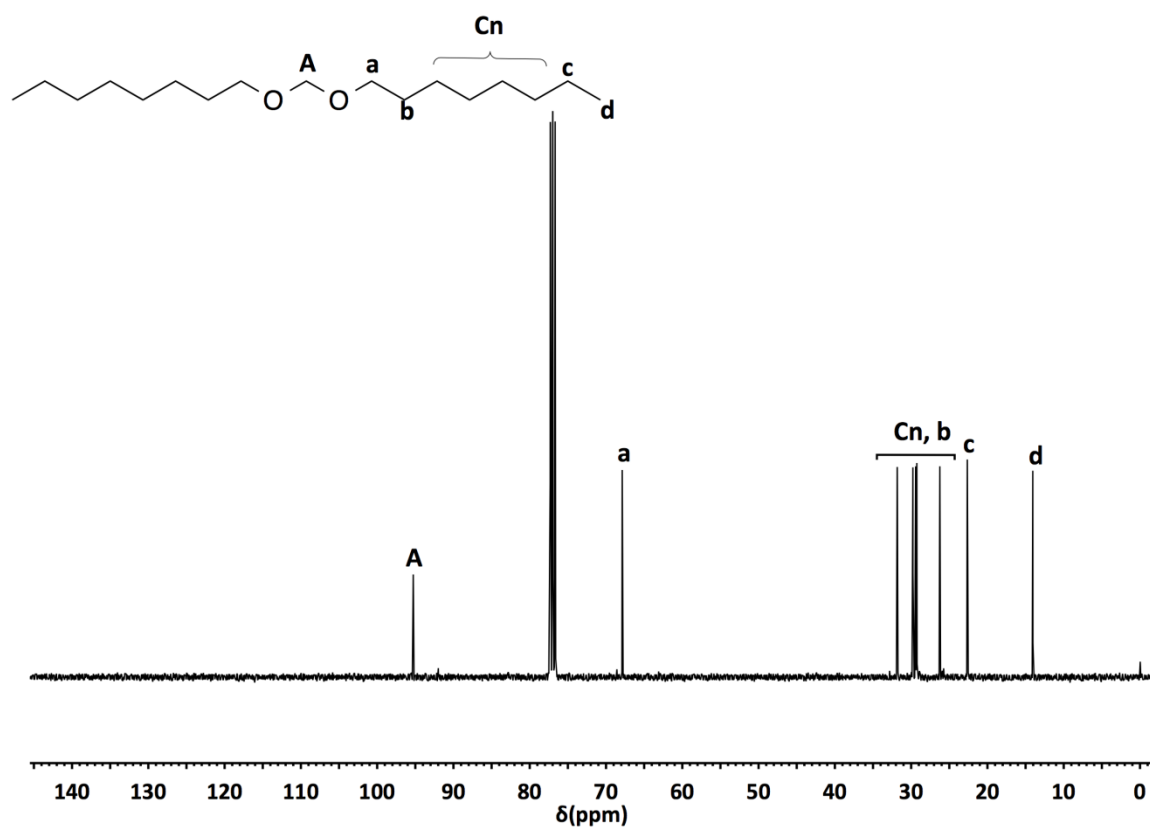


Figure S17. <sup>13</sup>C NMR spectrum of 9,11-dioxaoctadecane (δ (ppm), CDCl<sub>3</sub>)

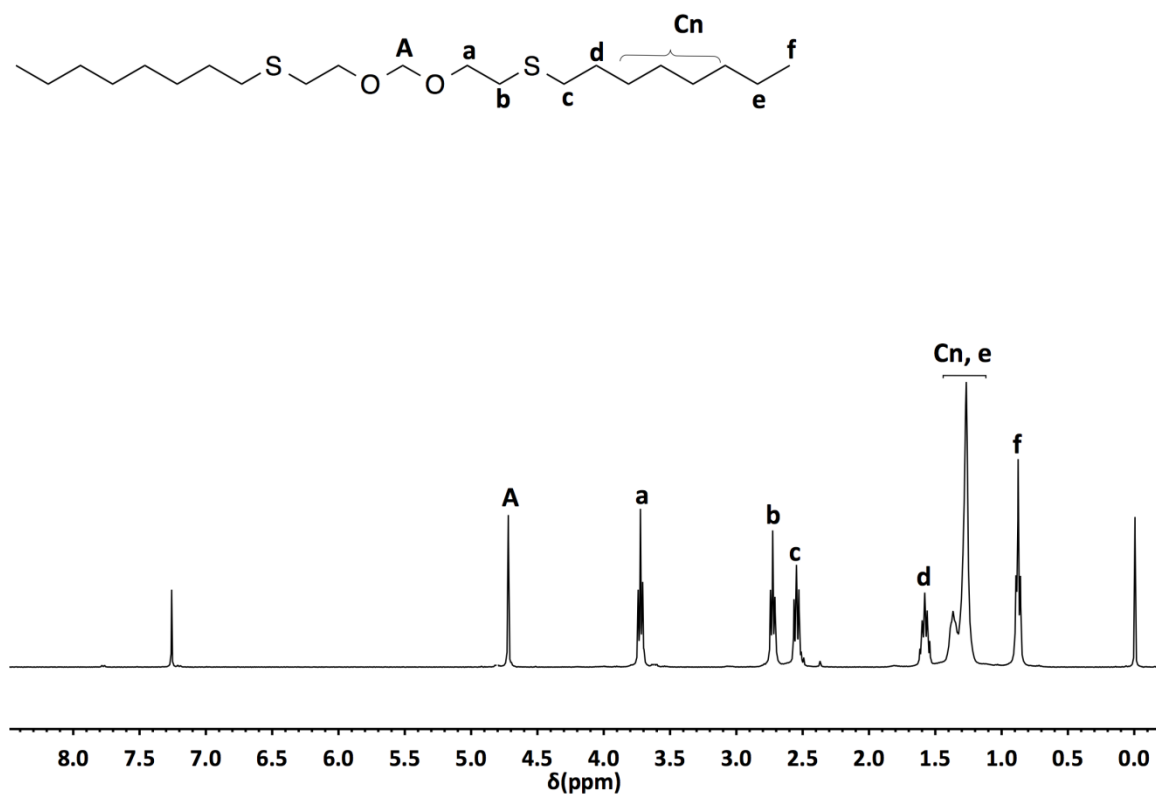


Figure S18. <sup>1</sup>H NMR spectrum of 12,14-dioxa-9,17-dithiapentacosane (δ (ppm), CDCl<sub>3</sub>)

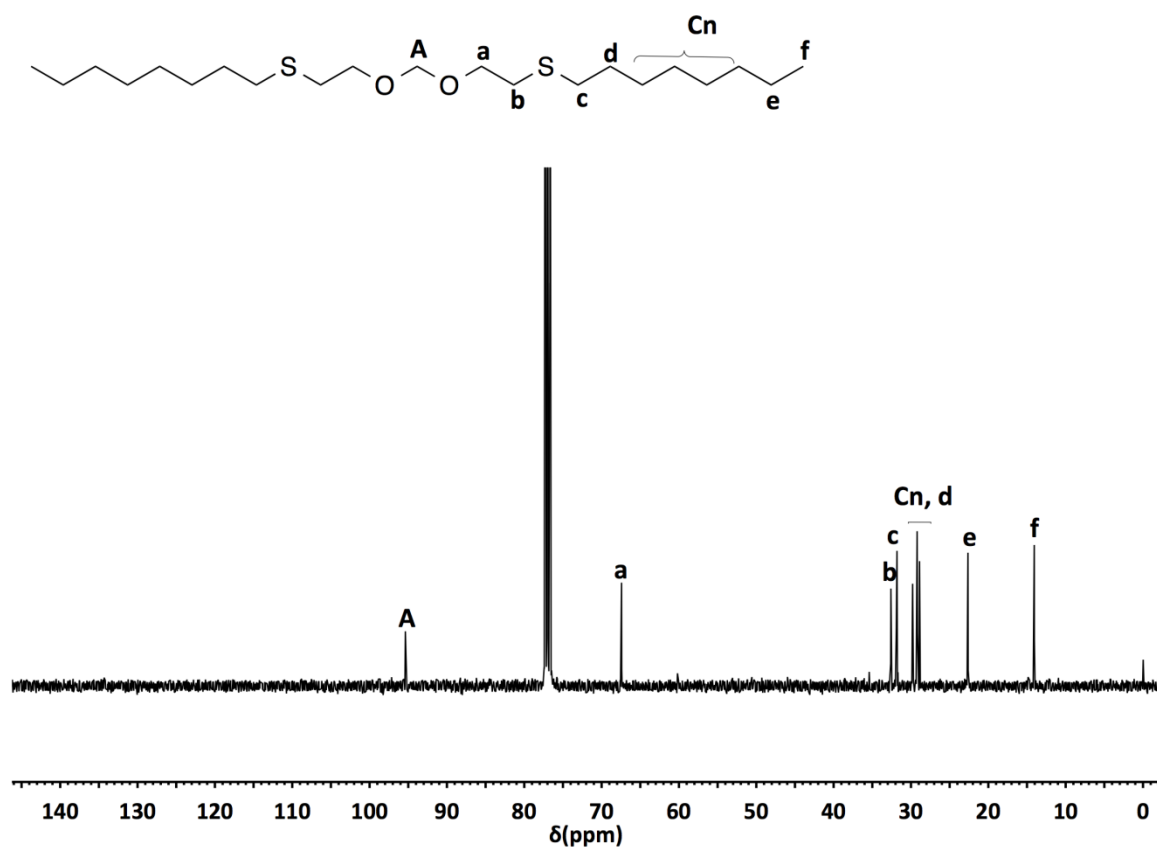


Figure S19.  $^{13}\text{C}$  NMR spectrum of 12,14-dioxa-9,17-dithiapentacosane ( $\delta$  (ppm),  $\text{CDCl}_3$ )

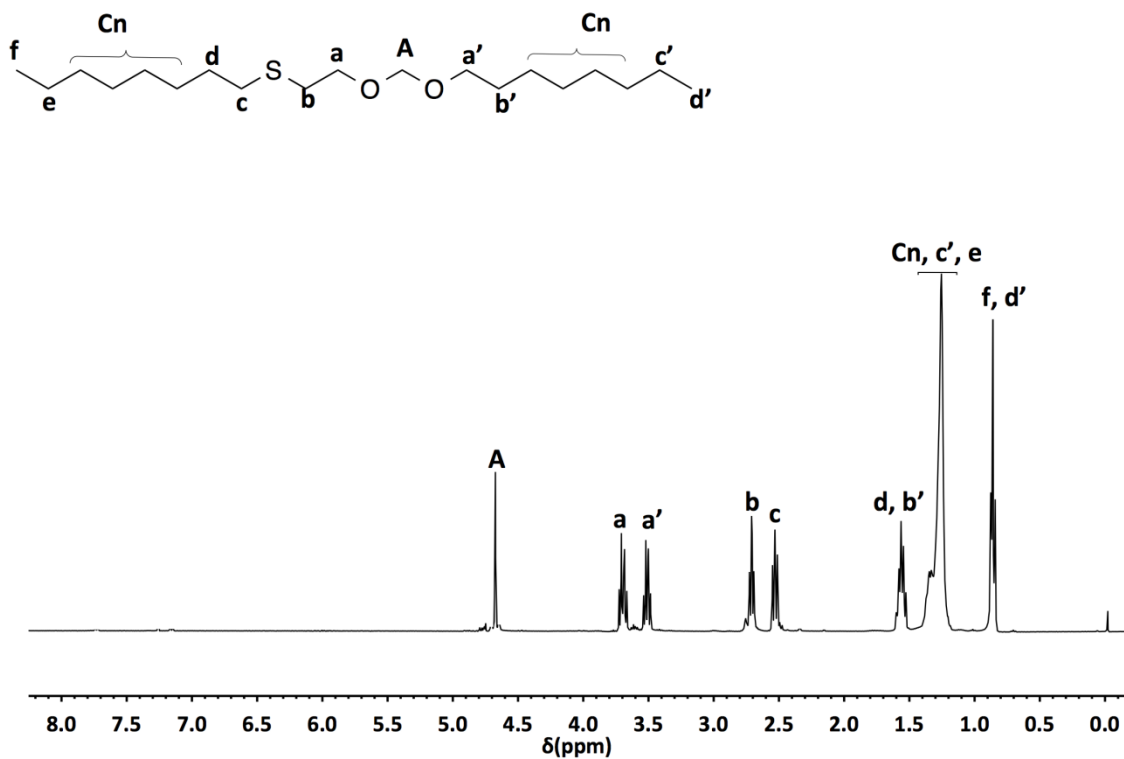


Figure S20.  $^1\text{H}$  NMR spectrum of 12,14-dioxa-9-thiadocosane ( $\delta$  (ppm),  $\text{CDCl}_3$ )

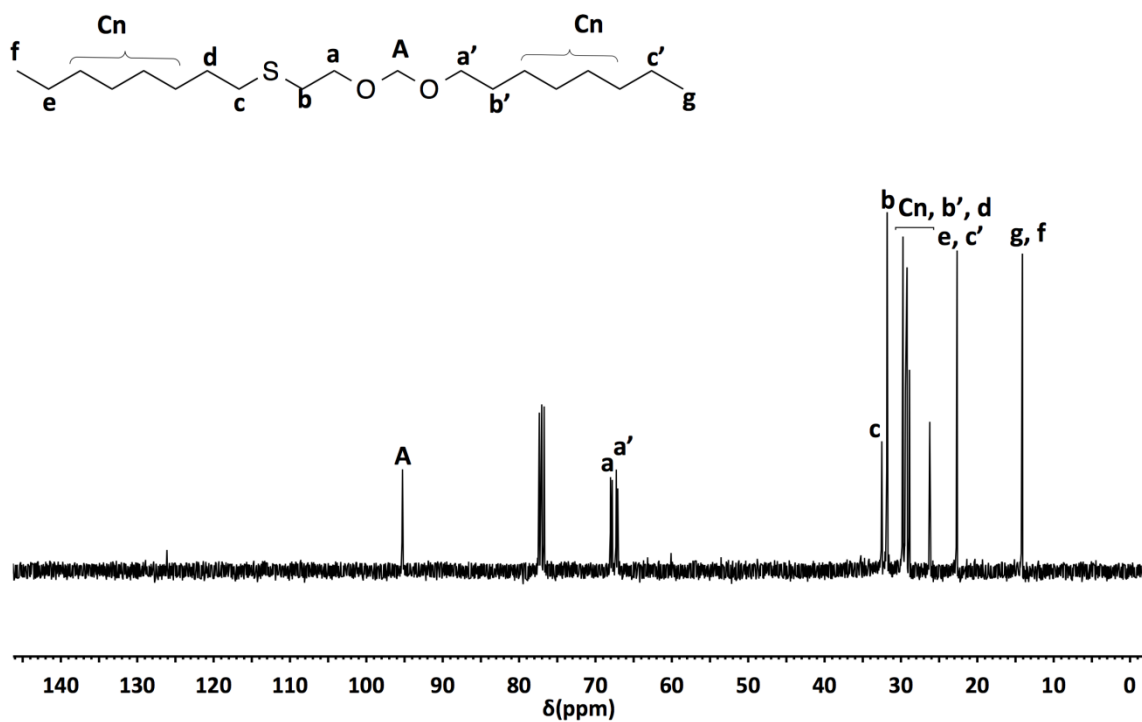


Figure S21.  $^{13}\text{C}$  NMR spectrum of 12,14-dioxa-9-thiadocosane ( $\delta$  (ppm),  $\text{CDCl}_3$ )

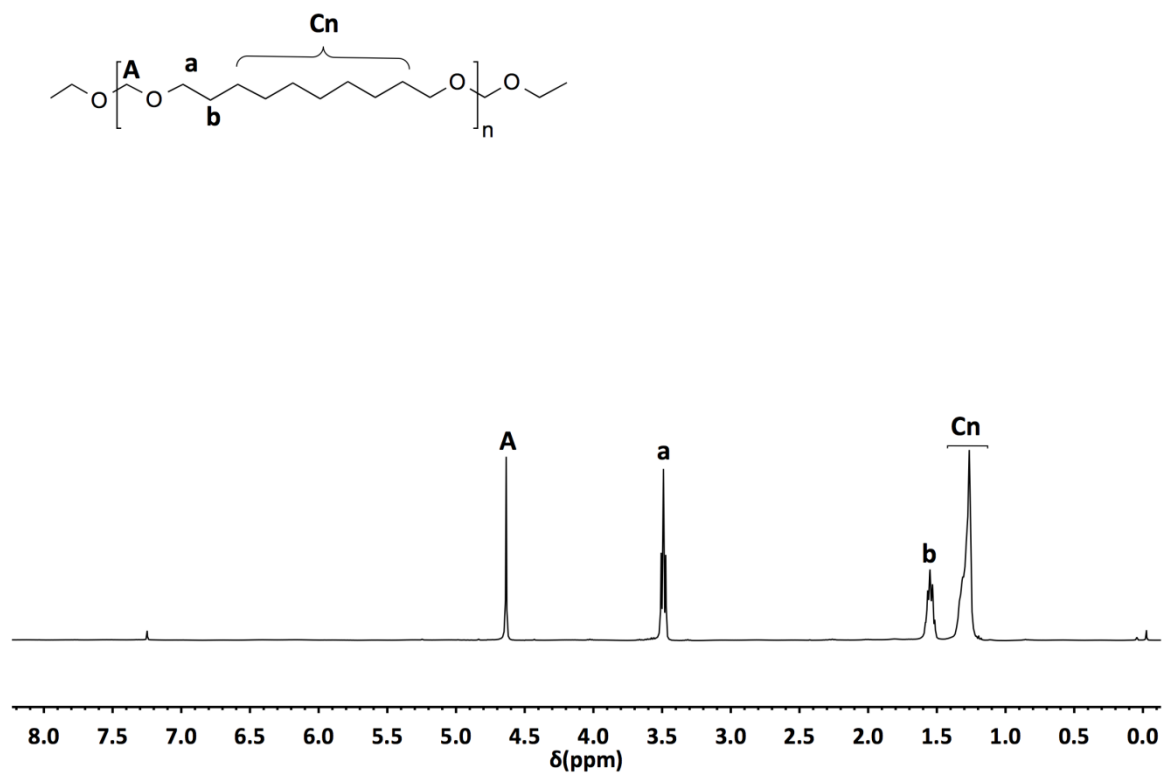


Figure S22.  $^1\text{H}$  NMR spectrum of PA1 ( $\delta$  (ppm),  $\text{CDCl}_3$ )

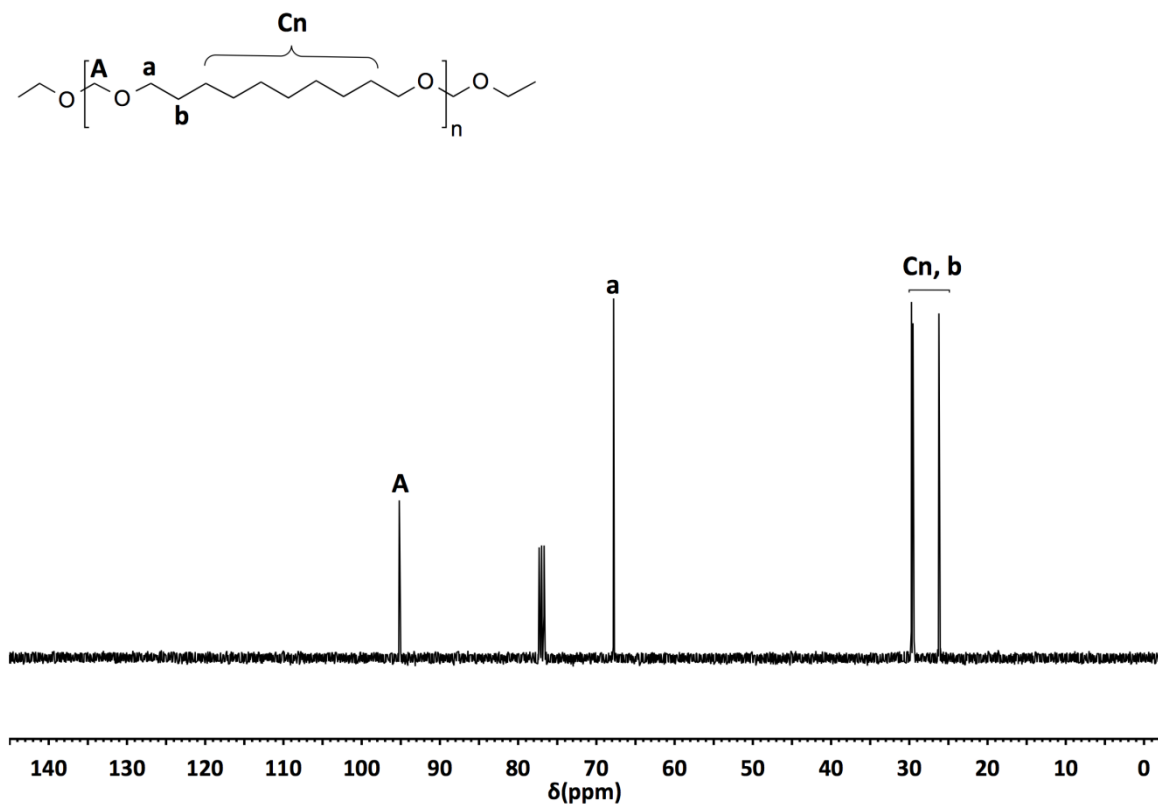


Figure S23.  $^{13}\text{C}$  NMR spectrum of **PA1** ( $\delta$  (ppm),  $\text{CDCl}_3$ )

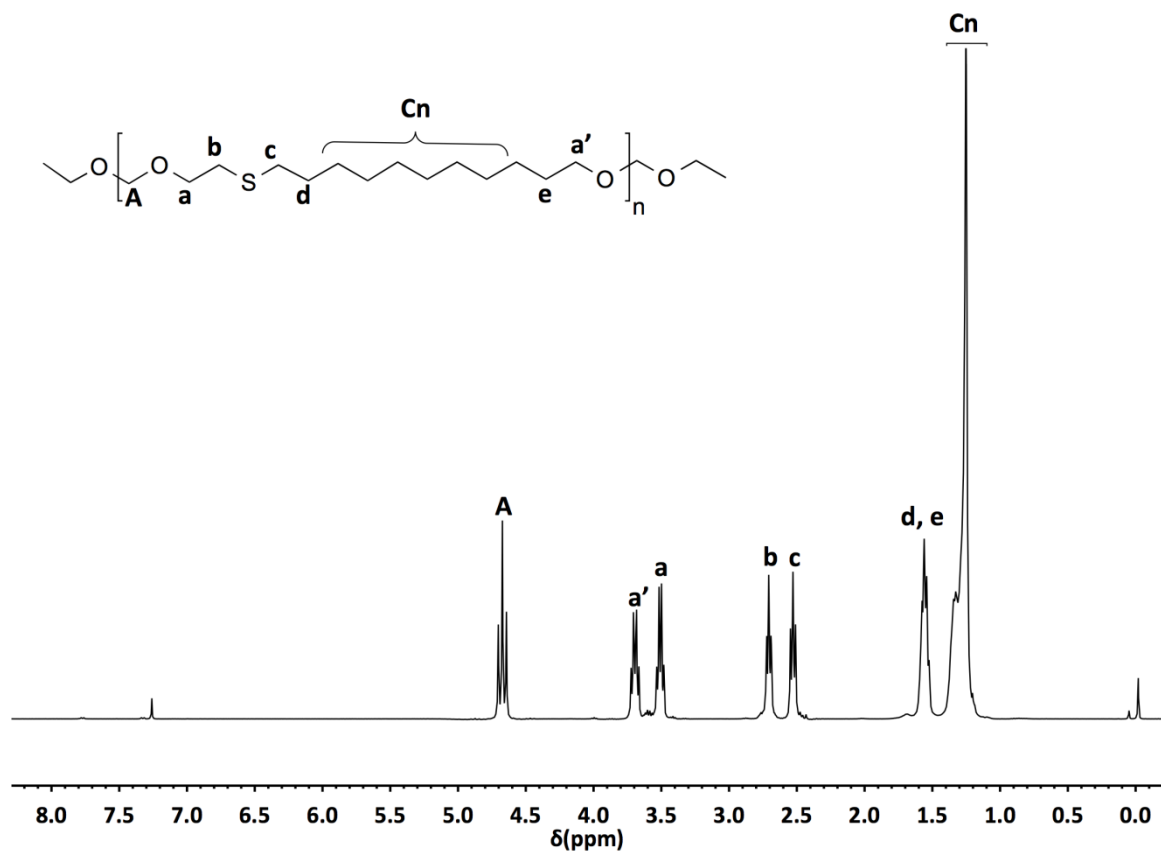


Figure S24.  $^1\text{H}$  NMR spectrum of **PA2** ( $\delta$  (ppm),  $\text{CDCl}_3$ )

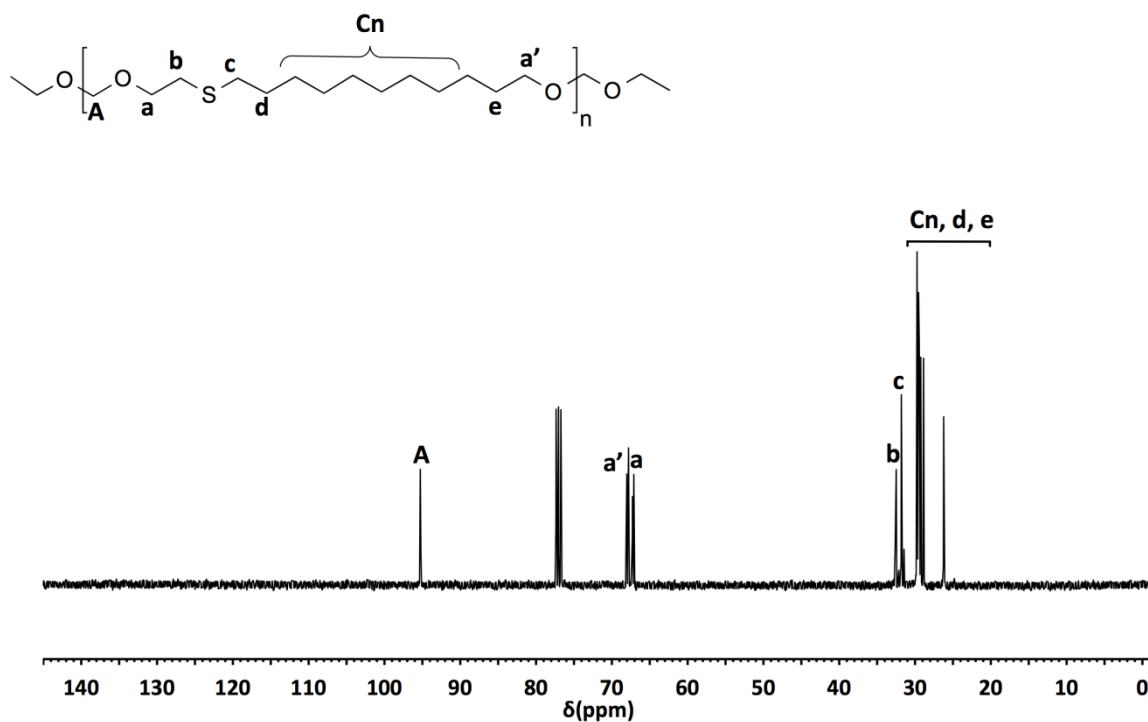


Figure S25.  $^{13}\text{C}$  NMR spectrum of PA2 ( $\delta$  (ppm),  $\text{CDCl}_3$ )

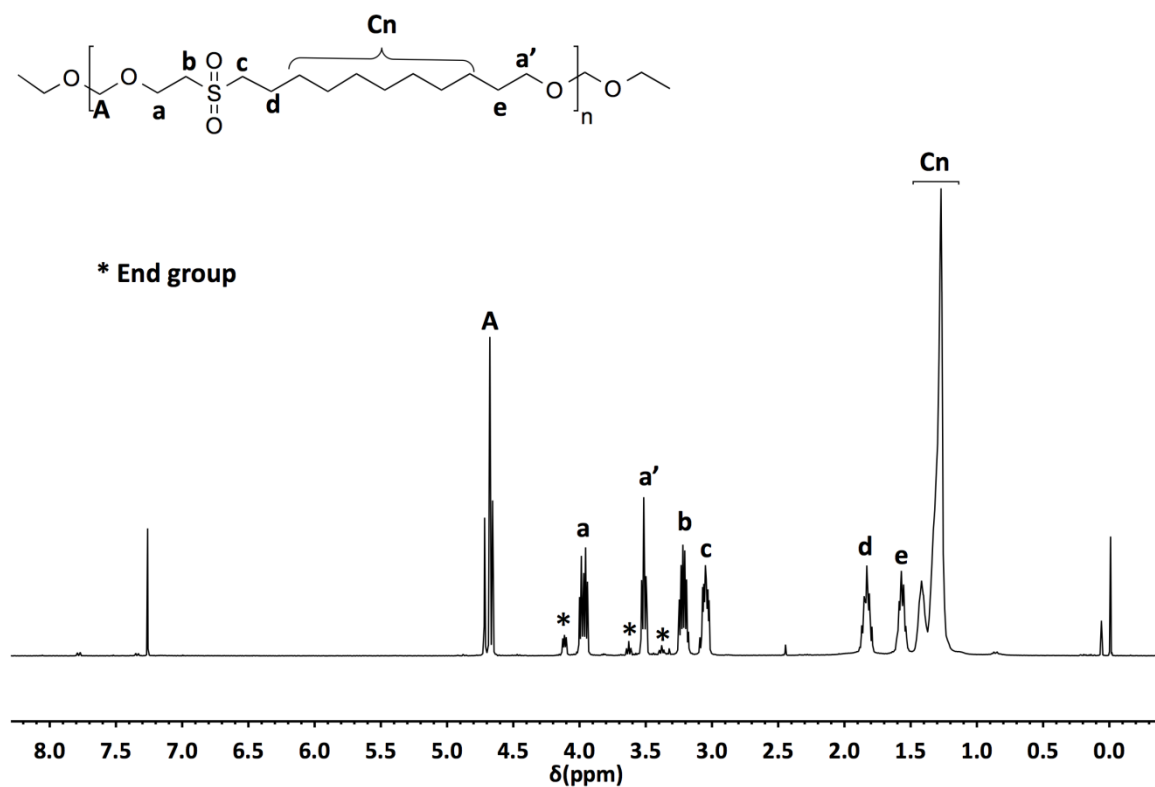


Figure S26.  $^1\text{H}$  NMR spectrum of PA3 ( $\delta$  (ppm),  $\text{CDCl}_3$ )

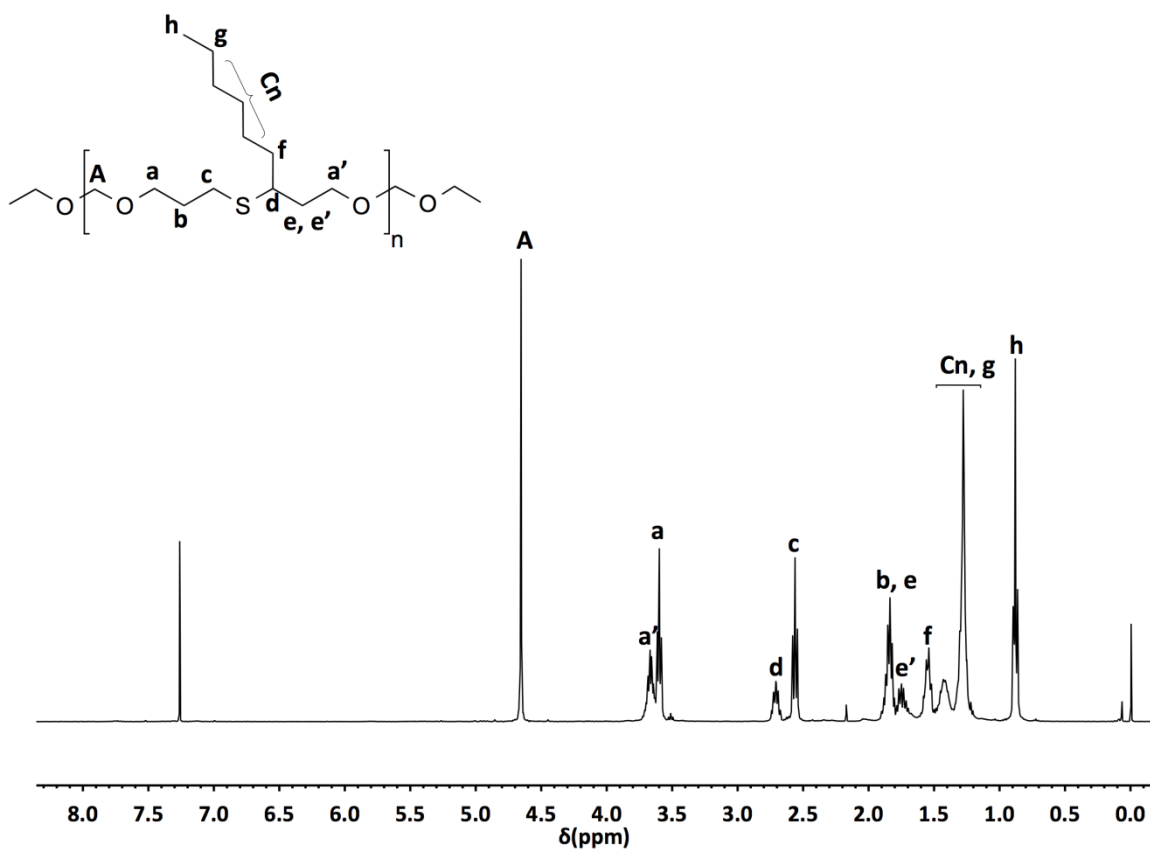
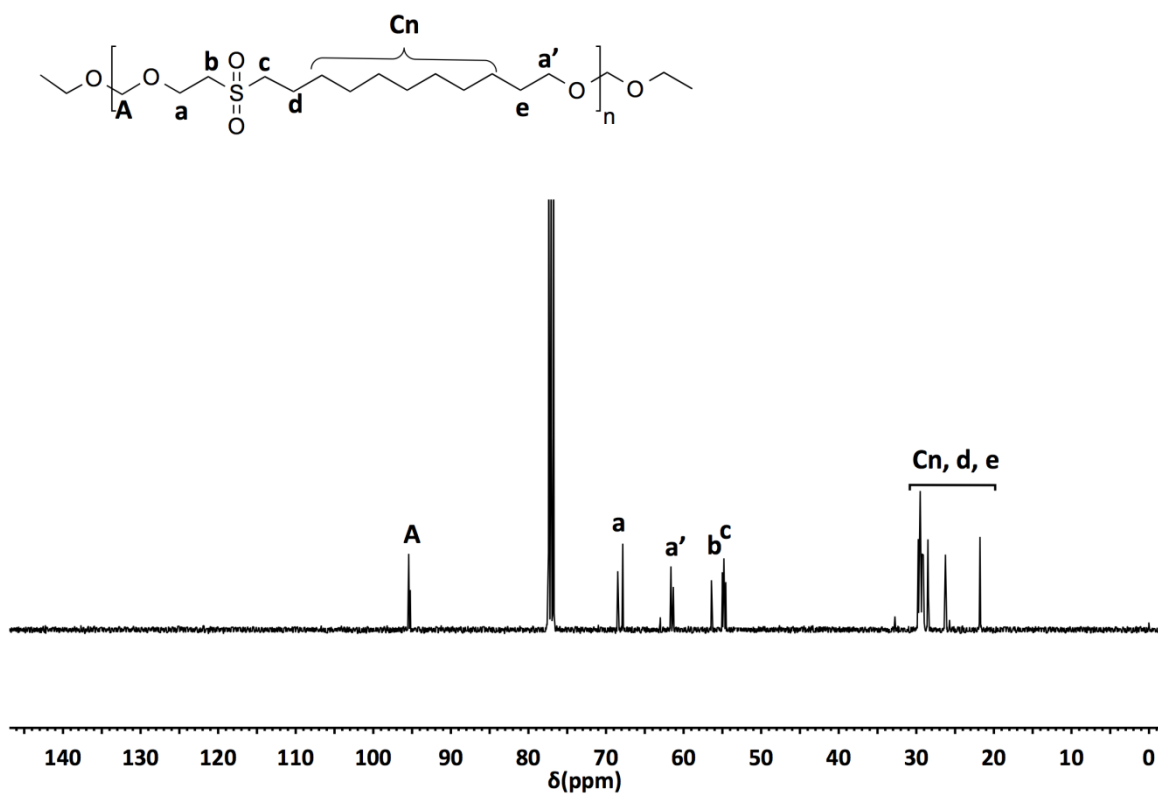
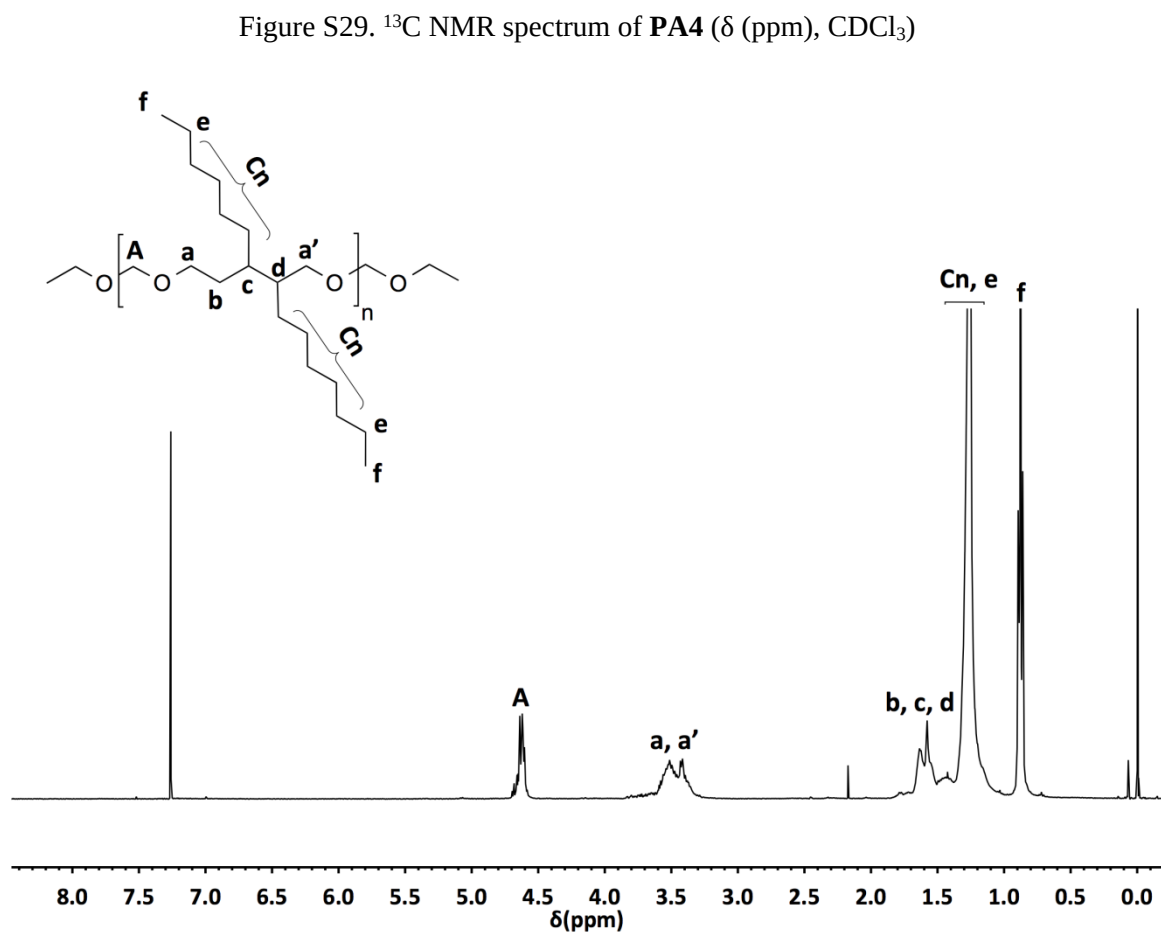
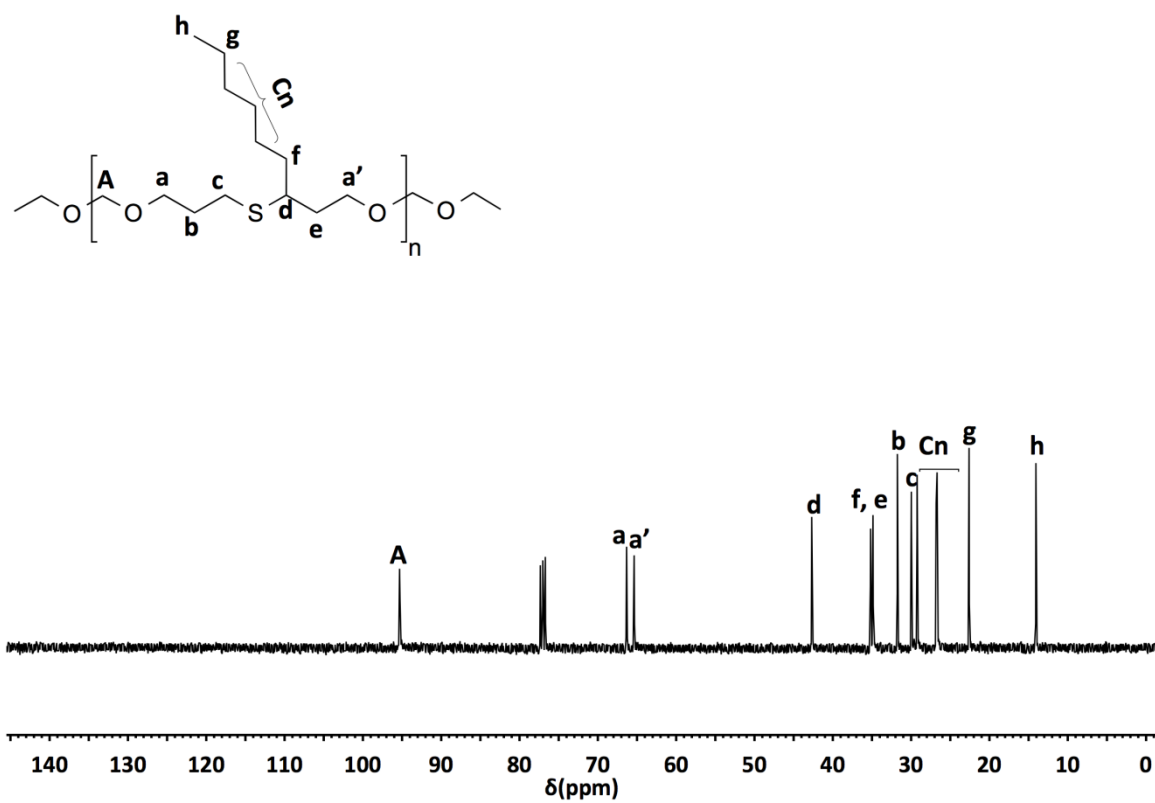
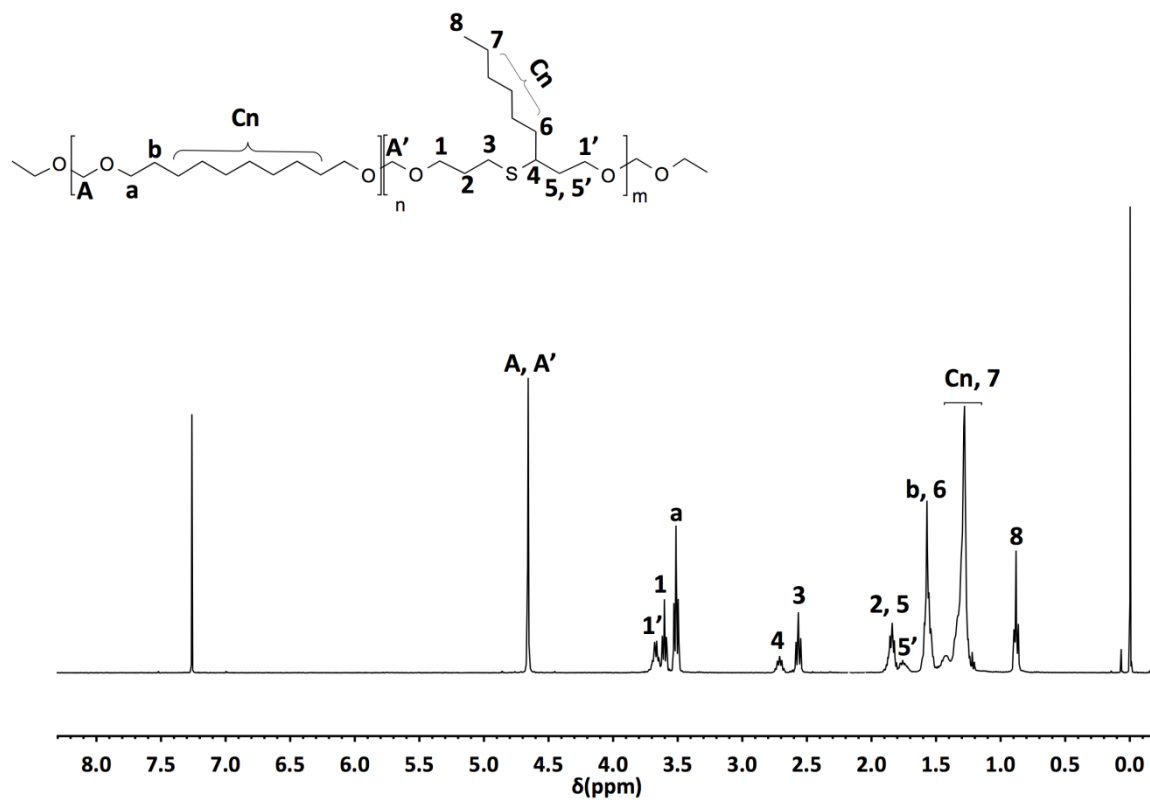
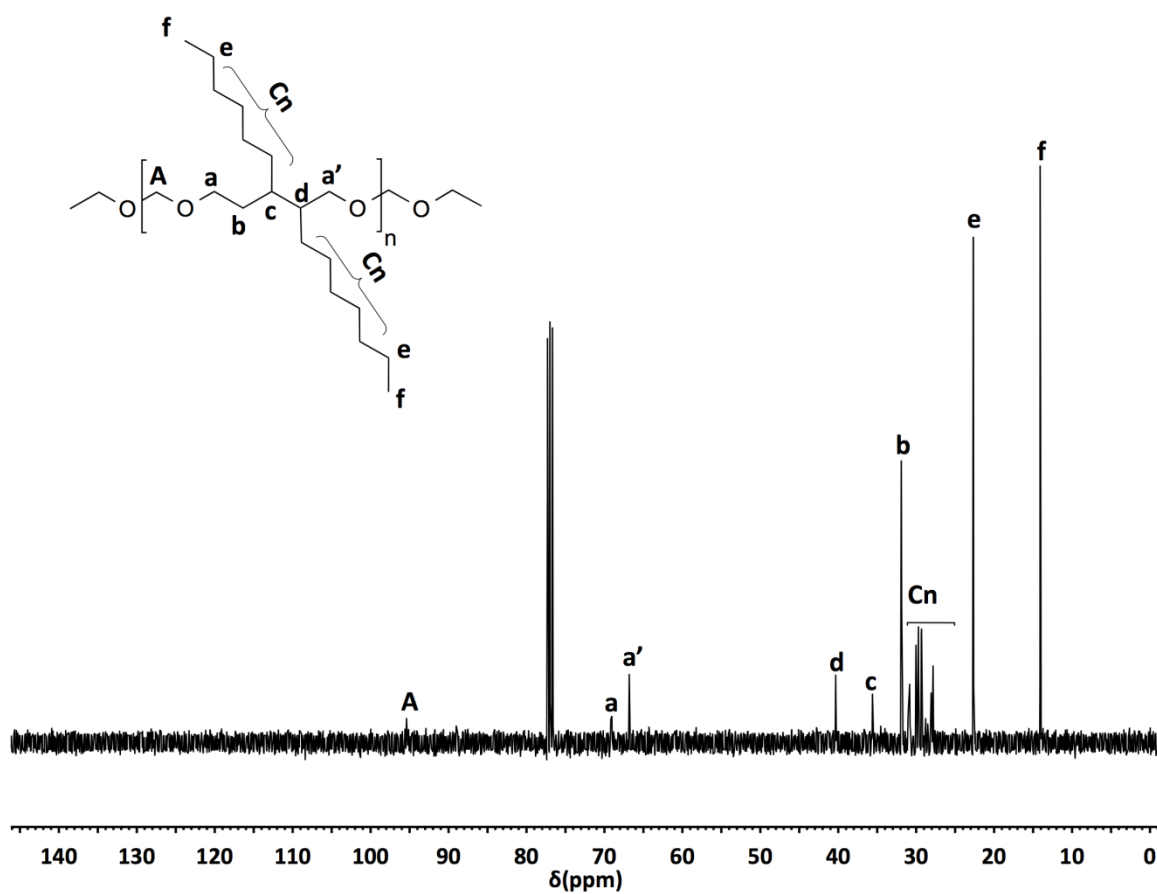


Figure S28.  $^1\text{H}$  NMR spectrum of **PA4** ( $\delta$  (ppm),  $\text{CDCl}_3$ )





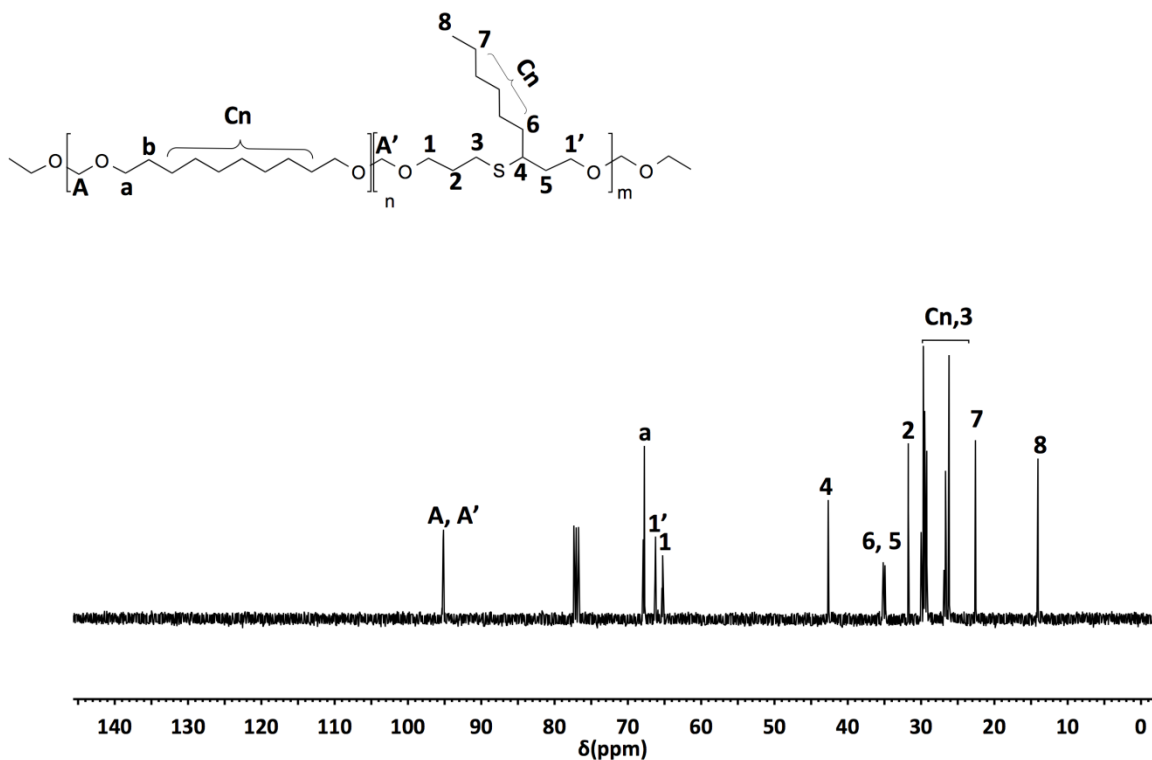


Figure S33.  $^{13}\text{C}$  NMR spectrum of PA1-4 ( $\delta$  (ppm),  $\text{CDCl}_3$ )

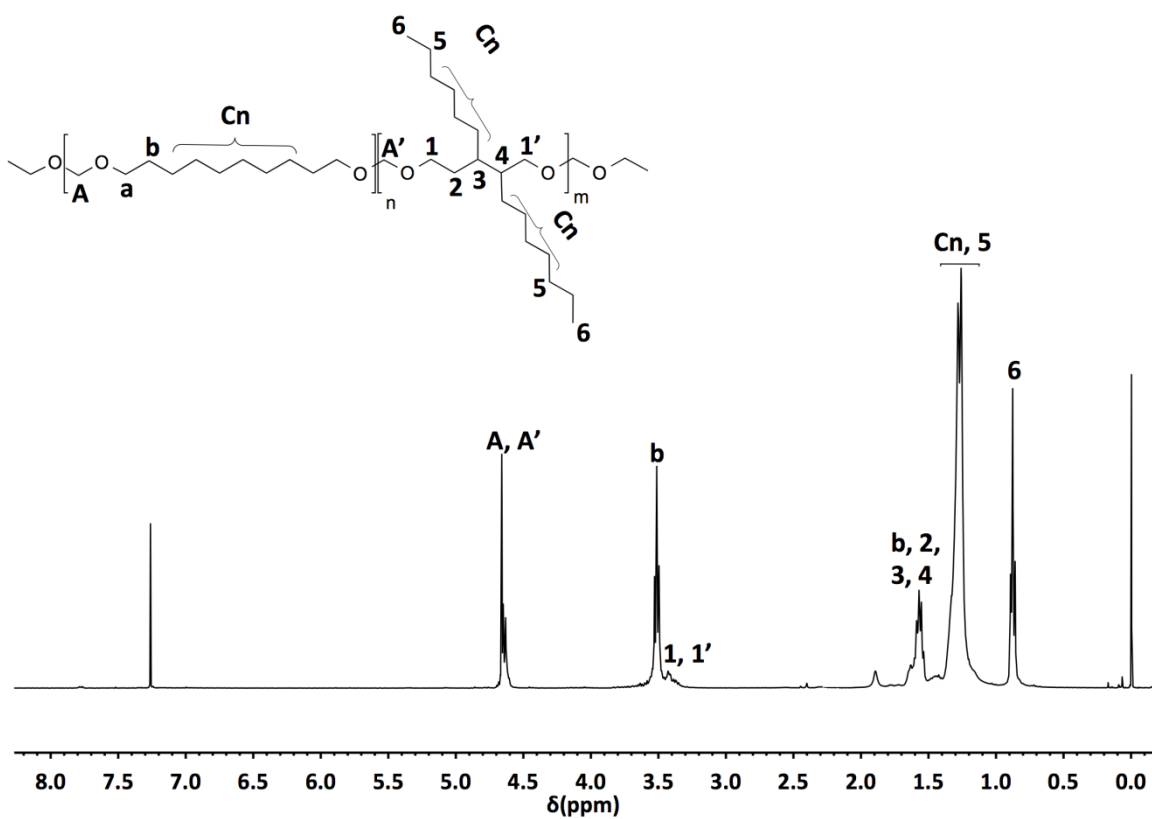


Figure S34.  $^1\text{H}$  NMR spectrum of PA1-5 1:1 ( $\delta$  (ppm),  $\text{CDCl}_3$ )

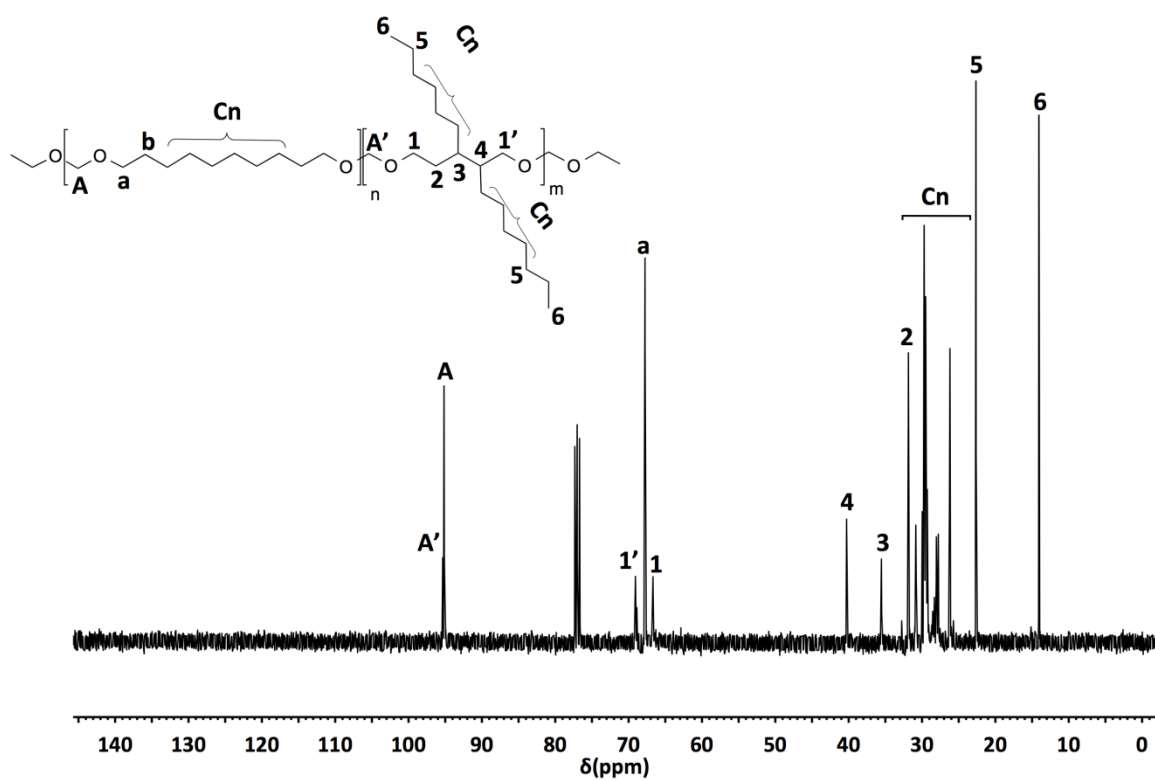


Figure S35.  $^{13}\text{C}$  NMR spectrum of PA1-5 1:1 ( $\delta$  (ppm),  $\text{CDCl}_3$ )

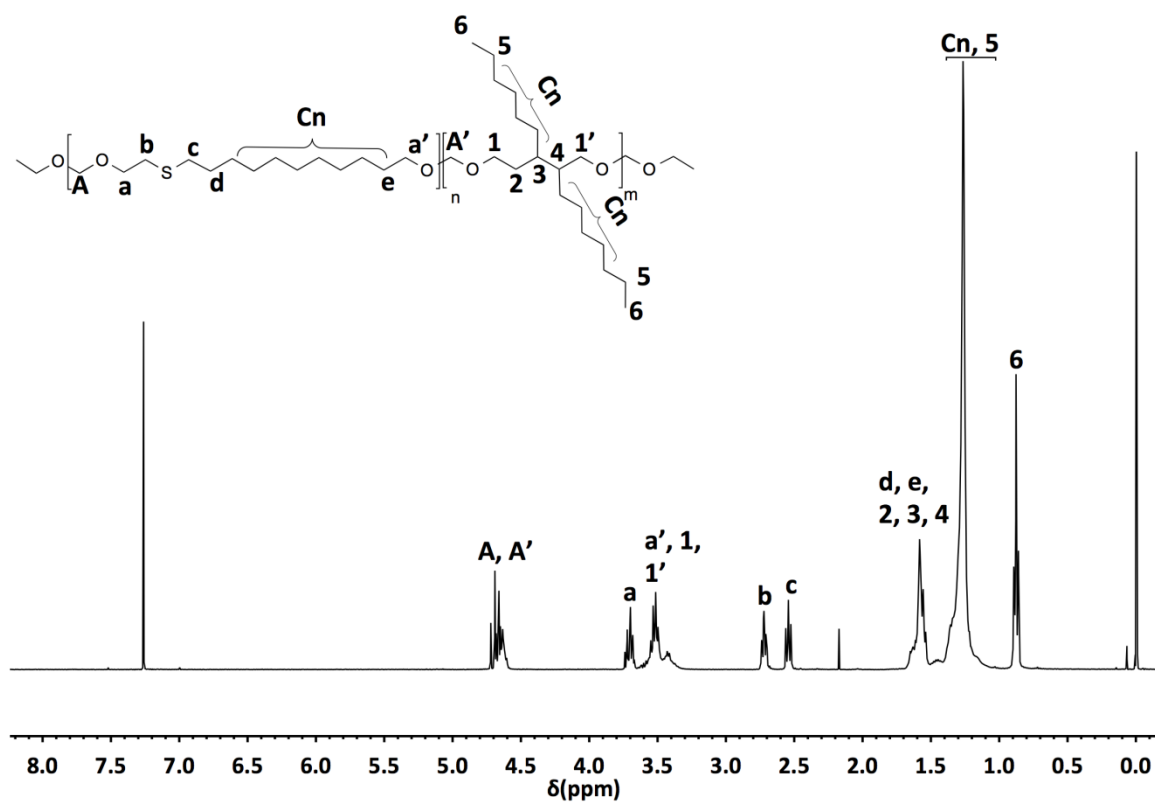


Figure S36.  $^1\text{H}$  NMR spectrum of PA2-5 ( $\delta$  (ppm),  $\text{CDCl}_3$ )

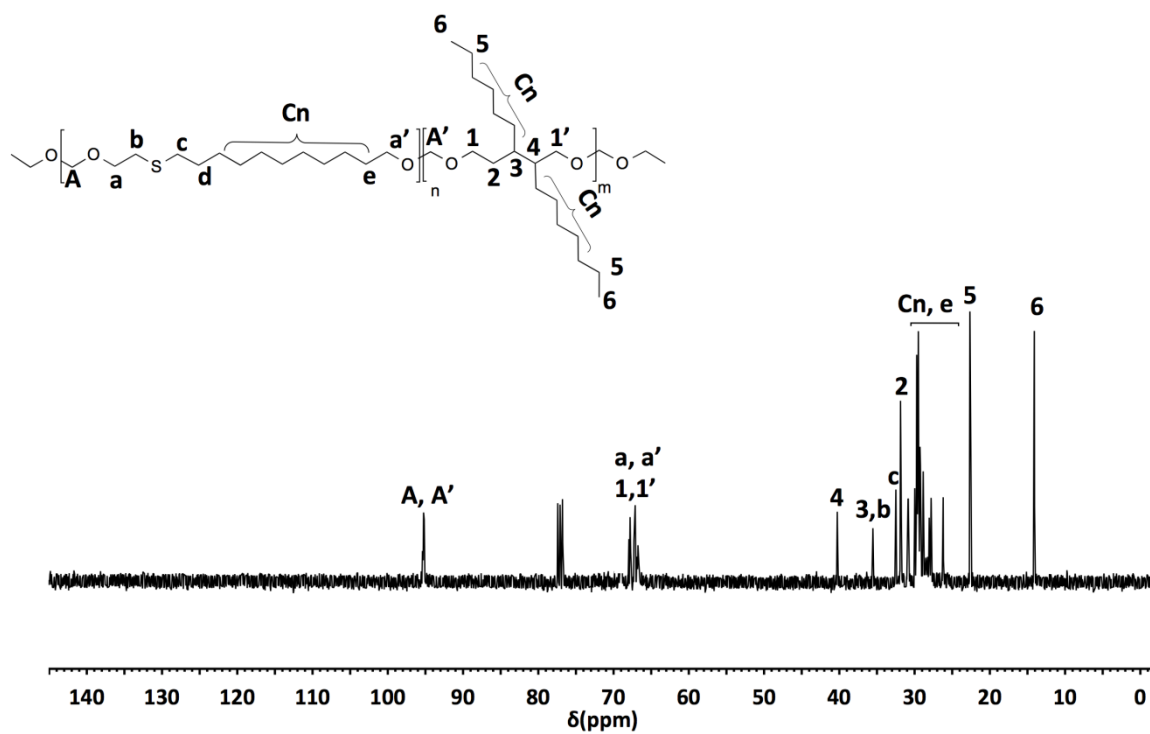


Figure S37. <sup>13</sup>C NMR spectrum of PA2-5 (δ (ppm), CDCl<sub>3</sub>)

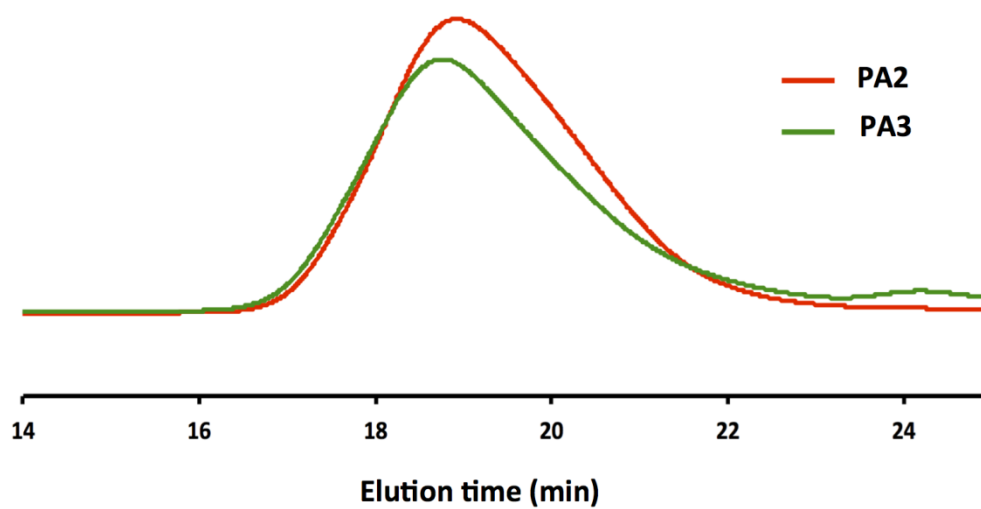


Figure S38. GPC traces of PA2 and PA3

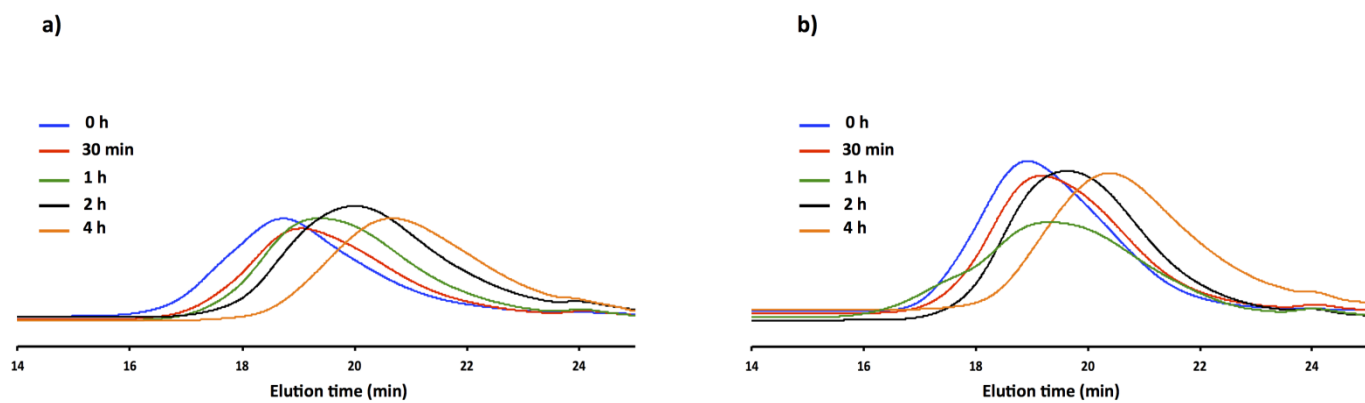


Figure S39. GPC degradation traces of **PA1** (a) and **PA2** (b) (0.04M, 25°C)